Universidade de Aveiro
2021

Mariana Fontoura Vassal

Diferentes estratégias para atenuar a toxicidade reprodutiva das nanopartículas de ZnO

Different strategies to attenuate the reproductive toxicity of ZnO Nanoparticles

Universidade de Aveiro
2021

Mariana Fontoura Vassal

Diferentes estratégias para atenuar a toxicidade reprodutiva das nanopartículas de ZnO

Different strategies to attenuate the reproductive toxicity of ZnO Nanoparticles

Dissertação apresentada à Universidade de Aveiro para cumprimento dos requisitos necessários à obtenção do grau de Mestre em Biologia Molecular e Celular, realizada sob a orientação científica da Professora Doutora Maria de Lourdes Gomes Pereira, Professora Associada com agregação do Departamento de Ciências Médicas da Universidade de Aveiro, e sob a co-orientação científica da Professora Doutora Sandra Maria Tavares da Costa Rebelo, Professora Auxiliar do Departamento de Ciências Médicas da Universidade de Aveiro

This work was supported by Fundação para a Ciência e Tecnologia (FCT) I.P. (PIDDAC), (project numbers UIDB/04501/2020 and UIDP/045011/2020). Project CICECO-Aveiro Institute of Materials, UIDB/50011/2020 and UIDP/50011/2020 was also supported by FCT/MCTES.

Dedico este trabalho aos meus incríveis pais que sempre apoiaram todas as minhas decisões, e à minha irmã que foi incansável comigo. Sem eles nada disto seria possível. Obrigada por todo o amor.

Ao meu avô Armindo, que partiu este ano e não teve oportunidade de me ver concluir os estudos.

À minha avó Mariana, que nunca tive oportunidade de conhecer, mas que trago sempre no meu coração. Espero que esteja orgulhosa.

o júri

Presidente	Doutora Clara Lúcia Ferreira Rodrigues Investigadora Auxiliar em Regime Laboral, CESAM & Departamento de Biologia, Universidade de Aveiro
Arguente	Prof. Doutor Carlos Pedro Fontes Oliveira Professor Auxiliar em Regime Laboral, Departamento de Química, Universidade de Aveiro
Orientadora	Prof. Doutora Maria de Lourdes Gomes Pereira Professora Associada com Agregação, Departamento de Ciências Médicas, Universidade de Aveiro

Agradecimentos

Em primeiro lugar, gostaria de agradecer às minhas orientadoras. À Professora Doutora Maria de Lourdes Pereira e Professora Doutora Sandra Rebelo, por todo o rigor, conselhos e revisões milimétricas. Obrigada pelo conhecimento que me transmitiram e pelas oportunidades que me deram.

Queria também agradecer à Doutora Vera Silva do Departamento de Química da Universidade de Aveiro, por me ter facultado diferentes compostos para explorar neste trabalho e pela disponibilidade em esclarecer todas as minhas dúvidas.

Aos meus pais, Dionísio Vassal e Agostinha Vassal por terem sido tão pacientes comigo ao longo do meu percurso académico. Nem sempre foi fácil, mas nunca desistiram de mim. À minha irmã Isabela por ter sido o meu pilar este ano, sem ela não conseguiria. Aos meus avós Carminda e Alberto por toda a preocupação e carinho, e aos meus avós que partiram, Armindo e Mariana. Obrigada por me ensinarem que a família é o melhor do mundo. Todo o vosso amor permitiu que eu chegasse aqui.

À Cátia, do grupo do Laboratório de Neurociências e Sinalização que me ensinou tudo o que sei sobre cultura de células e muito mais. O rigor e perfeição com que executa o seu trabalho é realmente incrível. Foi uma honra ter aprendido com ela. Ficarei para sempre grata.

À Ana Rita Pinho que foi incrivelmente paciente comigo ao longo destes meses, esclarecendo-me sempre dúvidas e dando sugestões para otimizar protocolos.

Às minhas amigas Diana Martins e Rita Moreira, pela grande amizade e bons momentos que me proporcionaram nos últimos dois anos.

A todos os meus colegas do iBiMED, em especial à Nélia e Margarida, um sentido obrigada pelo companheirismo e por toda a partilha de conhecimentos. À Isabela Santos que foi incansável, ajudando-me sempre no que podia e mostrando-se sempre disponível, mesmo quando não estava.

palavras-chave

Nanopartículas de óxido de metal, nanopartículas de óxido de zinco, espermatogónia, toxicidade reprodutiva, antioxidantes, calconas, reversibilidade

resumo

As nanopartículas de óxido de zinco (ZnO NPs) são das nanopartículas de óxido de metal mais sintetizadas, devido às suas propriedades físico-químicas e biológicas singulares. Existe, contudo, uma preocupação crescente relativamente ao impacto negativo que estes materiais têm na saúde reprodutiva masculina. Sendo assim, neste trabalho, foi feita uma revisão bibliográfica de forma a compilar os atuais estudos *in vitro* e *in vivo* que reportaram efeitos adversos das NPs de óxido de metal no sistema reprodutor masculino, de forma a facilitar a compreensão da sua toxicidade através de evidências moleculares, bioquímicas e histopatológicas. Contudo, ainda existem poucos dados relativamente à reversibilidade desta toxicidade. Para compreender melhor qual o impacto das NPs na saúde reprodutiva masculina, é essencial determinar se os danos induzidos são permanentes. Portanto, o passo seguinte deste trabalho foi avaliar a capacidade de recuperação de espermatogónias (GC-1 spg) após 6 e 12 horas de exposição a uma concentração citotóxica de ZnO NPs. Após um período de recuperação de 4 dias em que as células estiveram num ambiente desprovido de NPs, os resultados de viabilidade celular sugerem que as GC-1 não foram capazes de recuperar totalmente dos danos induzidos. Desta forma, foram utilizadas diferentes concentrações (0-12.5 μM) de uma calcona sintética (VS3) com propriedades antioxidantes, antes e durante a exposição das células de GC-1 às NPs de ZnO, numa tentativa de mitigar os danos induzidos pelas NPs. A capacidade protetora deste composto foi avaliada através de ensaios de viabilidade, deteção intracelular de espécies reativas de oxigénio (ROS), níveis de danos no DNA, e níveis de proteínas do citoesqueleto (α-tubulina acetilada, β-tubulina, e β-actina). Os resultados indicam que as concentrações testadas da calcona VS3 têm a capacidade de atenuar a genotoxicidade induzida pelas NPs de ZnO, para períodos de exposição mais curtos (6 horas). A suplementação com VS3 também aumentou a viabilidade celular e estabilizou os microtúbulos. No entanto, o potencial antioxidante deste composto revelou-se inconclusivo.

Em conclusão, este trabalho aborda os principais efeitos citotóxicos das NPs de óxido de metal nas células reprodutivas masculinas (GC-1 spg) e analisa duas estratégias diferentes para mitigar estes danos, o que representa um contributo significativo no âmbito da fertilidade masculina. Perspectiva-se a realização de estudos futuros com vista a uma melhor compreensão do potencial antioxidante da calcona sintética (VS3) na espermatogénese.

keywords

Metal oxide nanoparticles, zinc oxide nanoparticles, spermatogonia, reproductive toxicity, antioxidants, chalcones, reversibility

abstract

Zinc oxide nanoparticles (ZnO NPs) are between the most synthesized metal oxide nanoparticles (MONPs) due to their unique physicochemical and biological properties. There is, however, a growing concern about their negative impact on male reproductive health. Therefore, in this work, a literature review was carried out to summarize current *in vitro* and *in vivo* studies that reported adverse effects of MONPs on the male reproductive system, to provide understanding of their toxicity through molecular, biochemical, and histopathological evidence.

However, there are still limited data regarding the reversibility of this toxicity. To fully understand the impact of NPs on male reproductive health, it is crucial to determine if the induced damage is permanent. Therefore, the next step of this work was to assess the recovery ability of spermatogonia cells (GC-1 spg cell line) after 6 and 12 hours of exposure to a cytotoxic concentration of ZnO NPs. After a recovery period of 4 days where cells were left in NP-free conditions, cell viability results suggest that GC-1 cells were not able to fully recover from the induced damage. Thus, different concentrations (0-12.5 μM) of a synthetic chalcone (VS3) with antioxidant properties were used before and during GC-1 cells exposure to ZnO NPs in an attempt to mitigate the damage induced by NPs. The protective ability of this compound was evaluated through viability assays, intracellular detection of reactive oxygen species (ROS), DNA damage levels, and cytoskeleton protein levels (acetylated α-tubulin, β-tubulin, and β-actin). The results indicate that the tested concentrations of chalcone VS3 have the ability to attenuate the genotoxicity induced by ZnO NPs for shorter exposure periods (6 hours). VS3 supplementation also increased cell viability and stabilized microtubules. However, the antioxidant potential of this compound was inconclusive.

In conclusion, this work addressed the main cytotoxic effects of MONPs on male reproductive cells and analyzed two different strategies to mitigate this damage, which represent a significant contribution in the field of male fertility. Future studies are planned with a view to a better understanding of the antioxidant potential of synthetic chalcone (VS3) in spermatogenesis.

Index

List of figures

Chapter 1

Chapter 3

Chapter 4

List of tables

Chapter 1

Chapter 4

List of abbreviations

ACP	Acid Phosphatase
Ag_2O	Silver Oxide
AKP	Alkaline Phosphatase
Al_2O_3	Aluminium Oxide
ALT	Alanine Aminotransferase
AST	Aspartate Aminotransferase
Atg-5	Autophagy Related 5
ATP	Adenosine Triphosphate
Bax	Bcl2-associated X protein
Bcl-2	B cell lymphoma-2
BER	Base Excision Repair
BIP	Immunoglobulin-Binding Portein
BSA	Bovine Serum Albumin
BTB	Blood-testis-barrier
Ca^{2+}	Calcium ion
Casp-	Caspase
CAT	Catalase
Cdc-	Cyclin Dependent Kinase
$CdCl_2$	Cadmium Chloride
CDK2	Cyclin Dependent Kinase 2
CdS	Cadmium Sulfide
CeO	Cerium Ocide
CHOP	Transcription of CCAAT/enhancer-binding Protein (C/EBP)
CK	Creatine Kinase
CT	Computed Tomography
CuO	Copper Oxide
DCF	dichlorofluorescein
DCFH	dichlorodihydrofluorescein
DCFH-DA	2'-7'-dichlorodihydrofluorescein-diacetate
DMC1	DNA Meiotic Recombinase 1
DMEM	Dulbeccos' Modified Eagle's Medium
DMSO	Dimethylsulfoxide
DNA	Deoxyribonucleic Acid
DSBR	Double Strand Break Repair
E2	17β-estradiol
Erk1/2	Extracellular Signal-Regulated Kinase 1/2
FBS	Fetal Bovine Serum
Fe_2O_3	Iron Oxide
FRAP	Ferric Reducing Antioxidant Power
FSH	Follicle Stimulating Hormone
G6PD	Gluco-6-Phosphate Dehydrogenase
GnRH	Gonadotropin-Releasing Hormone
GPx	Glutathione Peroxidase
GSH	Reduced Glutathione
Gsk3-β	Glycogen synthase kinase 3 beta
GST	Glutathione S-transferase
H_2O_2	Hydrogen peroxide
HA	Hydroxyapatite
HR	Homologous Recombination Repair
HS	Hydrodynamic Size
ICR	Institute of Cancer Research
IL	Interleukin
IRE1α	Inositol-Requiring Protein 1α
JNK	Jun Kinase
K^+	Potassium ion

LDH	Lactate Dehydrogenase
LH	Luteinizing Hormone
LPO	Lipid Peroxidation
MDA	Malondialdehyde
Mg^{2+}	Magnesium ion
MgO	Magnesium Oxide
MMP	Mitochondrial Membrane Potential
MMR	Mismatch Repair
MnO_2	Manganese Dioxide
MONPs	Metal Oxide Nanoparticles
MRI	Magnetic Resonance Imaging
MtFA	Mitochondrial Transcription Factor A
Na^+	Sodium ion
NAC	N-acetyl-L-cysteine
NADH	Nicotinamide Adenine Dinucleotide
NHEJ	Nonhomologous End Joining Repair
NO	Nitric Oxide
NPs	Nanoparticles
NR	Nucleotide Repair
Nr5A1	Nuclear Receptor Subfamily 5 group A member 1
$O_2^{\bullet-}$	Superoxide radical
P450scc	Cytochrome P450 side-chain cleavage enzyme
P450scc	Cytochrome P450 side-chain cleavage enzyme
PA	Photoacoustic Imaging
PAGE	Polyacrylamide Gel Electrophoresis
PARP	Poly (ADP-ribose) Polymerase
PBS	Phosphate-buffered saline solution
PC	Protein Carbonyl
PDI	Polydispersity Index
PDI	Polydispersity Index
PEG	Polyethylene Glycol
PenStrep	Penicillin-Streptomycin
PET	Positron Emission Tomography
PGAM1/4	Phosphoglycerate Mutase 1
PLA	Polylactic Acid
PLGA	Poly Lactic-co-Glycolic Acid
PND	Post-Natal Days
PVA	Polyvinyl Alcohol
ROS	Reactive Oxygen Species
SA	Surface Area
SDH	Succinate dehydrogenase
SDS	Sodium Dodecyl Sulfate
SE	Seminiferous Epithelium
SEM	Scanning Electron Microscopy
SF-1	Steroidogenic Factor-1
SiO_2	Silicon Dioxide
SOD	Superoxide Dismutase
SODH	Sorbitol Dehydrogenase
ST	Seminiferous Tubules
StAR	Steroidogenic Acute Regulatory Protein
T3	Tri-iodothyronine
T4	Thyroxin
TAC	Total Antioxidant Capacity
TBARS	Thiobarbituric Acid-Reactive Substances
TBS	Tris-buffered saline
TBS-T	Tris-buffered saline-Tween
TEM	Transmission Electron Microscopy
TERT	Telomerase Reverse Transcriptase

Tesmin	Testis Expressed Metallothionein Like Protein
TESP-1	Testicular Serine Protease 1
TiO_2	Titanium Dioxide
TNF-α	Tumor Necrosis Factor Alpha
TNOS	Total Nitric Oxide Synthase
TOS	Total Oxidant Status
TSH	Thyroid Stimulating Hormone
UCP2	Uncoupling Portein 2
UV	Ultraviolet
VAP	Average Path Velocity
VCL	Curvilinear Velocity
VS3	I-3-(2,6-dichlorophenyl)-1-(2-hydroxyphenyl)prop-2-en-1-one)
VSL	Straight Line Velocity
XBP1s	X-Box-Binding protein 1 splicing
XRCC1	X-Ray Repair Cross Complementing 1
ZnO	Zinc Oxide
ZnS	Zinc Sulfide
ZO-1	Zonula Occludens-1
ZrO_2	Zirconium dioxide
γ-GT	γ-glutamyl-transpeptidase
●OH	Hydroxyl radical
17-KSR	17-Ketosteroid Reductase
17β-HSD	17β-hydroxysteroid dehydrogenase
$^1O_2$	Singlet Oxygen
3β-KSD	3β-hydroxysteroid dehydrogenase
8-OhdG	8-hydroxydeoxyguanosine

Theme framework and thesis organization

This dissertation was conducted in the scope of an interdisciplinary cooperation between CICECO-Aveiro Institute of Materials, Institute of Biomedicine iBiMED, Department of Medical Sciences and Department of Chemistry of Aveiro University.

This dissertation is organized into five chapters:

Chapter 1 consists of a published review article that includes *in vitro* and *in vivo* studies that assessed the impact of metal oxide nanoparticles (MONPs) on the male reproductive system. Briefly, it overviews the therapeutic potential of MONPs and their biomedical applications.

In the second chapter, the aims of this research are defined.

In Chapter 3, a spermatogonia cell line was used to assess the reversibility of the damage induced by a cytotoxic concentration of zinc oxide nanoparticles.

Chapter 4 proposes another strategy to reverse the adverse effects of zinc oxide nanoparticles (ZnO NPs). In this chapter, the protective potential of a synthetic chalcone (VS3) on spermatogonia cells exposed to zinc oxide nanoparticles is assessed.

In the last, the five, General conclusions and Future Perspectives are pointed out for future

Chapter 1

Metal Oxide Nanoparticles: Evidence of Adverse Effects on the Male Reproductive System

Mariana Vassal, Sandra Rebelo, Maria de Lourdes Pereira

Int. J. Mol. Sci. **2021**, *22*(15), 8061; **https://doi.org/10.3390/ijms22158061**

Abstract

Metal oxide nanoparticles (MONPs) are inorganic materials that have become a valuable tool for many industrial sectors, especially in healthcare, due to their versatility, unique intrinsic properties, and relatively inexpensive production cost. As a consequence of their wide applications, human exposure to MONPs has increased dramatically. More recently, their use has become somehow controversial. On one hand, MONPs can interact with cellular macromolecules, which makes them useful platforms for diagnostic and therapeutic interventions. On the other hand, research suggests that these MONPs can cross the blood–testis barrier and accumulate in the testis. Although it has been demonstrated that some MONPs have protective effects on male germ cells, contradictory reports suggest that these nanoparticles compromise male fertility by interfering with spermatogenesis. In fact, in vitro and in vivo studies indicate that exposure to MONPs could induce the overproduction of reactive oxygen species, resulting in oxidative stress, which is the main suggested molecular mechanism that leads to germ cells' toxicity. The latter results in subsequent damage to proteins, cell membranes, and DNA, which ultimately may lead to the impairment of the male reproductive system. The present manuscript overviews the therapeutic potential of MONPs and their biomedical applications, followed by a critical view of their potential risks in mammalian male fertility, as suggested by recent scientific literature.

Keywords: metal-oxide nanoparticles; nanotoxicity; spermatogenesis; male infertility; reproductive system; oxidative stress; biomedicine

1. Introduction

Nanotechnology is a field of science that studies the properties, design, manipulation, production, and applications of structures and devices at the nanoscale level (10^{-9} m). Objects on this scale, such as nanoparticles (NPs), have properties and functions that differ from those with a larger scale [1]. European and other International Committees have defined NPs, as particles of matter in which at least one of their phases has one dimension (length, width, or thickness) within the range of 1 to 100 nanometers (nm) [2,3].

Among the several types of NPs reported in the literature, metal oxide NPs (MONPs) stand out as the category of versatile materials. Being a type of metallic NPs that have controllable features and small size, making them able to easily cross cells and tissues within the body to reach a target location [4,5]. This makes MONPs a valuable tool for biomedical applications, such as anticancer, antidiabetic, antimicrobial purposes, as well as imaging applications, drug delivery, and even in reproductive medicine [6].

Most of these inorganic materials that make up MONPs are typically classified as biocompatible since their metallic precursors are already present in human tissues, whose vital role in body functions was reported [7,8]. Because they are essential to the body, they will be more readily

accepted by the organism [6]. Manganese (Mn), molybdenum (Mo), magnesium (Mg), iron (Fe), cobalt (Co), chromium (Cr), copper (Cu), zinc (Zn), and selenium (Se) are among some of the elements considered essential for humans [6,7]. Some of these metals are closely related to male fertility. Zinc transduces a sign that induces sperm to become motile [9,10]. Selenium deficiency was previously associated with a decline in sperm motility [11]. Copper-dependent enzymes are present at all stages of spermatogenesis, as well as in somatic cells of the testis and epididymis [12]. However, in high concentrations, these physiologically compatible metals have toxic effects on mammalian cells and can even cause cell death [13]. Depending on how many metal ions are readily available, they can be beneficial or harmful, making their use a double-edged sword [6,12,14]. This may be part of the reason why there are so many controversial reports on the reproductive toxicity of MONPs [15]. In fact, it has been proven that MONPs can cross the blood–testis barrier (BTB), a structural and physiological compartment that protects spermatogenesis [16]. This raises concerns about male fertility, especially as spermatogenesis is a highly vulnerable process that is sensitive to exogenous materials, such as NPs [17,18]. Thus, addressing the effects of MONPs on the male reproductive system is crucial.

This review summarizes in vitro and in vivo studies that describe the potential reproductive toxicity of MONPs, to clarify the accurate effects of these NPs on the male reproductive system. Gaps in knowledge and ideas for future research are highlighted.

2. Classification of Nanoparticles and MONP Synthesis

NPs are versatile nanosized structures and, therefore, can be classified according to their dimensions, morphology, materials properties, origin, and synthesis process (Figure 1) [19]. Regarding their classification, all NPs share some aspects: they are known to have reduced size, which is related to their high surface area to volume ratio, they have chemically alterable physical properties, easy surface functionalization, and they all have different physical properties in respect to the bulk material [5,20,21].

Based on morphology and dimensions, NPs are typically spherical, but they can have many other shapes, such as cylindrical, tubular, conical, hollow core, spiral, flat, or irregular in shape with variable size [22,23].

Nowadays, NPs can be produced incidentally because of human activities, as a by-product of industrial and domestic endeavors that result in the unintentional release of NPs into the environment. On the other hand, engineered NPs with new properties may be synthesized by rearranging atoms of an object. However, NPs are not entirely a product of modern technology. Some exist in the natural world and can be found everywhere on earth, that is, in the hydrosphere, atmosphere, lithosphere, and biosphere. Therefore, regarding their origin, NPs can be classified as incidental, synthetic/engineered, or natural [24]. This emphasizes the idea that nanotechnology has become even more pervasive, and that NPs are ubiquitous in the environment, becoming more deeply embedded in today’s life.

According to properties of their materials, engineered NPs can be classified as carbon-based if they are made completely of carbon (e.g.,: fullerenes, graphene, carbon nanotubes), metal-based if NPs are made purely from metal precursors (e.g.: Al, Cd, Co, Au Ag, Zn), metal oxides based if they have been synthesized to modify the properties of their respective metal based NPs (e.g.: Fe_2O_3, Al_2O_3, ZnO), ceramic NPs if they are nonmetallic solids (e.g.: HA, ZrO_2, SiO_2) and semiconductor NPs if they have properties between metals and nonmetals (e.g.: ZnS, CdS) [22]. Polymeric NPs (e.g.: PEG, PLGA, PLA) and lipid-based NPs (e.g.: liposomes, niosomes), unlike those just mentioned, are generally organic [3,19,25].

There is a broad variety of techniques that can be used to synthesize MONPs, each with its own advantages and disadvantages. Generally, they can be arranged into physical, chemical, and biological (green synthesis) methods [26]. Biologically synthesized NPs are preferred in biomedical applications since they are safer than those produced by traditional physicochemical approaches. This can be attributed to the fact that the metallic core of NPs is coated with non-toxic biomolecules, making them biocompatible [27]. Additionally, in this method, the use of dangerous substances, such as organic solvents and inorganic salts—which are commonly used in physical and chemical methods—is minimized [28].

However, unlike other methods, this green approach has the drawback of being unable to control the size, shape, and yield of NPs [29]. Essentially, no single technique is ideal in all aspects or for all applications. Therefore, the desired application should be considered to select the most appropriate method.

The exact physical and chemical properties of NPs depend on the different ways in which they are produced, namely the synthesis process, external factors (reaction temperature, concentration of reagents and type of capping agents used), and internal factors (morphology, size, concentration) during their production [30]. These parameters, in turn, will determine the interaction of NPs with biological systems [29].

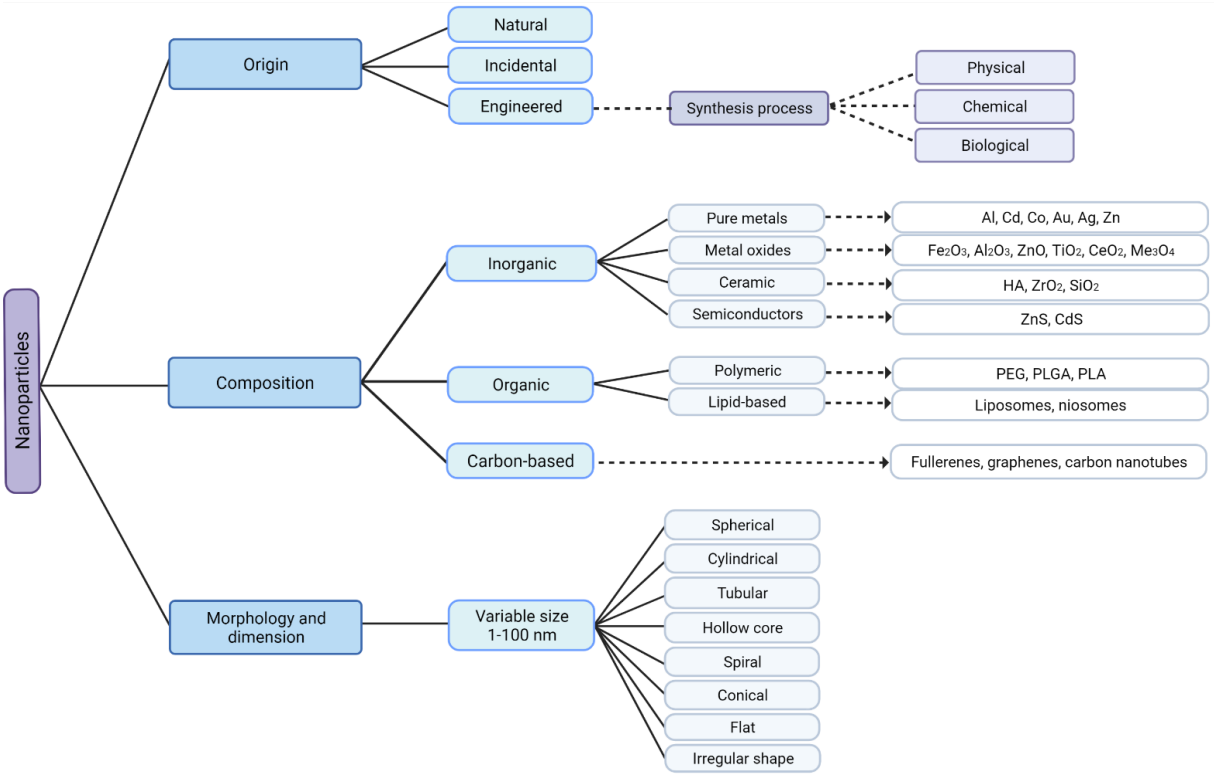

Figure 1. Classification of nanoparticles according to their origin, composition, morphology, and dimension with some examples. Metal oxide nanoparticles are engineered, inorganic nanoparticles, that can be synthesized by physical, chemical, or biological techniques, created with Biorender.com

3. Biomedical Applications of MONPs

MONPs are inorganic materials made to modify the properties of metallic elements. These have been subjected to intense biomedical research, mainly due to their unique intrinsic properties, such as good optical, electrical, catalytic, and magnetic behavior, chemical and mechanical stability, simple preparation process, easily engineered for the desired size, shape and porosity, and large surface area for reactions [4,5,31]. In addition, these materials can easily have their surface modified with several chemical functional groups, allowing their conjugation with antibodies, ligands and drugs of interest, which further enhances their potential in the biomedical field [5]. Although there is a wide spectrum of metals available, their use in the medical field is limited to those tolerated by the organism [32]. The fact that some metals exist in appreciable amounts in the body makes most MONPs biocompatible. For example, in the human body, iron (3–4 g) is mainly found associated with hemoglobin, making it the most abundant metal [33,34]. Followed by iron, zinc (~2 g) [35], and copper (~0.1 g) [36] are the second and third most common metals in the human body, and they are essential constituents of several enzymes. Unlike the previous metals, manganese is present in very small

amounts in the body (~12 mg). However, it is one of the most important nutrients for human health as it assists in the development of connective tissue, bones, blood-clotting factors, and sex hormones [33].

The use of MONPs to treat cancer, diabetes, and even to eradicate infectious diseases has been extensively studied, which proves the effort that has been made to create a symbiosis between nanoscience and medical science [31,37].

The common biomedical applications of MONPs and their main mechanisms of action are summarized in Figure 2.

Figure 2. Summary of the biomedical applications of MONPs. The latter were divided into six categories, namely antimicrobial activity, anticancer activity, antidiabetic activity, drug delivery, imaging, and reproductive medicine, created with Biorender.com

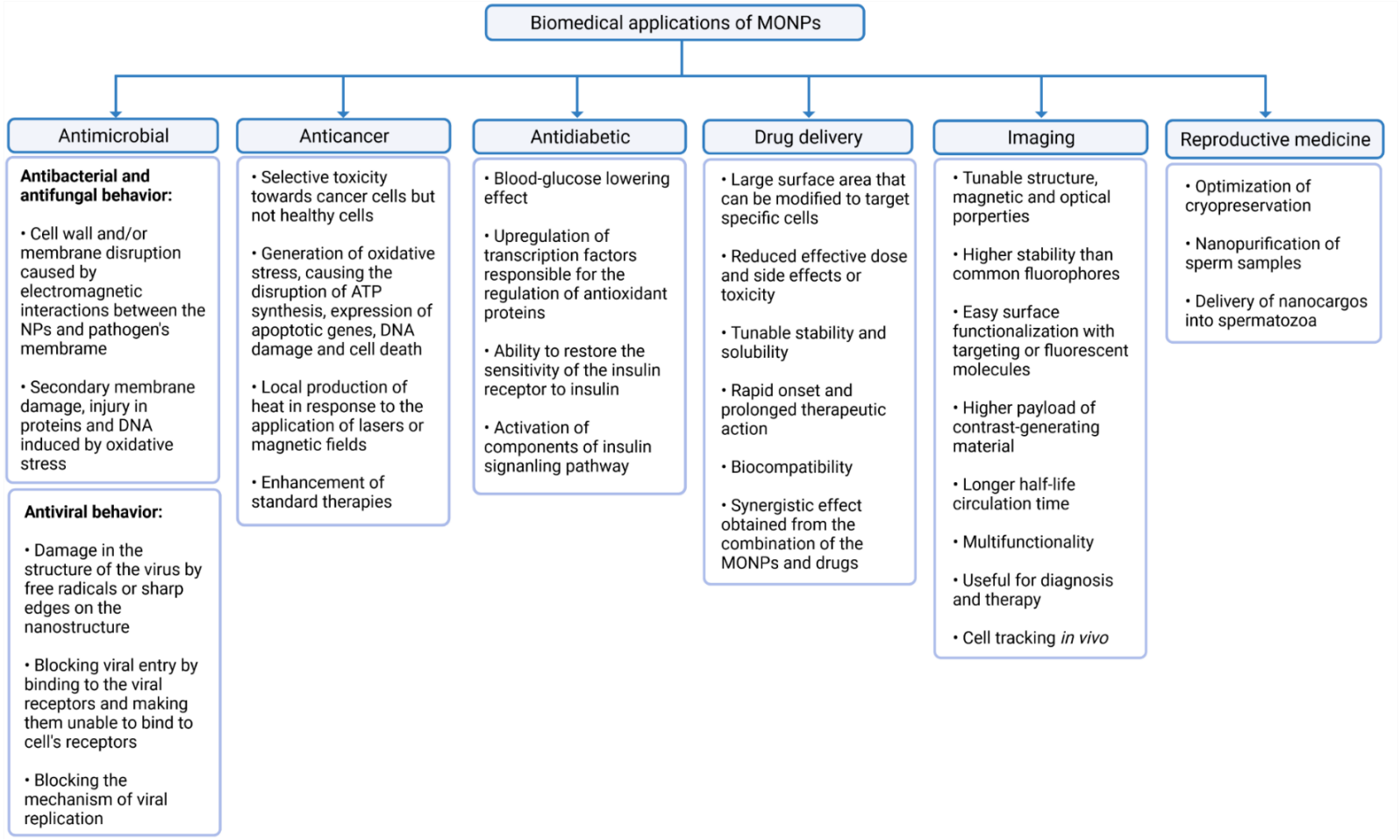

3.1. Antimicrobial, Anticancer, and Antidiabetic Activity

Although in excessive doses many metals are toxic to all cell types, in lower concentrations, MONPs may be able to selectively target bacteria, since their metal transport system and metalloproteins are different from those existing in mammalian eukaryotic cells [38,39]. To exert this microbial function, MONPs need to be in contact with microbial cells. This interaction increases microbes' membrane permeability, and allows the entry of NPs into the cytoplasm [38,40], where NPs induce damage to cellular macromolecules (Figure 2) [41]. This antimicrobial activity is enhanced for higher concentrations and smaller MONPs sizes [42,43], since smaller sizes allow a closer contact between NPs and the microbial membrane [4].

A wide range of MONPs seem to have antimicrobial abilities, including titanium dioxide (TiO_2) [44], magnesium oxide (MgO) [45], zinc oxide (ZnO) [46], copper oxide (CuO) [47], iron oxide (Fe_3O_4) [48], cerium oxide (CeO) [49], and silver oxide (Ag_2O) [50]. The molecular mechanisms of the antifungal activity of MONPs have been less studied because most studies have focused on antibacterial activity. Nonetheless, recent research suggests that these MONPs have similar mechanisms for bacteria and fungi [51].

Besides presenting antibacterial and antifungal activities, some MONPs also exert antiviral properties (Figure 2). MONPs can adhere to the virus envelope, causing its destruction [52], or they can block their mechanism of viral replication [53] or viral entry into a cell [54]. Metal oxides, such as TiO_2 [52] and Cu_2O [55], have already been shown to be effective antiviral agents against influenza A virus subtype H3N2 and Hepatitis C, respectively. These findings open a new perspective to prevent and treat viral diseases using MONPs.

MONPs can also selectively target cancer cells [56] and exert their anticancer activity mainly through the generation of oxidative stress [57]. This property can be further enhanced with the application of external stimuli such as magnetic fields or lasers, which induce the local production of heat in tumor sites [58]. Additionally, these NPs can also be used as enhancers of standard therapies, acting as co-adjuvants to improve the effect of radiation on radiotherapy, or to facilitate the action of conventional anticancer drugs, reducing the required dose and side effects of such drugs [59]. Therefore, different strategies take advantage of MONPs in the treatment of cancer: alone, conjugated with biological molecules, ligands, and anticancer drugs, or in combination with other conventional therapies to potentiate their therapeutic efficacy [60].

In addition, other MONPs such as MgO, MnO [61], CeO_2 [62], ZnO [63,64], and Fe_2O_3 [65] have been explored as possible antidiabetic agents, since recent studies have shown promising results. Essentially, the antioxidant ability of MONPs contributes to a decrease in oxidative stress, which is the main cause of β-cell damage [66]. However, concentration determines whether NPs elicit oxidative stress or increase the cell antioxidant capacity. Generally, small doses seem to be related to the antidiabetic potential [14,65].

3.2. Drug Delivery Platforms and Imaging

Medical imaging is essential for medical diagnosis. MONPs have been used as nanoparticle-based contrast agents in multiple modern imaging modalities that allow the visualization of abnormalities, such as tumor lesions or other regions of interest [67]. Of all the plethora of available NPs, metal oxides have advantages in imaging applications due to their diverse size- and shape-dependent optoelectronic properties [27,68] and high stability, which are not achievable with traditional lipid or polymer-based nanoparticles [69]. In addition, compared to molecular probes, MONPs are virtually inert, which means that they hardly interact with other cellular molecules and, therefore, their optical properties remain unaffected [70]. Their surface can also be easily functionalized with drugs, targeting or fluorescent molecules, or other components [71,72]. Therefore, these contrast agents can deliver therapeutic agents simultaneously, allowing for a dual diagnostic and therapeutic effect [73].

Considering all this, MONPs are attractive imaging agents. As a result, they have been exploited for different imaging modalities, such as magnetic resonance imaging (MRI) [74], photoacoustic imaging (PA) [75], positron emission tomography (PET) [76], computed tomography (CT) [77], fluorescent imaging [78], among many others. In addition, NPs can be multifunctional and, therefore, can provide contrast for more than one imaging modality [23].

3.3. An Asset for Reproductive Medicine

Although the detrimental effects of NPs on male fertility and sperm cell function have been suggested [16], some research teams have been exploring the properties of these materials to improve assisted reproductive techniques. Falchi et al. reported that the incubation of ram semen with CeO_2 NPs during cryopreservation improved sperm quantity and quality [79]. This study suggests that CeO_2 NPs can have beneficial effects on sperm preservation. Other research teams have functionalized Fe_2O_3 NPs with lectins and antibodies, to selectively bind to glycans expressed in acrosome reaction, or to ubiquitin, which is present on the surface of defective spermatozoa [79,80]. Then, aberrant spermatozoa can be removed from a sample using a magnetic force. This method of sperm purification may be used to increase conception rates following artificial insemination [80]. Nanoplatforms for the delivery of biological compounds to spermatozoa are another nanotechnology that has been investigated in the field of reproductive medicine [15].

Makhluf et al. described the spontaneous penetration of polyvinyl alcohol (PVA)-Fe3O4 NPs in bovine sperm, without affecting their motility and ability to undergo the acrosome reaction [81]. These interesting results suggest that, in the future, NPs may be conjugated with target nutrients or treatments for direct nutrient supplementation to sperm.

These and other research teams have presented interesting results that highlight the usefulness of MONPs. However, despite these promising results, uncertainty remains about the safety of MONPs. Therefore, it is crucial to investigate in more detail how MONPs interact with the male reproductive system and the consequences of this exposure.

4. The Impact of MONPs on Male Fertility

MONPs have received a lot of attention, especially in the biomedical field, due to their biological usefulness, as discussed in previous sections. In addition, due to their unique properties and versatility, the application of NPs extends to many other fields, making them ubiquitous in the environment. Consequently, human exposure to nanomaterials has increased dramatically. However, in recent years, the use of NPs of any material has become controversial [82]. On one hand, MONPs can interact with cellular macromolecules, leading to therapeutic effects [83]. On the other hand, cytotoxic effects were found in some tissues, presenting a health hazard [84].

Many studies suggest that human male infertility has increased significantly over the past few decades [85–87]. Due to this alarming trend, it has been hypothesized that environmental, dietary, and/or lifestyle changes are interfering with men's ability to produce spermatozoa with a consequent impact on male fertility [88,89]. In addition, the male reproductive system is known to be susceptible to environmental stress, as toxicants, vehicular pollutants, and even NPs [90]. As a result, the impact of MONPs on male reproductive health has become an important subject of study. While several reports suggest that some NPs might have protective effects on sperm cells [91], other reports suggest that they compromise male fertility by interfering with spermatogenesis [92]. In fact, spermatogenesis is prone to errors. Defects in any of its steps can result in the failure of the entire process and, in some cases, can lead to testicular diseases or male infertility [93,94].

Since spermatogenesis is a highly vulnerable process, it occurs in a protected environment, controlled by the BTB, whose purpose is to protect the developing germ cells from external insults [17]. It is formed by tight junctions between Sertoli cells that divide the epithelium of ST into two different compartments: basal and adluminal (Figure 3). Although it is one of the tightest blood–tissue barriers in the mammalian body [95], it was previously reported that NPs could cross this biological barrier due to their ultra-small size [16]. In fact, in mice treated with TiO_2 [96] and Fe_2O_3 [97], both NPs were able to penetrate the testis, despite the BTB. Takeda et al. even reported that TiO_2 NPs accumulated in the testis of male offspring from pregnant mice who were treated with these NPs [98]. Other animal studies have also demonstrated that NPs can move from the initial absorption site, for example, the lungs and skin, to secondary organs, such as the testis [99]. The integrity of BTB is a concern since NPs can easily permeate cells and their nuclei. This creates favorable circumstances for mutations appearance, which in germ cells may interfere with fertilization, embryogenesis [100], or even generate congenital defects in the offspring [101].

Therefore, a clear understanding of the impact of MONPs on reproductive health is fundamental. Tables 1 and 2 summarize the adverse effects of different MONPs on the male reproductive system, both in vitro and in vivo. However, it is important to keep in mind that these effects depend on several factors, such as dosage, duration of exposure, administration route, chemical nature of the compound (e.g., method of synthesis, size, shape, surface charge), as well as the biological system involved (e.g., strain and age of animal/cell, cell variability) [15].

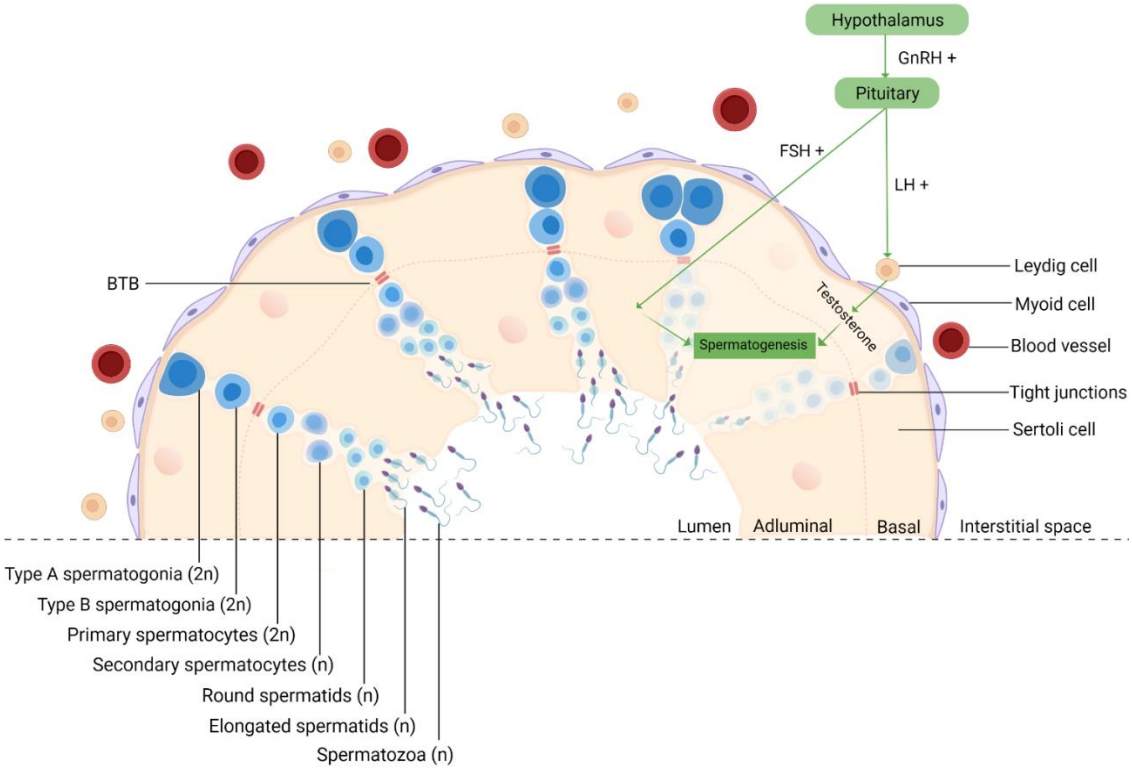

Figure 3. Schematic representation of spermatogenesis in the cross-section of a seminiferous tubule. Spermatogenesis is initiated at puberty by the hypothalamus, which produces GnRH, which, in turn, stimulates the release of FSH and LH at the reproductive tract. LH stimulates Leydig cells to produce testosterone and FSH stimulates Sertoli cells that provide support and nutrition for sperm survival, proliferation, and differentiation [102]. Sertoli cells then initiate the functional responses required for spermatogenesis. Spermatogenesis starts when type A spermatogonia (2n) commit to differentiating into type B spermatogonia. Then, through mitosis, B-spermatogonia (2n) give rise to primary spermatocytes (2n). The latter undergo a long meiotic phase that originates the secondary spermatocytes (n), which ends with spermatids (n) generation [103]. The round spermatids then go through substantial morphological changes during spermiogenesis originating highly specialized spermatozoa through the reorganization of the entire cell, where the nuclear envelope seems to be crucially involved [104,105]. The next event is spermiation, in which mature spermatids are released from the supporting Sertoli cells into the lumen of the seminiferous tubule, and the remainder of the spermatid cytoplasm, known as the residual body, is phagocytosed by the Sertoli cells [106]. However, at this stage, spermatozoa still lack motility. Immotile spermatozoa are then transported into the epididymis where the final steps of maturation occur [107]. GnRH, gonadotropin-releasing hormone; LH, luteinizing hormone; FSH, follicle-stimulating hormone; BTB, blood–testis-barrier; 2n, diploid cell; n, haploid cell, created with Biorender.com

4.1. *In Vitro* Studies

Few studies have focused on the adverse effects of NPs on male germ cells in vitro (Table 1).

The summary studies provide valuable information on the outcome of the interaction between MONPs and germ cells, which is useful for establishing the mechanisms of MONP toxicity. Parameters such as cell viability, oxidative stress, DNA damage, nanoparticle internalization, and mechanisms of cell death were assessed.

Table 1. *In vitro* studies of adverse effects of MONPs on mammalian male germ cells. The conditions where the main findings were observed are indicated in brackets.

MONPs	Characteristics	Concentration and Exposure Time	Cell Type	Parameters	Main Findings	Reference
Cerium oxide	**Formula:** CeO_2 **Size:** ~7 nm **SA:** 400 m^2/g **Shape:** Ellipsoidal crystallites	0.01, 0.1, 1, 10 µg/mL 1 h	Spermatozoa (Human)	- Sperm vitality; - DNA damage; - Uptake of NPs	- Sperm viability higher than the normality threshold—58% - Increased DNA damage (≥0.01 µg/mL); - Accumulation of NPs at the plasma membrane, particularly along the flagellum, without internalization	[108]
Iron oxide	**Formula:** Fe_3O_4 **Size:** 40 nm **Shape:** spherical	0.192 mg/mL 30, 45, and 60 min	Spermatozoa (Boar)	- Motility and kinetics	- No effects on sperm motility	[109]
Manganese oxide	**Formula:** Mn_3O_4 **Size:** ~ 20 ± 4.1 nm **Shape:** irregular sphere-like morphology	0, 5, 10, 20 µg/mL 6 and 24 h	Sertoli Cells (Rats)	- ROS production; - MMP and apoptosis;	- Increase in ROS (5 µg/mL, 24 h); - Alterations in the mitochondrial membrane integrity and increase in the apoptotic rates (≥5 µg/mL, 24 h)	[110]
Titanium oxide	**Formula:** TiO_2 **Size:** ~30–90 nm **Zeta potential:** −27.3 Mv	1, 10, 100 µg/mL 0, 3, 6 h	Spermatozoa (Bufallo)	- Viability; - Acrosomal and plasma membrane integrity; - Capacitation; - Acrosome-reaction; - DNA fragmentation; - Uptake of NPs	- Viability decrease (100 µg/mL, 3 and 6 h); - Decrease in the integrity of the plasma membrane (≥1 µg/mL, 6 h) and acrosomal membrane (100 µg/mL, 6 h); - Increase in capacitation (≥10 µg/mL, 6 h); - Increase in acrosomal reaction (≥1 µg/mL, 3 and 6 h); - Increased DNA fragmentation (≥10 µg/mL, 6 h); - Uptake of NPs mainly in the plasma membrane and sperms' head	[111]
	Formula: TiO_2 **Size:** ~21 nm **Shape:** spherical **Zeta potential:** −124.55 ± 13.20 Mv **HS:** 115.2 ± 11.3 nm **Purity:** >99.5% **PDI:** 0.19	0.1, 1, 10, 100 µg/mL 24 h	Spermatocytes and Sertoli cells (Mouse)	- Viability; - Apoptosis; - Uptake of NPs - Cytoskeleton; - Migration ability; - Phagocytic activity	- Cell viability was not affected; - Increase in the early apoptosis ratio for both cells and in the late apoptosis ratio for Sertoli cells (100 µg/mL); - Dose-dependent uptake of the nanoparticles, mainly in the cytoplasm; - Disordered microtubules (spermatocytes) and microfilaments (Sertoli cells); - Decreased migration ability of spermatocytes (100 µg/mL); - Weakened phagocytic capacity of Sertoli cells (100 µg/mL)	[112]
	Formula: TiO_2 **Size:** ~21 nm **Shape:** partly irregular and semispherical	1, 10 µg/L 15, 30, 45, 90 min	Spermatozoa (Human)	- Viability; - Motility characteristics; - DNA damage;	- Cell viability was not affected; - Increase in progressive and nonprogressive sperm (1, 10 µg/L for ≥ 45 min); - Increase in DNA damage (1, 10 µg/L for ≥ 30 min);	[113]

				- ROS production	- Increase in ROS production (1, 10 µg/L for ≥ 15 min)	
Zinc oxide	**Formula:** ZnO **Size:** ~50 nm **Shape:** amorphous	10, 100, 500, 1000 µg/mL 45, 90, and 180 min	Spermatozoa (Human)	- Viability	- Increase in cell death (≥100 µg/mL, 180 min and ≥ 500 µg/mL, ≥ 45 min)	[114]
	Formula: ZnO **Size:** ~70 nm **Shape:** spherical **Dispersion:** polydisperse **Surface roughness:** high (22.9 nm)	0, 5, 10, 15, 20 µg/mL 3, 6, 12, and 24 h	Leydig and Sertoli cells (Mouse)	- Viability; - ROS production; - Uptake of NPs; - MMP and apoptosis; - DNA damage	- Decreased viability in both cell types (≥15 µg/mL, ≥6 h); - Increase in ROS production (≥10 µg/mL, ≥6 h) - Accumulation and uptake of nanoparticles' aggregates in the cytoplasm and nucleus; - Loss of MMP and apoptosis increase (≥15 µg/mL, 6–12 h); - DNA leakage with an increase in chromosome breaks or loss (≥15 µg/mL, ≥12 h)	[115]
	Formula: ZnO **Size:** 177 nm **Shape:** spheroid or ellipsoid **Zeta potential:** −27.4 ± 1.0 Mv **Purity:** >97%	0, 0.04, 0.08, 0.4, 0.8, 4, 8, 16 µg/mL 24 h	Spermatocytes and Sertoli cells (Mouse)	- Viability; - Oxidative stress indexes (ROS, GSH, MDA) of both cell types; - Membrane permeability, MMP and cytochrome c of Sertoli cells; - TNF-α and Erk1/2 levels of Sertoli cells; - Connexin-43, occludin, claudin-5, ZO-1 expression of Sertoli cells; - DNA damage of spermatocytes; - Cell cycle analysis (cyclin E2, cyclin A2, CDK2) of spermatocytes	- Decrease in cell viability (≥8 µg/mL); - Increase in ROS and MDA levels and decrease in GSH (8 µg/mL); - Increase in membrane permeability with decrease in MMP (8 µg/Ml), but no significant changes in cytochrome c (8 µg/mL); - Increase in TNF-α and phosphorylation of Erk1/2 (8 µg/mL); - Decrease in claudin-5, occludin, ZO-1 and connexin-43 expression (8 µg/mL); - Increase in p-Chk1, p-Chk2 and Y-H2AX expression but decrease in APE1 (8 µg/mL) but DNA damage can be partly rescued by antioxidants; - Increase in cyclin E2, cyclin A2, CDK2 expression with an increase of cell numbers in the S phase (8 µg/mL)	[116]
	Formula: ZnO **Size:** 20–40 nm **Shape:** spherical **HS:** 75 nm	0–200 µg/mL 1, 4, and 12 h	Leydig cells (Mouse)	- Viability; - Cell morphology; - Uptake of NPs; - Apoptosis; - Oxidative stress indexes (SOD, CAT);	- Decrease in cell viability (≥2 µg/mL, ≥1 h); - Loss of normal morphology (≥5 µg/mL, 4 h); - Randomly dispersed agglomerates of NPs in the cytoplasm, autophagosomes, autolysosomes, mitochondria and in nuclear membranes (50 µg/mL, 4 h); - Apoptosis increase (5 or 20 µg/mL, 4 h);	[117]

			- Steroidogenesis-related genes expression (StAR, P450scc); - Antioxidant enzyme related gene (SOD); - Testosterone levels in cells' supernatant	- Increase in SOD (1, 5 µg/mL, 4 h and 5, 20, 50 µg/mL, 12 h), CAT (1, 5, 20 µg/mL, 4 h and 5, 20 µg/mL, 12 h) activity; - Increase in StAR (1, 5 µg/mL, 4 h and 1 µg/mL, 12 h) and P450scc expression (1, 5 µg/mL, 4 h); - Decrease in SOD Mrna (1, 5 µg/mL, 4 h); - Increase in testosterone production (2 µg/mL, 12 h)	
	Formula: ZnO **Size:** 30 nm **Zeta potential:** 38.25 ± 1.06 Mv **HS:** 66.36 ± 0.93 nm	0, 2, 3, 4, 8 µg/mL 24 h	Leydig cells (Mouse)	- Viability; - Oxidative stress indexes (GPx, GSH, SOD, MDA); - Apoptosis-related proteins (cleaved Casp-8 and Casp-3, Bcl-2, Bax); - Autophagy-related proteins (Atg-5, Beclin-1) and LC3-II/LC3-I ratio	- Decrease in cell viability (≥3 µg/mL); - Increase in MDA levels (≥3 µg/mL) and decrease in SOD, GSH (≥3 µg/mL) and GPx (≥2 µg/mL) levels; - Increase in the expression of cleaved Casp-8, Casp-3 and Bax and decrease in Bcl-2 expression; - Increase in LC3-II to LC3-I ratio and Atg-5 and Beclin-1 expression (4 µg/mL)	[118]
	Formula: ZnO **Size:** 88 nm **SA:** 12 m^2/g **Shape:** spherical **Crystal structure:** hexagonal wurtzite **Zeta potential:** −15 Mv (Ph = 6) and −55 Mv (Ph = 12)	1, 5, 8, 10, 20 µg/mL 6 and 12 h	Spermatogonia(Mouse)	- Viability; - Apoptosis and necrosis; - ROS production; - DNA damage; - Cytoskeleton dynamics; - Nucleoskeleton dynamics; - Nuclei morphological changes	- Decrease in cell viability (20 µg/mL, 12 h); - Cell death by necrosis (20 µg/mL, 12 h); - Increase in ROS levels (20 µg/mL, 6 h and ≥5 µg/mL, 12 h); - Increase in DNA damage (20 µg/mL, ≥6 h); - Interference with microtubule and microfilament protein levels (20 µg/mL for 6 h and 12 h); - Alterations of the basal levels and distribution of the nuclear lamina and nuclear envelope proteins (20 µg/mL, 12 h); - Visible morphological deformities in the cells' nuclei.	[92]

Abbreviations: Atg-5, Autophagy Related 5; Bax, Bcl2-associated X protein; Bcl-2, B cell lymphoma-2; Casp-, Caspase; CAT, Catalase; CDK2, Cyclin Dependent Kinase 2; DNA, Deoxyribonucleic Acid; Erk1/2, Extracellular Signal-Regulated Kinase 1/2; GPx, Glutathione Peroxidase; GSH, Reduced Glutathione; HS, Hydrodynamic Size; MDA, Malondialdehyde; MMP, Mitochondrial Membrane Potential; PDI, Polydispersity Index; P450scc, Cytochrome P450 side-chain cleavage enzyme; ROS, Reactive Oxygen Species; SA, Surface Area; SOD, Superoxide Dismutase; StAR, Steroidogenic Acute Regulatory Protein; TNF-α, Tumor Necrosis Factor Alpha; ZO-1, Zonula Occludens-1.

The *in vitro* studies reported in Table 1 were carried out with NPs made from Cerium (Ce), Iron (Fe), Manganese (Mn), Titanium (Ti), and Zinc (Zn) oxides. However, TiO_2 and ZnO NPs are, by far, the most explored NPs.

The studies listed were conducted in different reproductive cells at three stages of maturation: spermatogonia, spermatocyte, and spermatozoa. Additionally, the cells responsible for testicular architecture and function, namely Sertoli and Leydig cells, were also used in the listed studies. In addition, most studies have carried out the extensive chemical and physical characterization of NPs, which is crucial for a better understanding of the toxicity mechanisms of NPs on reproductive cells.

A wide range of concentrations of MONPs has been studied, from very low (0.04 µg/mL) to high concentrations (1000 µg/mL). It is crucial to evaluate different concentrations of MONPs to establish their cytotoxic effect. However, the results still were conflicting. Préaubert et al. reported that the lowest concentrations of CeO_2 NPs (0.01 µg/mL) were associated with higher levels of DNA damage in human spermatozoa [108]. ZnO NPs were also highly cytotoxic to mouse Leydig cells, even at low concentrations and incubation times [117]. Those are the exceptions since most studies indicate that MONP cytotoxicity is dose and time-dependent. Other authors even reported that lower MONPs concentrations were inefficient to cause genotoxicity [92,111].

The periods of incubation were also variable, ranging from 15 min to 24 h. From the results summarized in Table 1, it can be deduced that the reproductive toxicity of MONPs depends mainly on the concentration used and on the time of incubation.

The size of the NPs used ranges from ultrafine particles (7 nm) to much larger NPs (177 nm). Previous studies reported that even a small difference in size can make particles up to six times more harmful [119]. Gromadzka-ostrowska et al. also found that the toxicity of NPs is not only dependent on dose and time, but also depends on size, which seems to be inversely proportional to the cytotoxicity of NPs [120]. However, none of the studies reported in Table 1 evaluated the effect of the size of NPs on male germ cells.

The most studied parameters were oxidative stress indexes, cell viability, apoptosis, and genotoxicity. The principal suggested mechanism by which MONPs may exert that their toxic and genotoxic effect is oxidative stress [113,117]. In fact, increased oxidative stress was observed in almost all studies where this parameter was tested, except one [117]. Bara and Kaul reported an increase in the levels of antioxidant enzymes SOD and CAT in Leydig cells after exposure to ZnO NPs [117]. However, it has also been reported by other studies that NPs initially induce antioxidant enzyme activities in response to stress, as a defense mechanism, but, eventually, ROS production overcomes the capacity of the antioxidant response mechanisms [121].

Both exogenous stimuli and endogenous physiological stress can induce ROS production [117]. Oxidative stress is known to induce DNA damage through the oxidation of DNA bases [108] (Figure 4). However, it can also induce injury to biomolecules and organelles in other cells, mainly mitochondria [117]. In addition, under stress conditions, cells activate different cellular processes important for cell adaption to adverse conditions or to activate cell mechanisms of cell death, such as apoptosis or necrosis [117]. Pinho et al. reported an increase in the number of spermatogonia in

necrosis (but not apoptosis) after ZnO NP exposure [92], while other studies have reported apoptosis as the preferred mechanism of cell death [110,117,118]. Autophagy is an example of an adaptive mechanism under stress conditions, and it was reported in Leydig cells after ZnO NPs exposure [118].

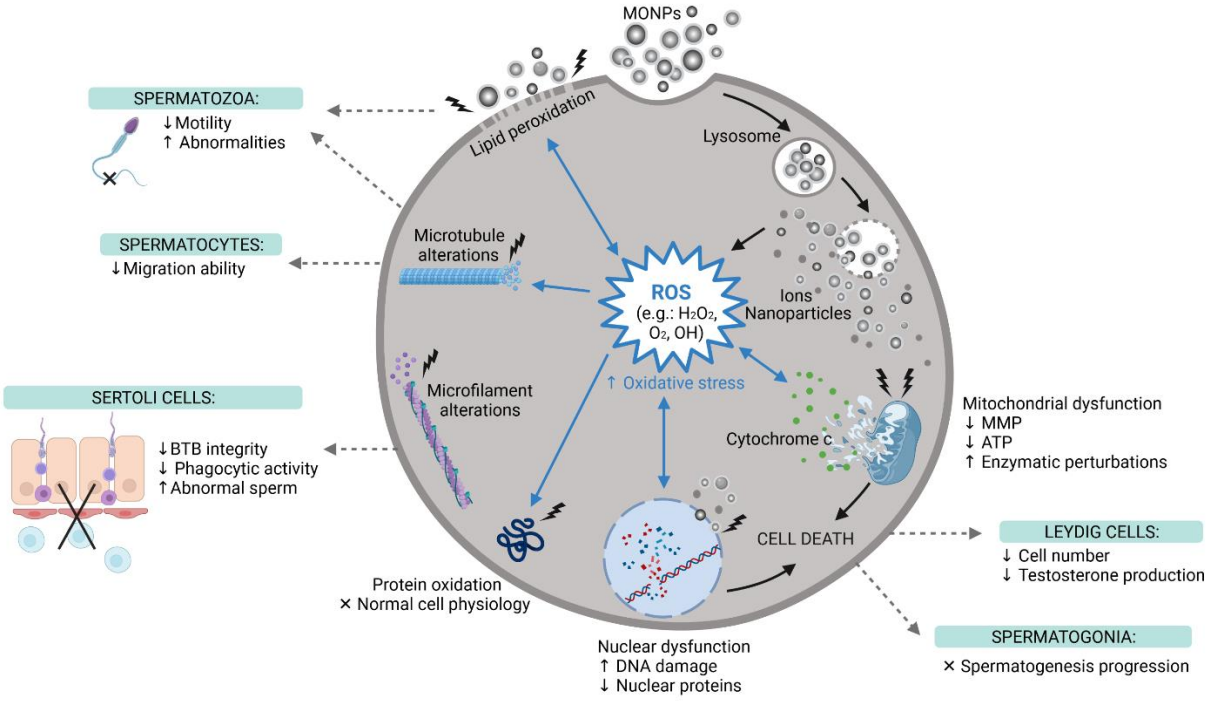

Figure 4. The main reproductive toxic events induced by MONPs at the cellular level. MONPs, Metal Oxide Nanoparticles; ROS, Reactive Oxygen Species; MMP, Mitochondria Membrane Potential; ATP, Adenosine Triphosphate; BTB, Blood-Testis-Barrier; ↑, increase; ↓, decrease; x, impaired. Created with Biorender.com

The mechanism of MONPs internalization by cells was explored in some studies. Pawar and Kaul , using Scanning Electron Microscopy (SEM) and Transmission Electron Microscopy (TEM) images, reported that TiO_2 in both agglomerated and single forms can remain attached to the spermatozoon surface (head and tail) after the addition of NPs to the sperm suspension, even after washing [111]. This indicates that NPs can attach and remain intact on the cell membrane immediately after mixing the NPs with the cell suspension. When in direct contact with cells, NPs cause mechanical damage to the membrane and destabilization of the plasma membrane, allowing NP entrance. The latter will exert pro-oxidant effects. In fact, Mao et al. monitored the internalization of TiO_2 NPs by spermatocytes and Sertoli cells, both by flow cytometry and by TEM [112]. Bara and Kaul TEM results also revealed that ZnO NPs can enter Leydig cells and cross their nuclear membranes [117]. Moreover, Préaubert et al. also found an accumulation of CeO_2 NPs at the spermatozoon plasma membrane [108]. However, in this case, the NPs were not internalized by the cells, but genotoxicity was still present. These authors proposed that MONPs do not need to be

internalized to induce cell damage. To date, the exact mechanism by which the NPs induce cell damage is far to be elucidated, and, therefore, more comprehensive studies are needed.

Changes in the cytoskeleton were assessed only by Mao et al. and Pinho et al. , using TiO_2 NPs and ZnO NPs, respectively [92,112]. The latter reported disturbances in both microtubules and microfilament networks in spermatogonia cells [92]. Mao et al. also studied the effect of TiO_2 NPs on the cytoskeleton of two different germ cells, spermatocytes, and Sertoli cells. TiO_2 NPs interfered with microtubules of spermatocytes, but Sertoli cells only had their microfilaments altered [112]. These studies indicate that different germ cells respond differently to MONP insults. Additional studies should investigate alterations in the cytoskeleton since changes in the microtubule dynamics affect the formation of sperm flagella and migration abilities, and changes in the microfilament dynamics can affect the formation of tight junctions of Sertoli cells, which altogether interfere with spermatogenesis [112]. Although Liu et al. did not study cytoskeleton dynamics, their results indicate downregulation of tight junction proteins in Sertoli cells, leading to BTB impairment [116]. In addition, the disturbed microfilament arrangement interferes with the phagocytic capacity of Sertoli cells, which makes cells unable to properly phagocytose abnormal sperm cells [112].

Besides studying the cytoskeleton, Pinho et al. also reported, for the first time, the impact of ZnO NP exposure in the nucleoskeleton [92]. These authors reported several nuclear alterations in spermatogonia that may affect the progression of spermatogenesis.

Bara and Kaul was the only in vitro study to investigate the effect of NPs on steroidogenesis and testosterone biosynthesis in male reproductive cells. Interestingly, they found that a low concentration treatment with ZnO NPs for short incubation periods enhanced the steroidogenic ability of Leydig cells [117]. However, the exact mechanism is still unclear and therefore should be explored in future studies.

Overall, the interesting data collected indicate that the reproductive toxicity of NPs is not simply a matter of the NP material type, size, concentration, and exposure time, but also the result of intricate interactions at the nano-bio interface, which is influenced by many factors [13].

Since in vitro studies cannot consider tissue distribution, organs accumulation, clearance, or diffusion across biological barriers, such as the BTB, *in vivo* studies must be considered [122] and are of paramount importance to understand NP cytotoxicity.

4.2. *In Vivo* Studies

Table 2 lists the biochemical, molecular, and histopathological evidence of reproductive toxicity of MONPs. All MONPs that have been used in previous in vitro studies were also applied in in vivo studies. Considering the aluminum oxide (Al_2O_3) NPs, they have not been evaluated under cell culture conditions, only *in vivo*.

Table 2. *In vivo* studies of adverse effects of MONPs on the mammalian male reproductive system. The conditions where the main findings were observed are indicated in brackets.

MONPs	Characteristics	Dosage and Exposure Duration	Route of Administration	Animal Model/Tissue/Organ/ Fluid	Parameters	Main Findings	Reference
Aluminum oxide	**Formula:** Al_2O_3 **Size:** 50 nm	70 mg/kg/day 75 days	Oral	Wistar Rats Testis Prostate Epididymis Sperm Plasma	- Reproductive organs weight; - mtTFA, UCP2 testis levels; - DNA fragmentation ; - p53, TNF-α, IL-6 testis levels ; - Oxidative stress indexes (GPx, GST, CAT, SOD, GSH, TAC, TBARS, NO); - Steroidogenic enzymes levels (17-KSR, 17β-HSD); - Sperm quality; - Reproductive and thyroid hormones levels (testosterone, FSH, LH, TSH, T3, T4); - Testis histopathology	- Decline in testis and epididymis weight but increase in prostate weight; - Suppression and increase of MtTFA and UCP2 expression, respectively; - Massive DNA fragmentation; - Increase in p53, TNF-α and IL-6 levels; - Decrease in GPx, GST, CAT, SOD, GSH, TAC levels and increase in TBARS and NO levels; - Increase and decrease in 17β-HSD and 17-KSR levels, respectively; - Reduction in sperm quality; - Decrease in testosterone and TSH levels, increase in FSH, LH, T3 and T4 levels; - Degenerative changes in testis	[123]
Cerium oxide	**Formula:** CeO_2 **Size:** <25 nm **Purity:** >99%	10, 20, 40 mg/kg/day 32 days	Oral	C57BL/6J Mice Testis Epididymis Epididymis Sperm Plasma	- Ce accumulation; - Testis weight; - Sperm quality; - Testis histopathology; - Testicular marker enzymes levels (ACP, G6PD, γ-GT, SDH); - Testosterone and transcription factors genes expression (StAR, P450scc, P450c17, 3β-HSD, 17β-HSD, SF-1)	- Increase of Ce content in testis and in denatured sperm DNA (≥20 mg/kg); - Decrease in testis weight (40 mg/kg); - Reduction in sperm quality (≥20 mg/kg); - Seminiferous tubules damage and apoptosis in interstitial tissue (≥20 mg/kg); - Decreased activities of G6PD, SDH, γ-GT (≥20 mg/kg) and ACP (40 mg/kg); - Decrease in testosterone levels and expression of SF-1, StAR, P450scc, P450c17, 3β-HSD (≥20 mg/kg)	[124]
Iron oxides	**Formula:** Fe_2O_3 **Size:** 20 ± 5 nm	5, 10, 20, 40 mg/kg 2 weeks	Intraperitoneal	Mice Testis Epididymis Epididymis Sperm	- Sperm quality; - Testis histopathology	- Reduction in sperm quality (≥5 mg/kg); - Reduction of spermatids and spermatocytes in ST and detachment	[125]

					of spermatogonia and spermatocytes from ST wall	
	Formula: Fe_2O_3 **Size:** <50 nm	25, 50 mg/kg/week 4 weeks	Intraperitoneal	Albino Mice Testis Epididymis Serum	- Total protein in the testis; - Sperm quality; - Testis and serum LDH and testosterone levels; - Testis histopathology; - Fe accumulation; - Oxidative stress indexes (ROS, MDA, SOD, NO, LPO, PC, CAT, GPx, GSH, vitamin C); - DNA damage and apoptosis (Bax, cleaved-Casp3 and -PARP)	- Decrease in total protein in the testis (≥25 mg/kg); - Reduction in sperm quality (≥25 mg/kg); - Increase in testosterone and LDH levels (≥25 mg/kg); - Detachment, sloughing and vacuolization of ST (≥25 mg/kg); - Increased Fe levels in the testis and in serum (≥25 mg/kg); - Increase in ROS, LPO, PC, SOD, NO, CAT, GPx (≥25 mg/kg), decrease in CAT, GSH (50 mg/kg) and vitamin C (≥25 mg/kg) levels; - Increase in the expression of Bax, cleaved-PARP and -Casp3, confirming DNA damage and apoptosis	[97]
	Formula: Fe_3O_4 **Size:** 20–30 nm	50, 150, 300 mg/kg/day 4 days	Intraperitoneal	NMRI Mice Epididymis Testis Semen	- Sperm quality; - Testis cell number (spermatogonia, primary spermatocytes, spermatids, Sertoli and Leydig cells); - ST morphometry; - Volume of testis and interstitial tissue	- No significant changes in sperm number, decrease in VCL, VSL, VAP and rapid progressive motility values and increase in the percentage of immotile sperm (300 mg/kg/day); - Reductions in the total number of testicular cells; - Reduction in ST length, volume of the testis and interstitial tissue (300 mg/kg/day)	[126]
	Formula: Fe_3O_4 **Size:** <50 nm	5 mg/kg/day 79 days	Oral	Wistar Rats Epididymis Sperm Plasma Testis	- Sperm quality; - Reproductive and thyroid hormones levels (testosterone, TSH, FSH, LH, T3, T4); - Activity enzymes related to testosterone production (17β-HSD and 17-KSR activity)	- Reduction in sperm count, motility and increase in abnormal sperm; - Decrease in testosterone and TSH levels, increase in FSH, LH, T3 and T4 levels; - Reduction in 17β-HSD and 17-KSR activity	[127]
Manganese oxides	**Formula:** Mn_2O_3 **Size**: ~70 nm	100, 200, 400 mg/kg/day 14 days	Oral	Wistar Rats Testis Epididymis Blood	- Reproductive hormones levels (testosterone, LH and FSH); - Testis cell number (spermatogonia, primary spermatocytes, spermatids, Leydig cells);	- Decrease in testosterone, LH and FSH levels (400 mg/kg); - Reduction in testicular cell number (400 mg/kg); - Cellular disruption of ST (≥200 mg/kg), interstitial edema of ST,	[128]

					- Testis histopathology	appearance of vacuoles in epithelium and reduction in cell regulation (400 mg/kg)	
	Formula: MnO_2 **Size:** 25–85 nm	100 mg/kg/week 4 weeks	Subcutaneous	Wistar Rats Testis Epididymis Seminal vesicle Prostate Serum Epididymis Sperm	- Testis cell number (sperm, spermatozoa, spermatogonia and spermatocytes); - Reproductive organs weight; - Reproductive hormones levels (testosterone, E2, FSH); - Sperm quality; - Testis histopathology; - ST morphometry;	- Reduction in testicular cell number; - No difference in the prostate, epididymis and left testicle's weight; - No significant difference in FSH, E2 and testosterone levels (4^{th} week); - Decrease in sperm number and motility (100% immotile sperm, 4^{th} week); - Fluid accumulation in the interstitial space of germline cells; - Decrease in ST mean diameter	[129]
	Formula: Mn_3O_4 **Size:** ~20 ± 4.1 nm **Shape:** irregular sphere-like morphology	10 mg/kg/week 0, 60, 120 days	Intravenous	Sprague–Dawley Rats Testis Epididymis Sperm Serum	- Mn biodistribution in testis and serum; - Testis morphometry and histopathology; - Reproductive hormones levels (testosterone, LH, FSH); - Oxidative stress indexes (MDA, SOD); - Sperm quality; - Fertility evaluation; - Transcription profiling in the testis	- Increase in Mn content in serum and testis (≥60 days); - Reduction of the thickness of germinative layer (≥60 days) and ST degeneration (120 days); - Decline in testosterone and FSH but increase in LH levels (120 days); - Increase in SOD and MDA levels (120 days); - Increase in sperm abnormalities, decrease in sperm concentration and motility (120 days); - Decrease in fertility and fetal survival rate (120 days); - Upregulation of PPAR-signaling pathway and increased expression of cytochrome P450	[110]
Titanium oxide	**Formula:** TiO_2 **Size:** 5–6 nm **SA:** 174.8 m^2/g **HS:** 294 nm **Zeta potential:** 9.28 Mv	2.5, 5, 10 mg/kg/day 60 days	Intragastric	ICR Mice Testis Epididymis Epididymis Sperm	- Testis weight; - Sperm quality; - LDH, SODH, SDH, G-6PD, ACP, AKP, TNOS, Ca^{2+}-ATPase, Ca^{2+}/Mg^{2+}-ATPase, and Na^+/K^+ -ATPase levels; - Oxidative stress indexes (ROS, MDA, PC, 8-OhdG); - Testis and epididymis histopathology	- Reduction in testis weight (≥5 mg/kg); - Decline in sperm concentration, motility (≥5 mg/kg) and increase in morphological abnormalities (≥2.5 mg/kg); - Decreased activity of LDH, SODH (≥5 mg/kg), SDH, G6PD, ATPases (≥2.5 mg/kg), and elevated activity of ACP (≥5 mg/kg), AKP and NOS (≥2.5 mg/kg);	[130]

					- Increase in ROS (≥2.5 mg/kg), MDA, PC and 8-OhdG (≥5 mg/kg) levels; - ST degeneration, reduced number of Leydig cells and mature sperm within the lumen, sperm breakages, spermatolysis, androgone fusion and/or pycnosis (≥2.5 mg/kg);	
Formula: TiO_2 **Size:** ~ 5.5 nm **SA:** 174.8 m^2/g **HS:** 208–330 nm **Zeta potential:** 9.28 Mv	1.25, 2.5, 5 mg/kg/day 6 months	Intragastric	CD-1 Mice Testis Epididymis Sperm	- Reproductive organs weight; - Ti accumulation; - Sperm quality; - Testis and epididymis histopathology; - Cdc2, Cyclin B1, Gsk3-β, TERT, Tesmin, TESP-1, XPD, XRCCI, PGAM1/4 and DMC1 expression	- Decrease in testis (≥2.5 mg/kg) and epididymis weight (≥1.25 mg/kg); - Increase in Ti content in testis and epididymis (≥2.5 mg/kg); - Decrease in sperm number, motility rate and increase in abnormalities (≥1.25 mg/kg); - Pathological changes in the testis and epididymis with NPs agglomerates in the ST and few spermatozoa in epididymis lumen (≥1.25 mg/kg); - Decreased expression of Cdc2, DMC1, TERT, Tesmin, Cyclin B1, XRCC1 and XPD and increased expression of Gsk3-β and PGAM4 (≥1.25 mg/kg)	[131]
Formula: TiO_2 **Size:** 21 nm	5, 25, 50 mg/kg/week 4 weeks	Intravenous	Wistar Rats Testis Serum	- Ti accumulation; - Oxidative stress indexes (CAT, SOD, GPx, LPO); - CK, testosterone and Casp-3 levels; - Sperm number; - DNA damage and apoptosis; - Testis histopathology	- Accumulation of Ti in the testis (≥5 mg/kg); - Decrease in SOD and GPx and increase in CAT and LPO levels (≥25 mg/kg); - Increase in CK levels and in Casp3 activity (50 mg/kg) but decrease in testosterone levels (≥25 mg/kg); - Decline in sperm count; - DNA damage and apoptosis (≥25 mg/kg); - Disorganized and disrupted ST with NPs aggregates in spermatids, Sertoli and Leydig cells (50 mg/kg)	[132]
Formula: TiO_2 **Size:** 10 nm	100 mg/kg/day 4 and 8 weeks	Oral intubation	Albino Rats Testis Epididymis Seminal vesicle Prostate gland	- Reproductive organs weight; - Testosterone levels; - Sperm quality; - Testis, epididymis, prostate gland and seminal vesicle histopathology	- Decrease in testis, epididymis (8^{th} week), and seminal vesicle weight (4^{th} week); - Decrease in testosterone levels (≥4^{th} week);	[133]

			Epididymis Sperm Serum		- Decrease in sperm motility, concentration and viability with increase of sperm abnormalities (≥4th week); - Interstitial edema and sloughing of SE, pyknosis, karyolysis and karyoschisis in testis; congestion, vacuolation and inflammatory cells infiltration with spermatid coagulum in epididymis; congestion, hyperplasia and desquamation of prostate's epithelial lining; congestion in seminal vesicle	
Formula: TiO_2 **Z-average size:** 150 d.nm	0.1, 1, 2, 10 mg/kg/week 4 weeks	Intravenous	C57BL/6J Mice Testis Epididymis Sperm Epididymis Plasma	- Reproductive organs weight; - Sperm quality; - Reproductive hormones levels (testosterone, LH, FSH, GnRH); - Ti accumulation	- No significant changes in the testis and epididymis weight; - Decrease in sperm number (10 mg/kg) and in motile and progressive sperm (≥0.1 mg/kg); - Only testosterone levels were decreased (0.1 mg/kg); - No significant accumulation of Ti in the testis	[134]
Formula: TiO_2 N/A	100 mg/kg/day 8 weeks	Oral intubation	Albino Rats Epididymis Sperm Serum Blood Testis	- Sperm quality; - Oxidative stress indexes (CAT, GSH, MDA); - Testosterone, Casp-3 and Testin levels; - Testis histopathology	- Decrease in sperm quality; - Decline in the levels of testosterone and GSH and increase in MDA levels, with non-significant effect on CAT; - Activation of Casp3, indicating apoptosis and upregulation of Testin gene; - Interstitial edema and sloughing of the germinal epithelium with apoptotic changes	[135]
Formula: TiO_2 **Size:** ~10 nm **SA:** 120 m^2/g **Purity:** >99.8% **Shape:** rhabditiform **Zeta potential:** −20.7 to −3.77 Mv	0, 10, 50, 100 mg/kg/day 28 days	Intragastrical	ICR Mice Epididymis Sperm Epididymis Testis	- Reproductive organs weight; - Sperm quality; - Oxidative stress indexes (SOD, MDA); - Testis histopathology	- No significant changes in testis and epididymis weight; - No significant changes in sperm density and increase in sperm malformation (≥50 mg/kg); - Decrease in SOD (100 mg/kg) and increase in MDA (≥50 mg/kg) content; - Disordered and vacuolized spermatogenic cells with reduced number (≥50 mg/kg)	[136]

	Formula: TiO_2 **Size:** 17 nm **SA:** 107.7 m^2/g **Z-average size:** 218 nm **PDI:** 0.24	63 µg/week 7 weeks	Intratracheal	C57BL/6J Testis Epididymis	- Reproductive organs weight; - Sperm count; - Testosterone levels;	- No significant changes in testis and epididymis weight; - No significant changes in sperm count; - No significant effect on testosterone levels;	[137]
	Formula: TiO_2 **Z-average size:** 150 d.nm	0, 2, 10 mg/kg/week 4 weeks	Intravenous	C57BL/6J Mice Testis Epididymis Sperm Epididymis	- Reproductive organs weight; - Sperm quality; - Ti accumulation	- No significant changes in testis and epididymis weight; - Decrease in sperm number and in motile and progressive sperm (≥2 mg/kg); - No significant accumulation of Ti in the testis	[138]
	Formula: TiO_2 **Size:** ~40 nm	100 mg/kg/day 60 days	Oral gavage	Wistar Rats Testis Epididymis Sperm	- Sperm quality; - Oxidative stress indexes (CAT, SOD, GPx, MDA, GSH, FRAP values); - SE and ST morphometry; - Testis histopathology	- Decline in sperm quality; - Increase in MDA levels, decrease in CAT, SOD, GPx, GSH and FRAP values; - Decline in the diameter of ST and height of SE; - ST with irregular shape, wide interstitial space with reduced number of Leydig cells	[139]
	Formula: TiO_2 **Size:** < 25 nm **Shape**: spherical **Zeta potential:** + 2.8 to +5.8 Mv **PDI:** 0.822 **HS:** 1492 nm	9.38, 18.75, 37.5, 75 mg/kg/day 35 days	Intraperitoneal	Swiss Mice Testis Serum Epididymis Sperm	- Testis weight; - Sperm quality; - Reproductive hormone levels (testosterone, LH, FSH); - Oxidative stress indexes (SOD, CAT, GSH, MDA); - Testis tissue morphometry; - Testis histopathology	- No significant changes in testicular weight; - Decrease in motile sperm (≥9.38 mg/kg) and in sperm count with an increase in sperm abnormalities (≥18.75 mg/kg); - Decrease in LH (≥9.38 mg/kg) and FSH (75 mg/kg) levels, with no significant changes in testosterone levels; - Reduced activity of SOD (≤37.5 mg/kg), CAT (≥9.38 mg/kg) and GSH (9.38 mg/kg) and increased MDA levels (≥18.75 mg/kg); - Decrease in germinal height (9.38, 37.5, 75 mg/kg) and increase of luminal width (≥9.38 mg/kg); - Increased number of damaged ST, Leydig cell degeneration and necrosis of spermatogenic cells (75 mg/kg)	[140]

Zinc Oxide	**Formula:** ZnO N/A	0, 5, 50, 300 mg/kg/day 35 days	Oral	NMRI Mice Epididymis Testis Epididymis Sperm	- Testis weight; - Sperm quality; - ST histopathology; - SE maturity; - ST and SE morphometry	- Decrease in testis weight (300 mg/kg); - Decrease in sperm number and motility, increase in abnormalities (≥50 mg/kg); - Increase in detached, sloughed (≥50 mg/kg), vacuolized (≥5 mg/kg) and multinucleated ST (300 mg/kg); - SE maturation arrest with abnormal spermatogenesis (≥50 mg/kg); - Decrease in ST diameter and SE height (≥50 mg/kg)	[141]
	Formula: ZnO **Size:** 10–30 nm **SA:** 20/30 m^2/g **Crystal phase:** single **Crystal morphology:** nearly spherical **Density:** 5.606 g/cm^3 **Purity:** ≥99%	0, 50, 100, 150, 200 mg/kg/day 10 days	Intraperitoneal	Wistar Rats Liver Kidneys Epididymis Sperm Serum	- SOD, GPx, MDA, TAC, TOS levels; - Sperm quality;	- No difference in the levels of SOD and GPx, increase in MDA (≥100 mg/kg) and TOS (200 mg/kg) and decrease in TAC (200 mg/kg) levels; - Decrease in sperm count, viability, normal morphology (≥50 mg/kg) and motility (≥100 mg/kg);	[142]
	Formula: ZnO **Size:** 20 nm **SA:** >90 m^2/g **Color:** white **Crystal morphology:** nearly spherical **Purity:** ≥99%	0, 250, 500, 700 mg/kg/day 7 days	Intraperitoneal	NMRI Mice Testis	- Testis weight; - Testis histopathology	- No alterations in testis weight; - No alterations in the tunica albuginea thickness and no increase in degenerated ST. Decrease in ST and SE diameter (250 and 500 mg/kg). Decrease in the number of A type spermatogonia (≥500 mg/kg), primary spermatocytes (500 mg/kg) and fibroblasts (≥250 mg/kg). Higher number of degenerated cells, and multinucleated spermatids (≥250 mg/kg). No alterations in the number of Sertoli, spermatids, spermatozoa, and B type spermatogonia cells	[143]
	Formula: ZnO **Size:** ~ 70 nm **Shape:** spherical **Nature:** crystalline	0, 1, 5 mg/kg single dose at PND21	Intravenous	CD-1 Mice Epididymis Testis Epididymis Sperm	- SE and ST morphometry; - Sperm morphology	- Reduction in SE thickness (5 mg/kg, PND28 and PND42) but no differences in ST diameter; - Increase in sperm abnormalities (≥1 mg/kg, 49 days after injection)	[115]

Dispersion: polydisperse **Surface roughness:** high (22.9 nm)						
Formula: ZnO **Size:** <50 nm **SA:** >10.8 m^2/g **Purity:** >97%	0, 100, 400 mg/kg/day 12 weeks	Intragastric	Albino Rats Epididymis Testis Epididymis Sperm Serum	- Sperm quality; - Oxidative stress indexes (MDA, CAT, SOD, GPx, GSH); - Testosterone levels; - Expression of enzymes related to testosterone production (3β-HSD, 17β-HSD and Nr5A1); - Testis histopathology	- Decline in sperm motility, viability (≥100 mg/kg) and concentration and increase in sperm abnormalities (400 mg/kg); - Increase in MDA (400 mg/kg), decrease in GSH, GPx, SOD and CAT (≥100 mg/kg) levels; - Reduction in testosterone production (≥100 mg/kg); - Reduction in the expression of 3β-HSD, 17β-HSD and Nr5A1 (≥100 mg/kg); - Increased cell apoptosis, ST damage, sloughing of immature germ cells from ST (≥100 mg/kg)	[144]
Formula: ZnO **Size:** 39.45 ± 19.88 nm **HS:** 447.5 nm **Aggregation:** large and irregular **PDI:** 0.13 nm **Shape:** hexagonal **Zeta potential:** −32.1 Mv	300, 2000 mg/kg twice at 24 h interval	Oral	Swiss Mice Liver Epididymis Sperm	- Sperm quality; - Liver ROS and 8-oxo-G levels	- Decline in sperm count (2000 mg/kg), motility, viability (≥300 mg/kg) and increase in aberrant sperm during the maturation phase (2000 mg/kg); - Increase in ROS levels and 8-oxo-G expression (2000 mg/kg)	[145]
Formula: ZnO **Size:** <100 nm **Purity:** ≥99.5% **Color:** white	0, 422 mg/kg/day 4 weeks	Oral gavage	Albino Rats Testis Prostate Serum	- Oxidative stress indexes (MDA, GSH, CAT, SOD); - Testis and prostatic cytokines content (TNF-α, IL-4); - Testis and prostate DNA fragmentation; - Testis and prostate histopathology;	- Elevation of MDA and reduction of GSH, CAT, SOD; - Increase in TNF-α and decrease in IL-4; - Confirmed DNA fragmentation; - Tunica albuginea with congested blood vessels, disorganized ST with cell loss and absence of spermatozoa, SE separated from basement membranes and some germ cells with dark pyknotic nuclei;	[146]

Formula: ZnO **Size:** 50 nm **Shape:** cube **Color:** white **Purity:** 99.99%	100, 200 mg/kg/day 7 and 14 days	Oral gavage	Albino Mice Testis Epididymis Seminal vesicle Prostate Epididymis Sperm	- Reproductive organs weight; - Sperm abnormalities	- Decline in testis and epididymis weight but hypertrophy of seminal vesicle and prostate (≥100 mg/kg, ≥7 days); - Increase in sperm abnormalities (≥100 mg/kg, ≥7 days)	[147]
Formula: ZnO **Size:** 30 nm **Zeta potential:** 38.25 ± 1.06 Mv **HS:** 66.36 ± 0.93 nm	0, 100, 200, 400 mg/kg/day 28 days	Intragastric	Kunming Mice Testis Epididymis Serum	- Testosterone levels; - Testis and epididymis histopathology; - Gene expression related to apoptosis (cleaved Casp-3 and -8, Bax, Bcl-2) and autophagy (Atg-5, Beclin-1, ratio LC3-II/LC3-I)	- Decrease in testosterone levels (≥200 mg/kg); - Mildly disorganized ST (200 mg/kg), disintegration of SE, germ cell depletion and reduction in round sperm in the ST (400 mg/kg); - Upregulation of cleaved Casp-8 (≥100 mg/kg), Casp-3 and Bax (400 mg/kg) and downregulation in Bcl-2 (≥100 mg/kg) expression in the testis. Increase in Atg-5, Beclin-1 expression, and LC3-II/LC3-I ratio in the testis (≥100 mg/kg);	[118]
Formula: ZnO **Size:** 30 nm **Shape:** spherical	0, 50, 150, 450 mg/kg/day 14 days	Oral gavage	Kunming Mice Epididymis Testis Testis Sperm Serum	- Reproductive organs weight; - Sperm count; - Testis histopathology; - Zinc accumulation; - Gene expression related to apoptosis (Casp-3, -9 and -12, JNK, Bcl-2/Bax) ER stress (BIP, XBP1s, IRE1α, CHOP) and testosterone production (StAR, cytochrome P450scc); - Testosterone levels	- Increase in testis (150 mg/kg) and epididymis weight (50 and 450 mg/kg); - Low number of sperm in the ST lumen (50 mg/kg), ST degeneration and vacuolization of Sertoli cells (150 mg/kg), Leydig cells vacuolization, absent ST with degenerated and necrotic spermatogenic cells (450 mg/kg); - Zinc accumulation in the epididymis (50 and 450 mg/kg) but not in the testis; - Upregulation of BIP, XBP1s, Casp-12 (450 mg/kg), IRE1α, Casp-3 (≥50 mg/kg), CHOP (≥150 mg/kg) and Casp-9 (150 mg/kg). Downregulation of JNK at 50 mg/kg but upregulation at 150 mg/kg and down-regulation of Bax/Bcl-2; - Decrease in sperm number and testosterone levels (≥150 mg/kg), related to the downregulation of StAR	[90]

Formula: ZnO **Size:** 100 nm	100 mg/kg/day 75 days	Oral	Wistar Rats Testis Prostate Epididymis Sperm Plasma	- Reproductive organs weight; - mtTFA, UCP2 testis levels; - DNA fragmentation; - p53, TNF-α, IL-6 testis levels; - Oxidative stress indexes (GPx, GST, CAT, SOD, GSH, TAC, TBARS, NO); - Steroidogenic enzymes levels (17-KSR, 17β-HSD); - Sperm quality; - Reproductive and thyroid hormones levels (testosterone, FSH, LH, TSH, T3, T4); - Testis histopathology	- Decline in testis and epididymis weight but increase in prostate weight; - Suppression and induction of MtTFA and UCP2 expression, respectively; - Massive DNA fragmentation; - Increase in p53, TNF-α and IL-6 levels; - Decrease in GPx, GST, CAT, SOD, GSH, TAC levels and increase in TBARS and NO levels; - Increase and decrease in 17β-HSD and 17-KSR levels, respectively; - Reduction in sperm count, motility and increase in sperm abnormalities; - Decrease in testosterone and TSH levels, increase in FSH, LH, T3 and T4 levels; - ST with irregular shaped and empty lumina, spermatogenic cells with pyknotic nuclei, few Leydig cells	[123]
Formula: ZnO **Size:** <100 nm **Shape:** rod-like **Zeta potential:** + 17 to +20.6 Mv **PDI:** 0.729 **HS:** 882.8 nm	9.38, 18.75, 37.5, 75 mg/kg/day 35 days	Intraperitoneal	Swiss Mice Serum Epididymis Sperm Testis	- Testis weight; - Sperm quality; - Reproductive hormones levels (testosterone, LH, FSH); - Oxidative stress indexes (SOD, CAT, GSH, MDA); - Morphometric parameters; - Testis histopathology;	- No significant changes in testis weight; - Decrease in motile sperm, lower sperm number (≥9.38 mg/kg), increase in sperm abnormalities (18.75 and 37.5 mg/kg) and higher testosterone levels (≥9.38 mg/kg); - Decrease in LH (9.38, 18.75 and 75 mg/kg) and FSH (≥37.5 mg/kg) levels; - Reduced SOD and CAT activity but increased MDA activity (≥9.38 mg/kg) with no significant changes in GSH; - Decrease in germinal height (≥9.38 mg/kg) and increase of luminal width (9.38, 37.5, 75 mg/kg); - Increased number of damaged ST, Leydig cell degeneration and necrosis of spermatogenic cells (≥9.38 mg/kg)	[140]
Formula: ZnO **Size:** 80 nm	0, 150, 350 mg/kg 15 days	Oral	Albino Mice Testis Prostate Seminal Vesicle	- Testis, prostate, seminal vesicle, and epididymis histopathology	- Mild damage in seminal vesicles and epididymis (150 mg/kg) and severe damage in all tissues of the reproductive system (350 mg/kg)	[148]

Epididymis

Abbreviations: ACP, Acid Phosphatase; ALT, Alanine Aminotransferase; AST, Aspartate Aminotransferase; AKP, Alkaline Phosphatase; Bax, Bcl2-associated X protein; Bcl-2, B cell lymphoma-2; BIP, Immunoglobulin-Binding Protein; Casp-, Caspase; CAT, Catalase; Cdc-, Cyclin Dependent Kinase; CHOP, Transcription of CCAAT/enhancer-binding Protein (C/EBP); CK, Creatine Kinase; DMC1, DNA Meiotic Recombinase 1; DNA, Deoxyribonucleic Acid; E2, 17β-estradiol; FRAP, Ferric Reducing Antioxidant Power; FSH, Follicle Stimulating Hormone; GnRH, Gonadotropin-Releasing Hormone; GST, Glutathione S-transferase; GSH, Reduced Glutathione; Gsk3-β, Glycogen synthase kinase 3 beta; GPx, Glutathione Peroxidase; G6PD, Gluco-6-Phosphate Dehydrogenase; HS, Hydrodynamic Size; IL-, Interleukin; IRE1α, Inositol-Requiring Protein 1α; JNK, Jun Kinase; LDH, Lactate Dehydrogenase; LH, Luteinizing Hormone; LPO, Lipid Peroxidation; MDA, Malondialdehyde; mtTFA, mitochondrial Transcription Factor A; NO, Nitric Oxide; Nr5A1, Nuclear Receptor Subfamily 5 group A member 1; PARP, Poly (ADP-ribose) Polymerase; PC, Protein Carbonyl; PDI, Polydispersity Index; PGAM1/4, Phosphoglycerate Mutase 1; PND, Post-Natal Days; P450scc, Cytochrome P450 side-chain cleavage enzyme; ROS, Reactive Oxygen Species; SA, Surface Area; SDH, succinate dehydrogenase; SE, Seminiferous Epithelium; SF-1, Steroidogenic Factor-1; SOD, Superoxide Dismutase; SODH, Sorbitol Dehydrogenase; ST, Seminiferous Tubules; StAR, Steroidogenic Acute Regulatory Protein; TAC, Total Antioxidant Capacity; TBARS, Thiobarbituric Acid-Reactive Substances; TERT, Telomerase Reverse Transcriptase; Tesmin, Testis Expressed Metallothionein Like Protein; TESP-1, Testicular Serine Protease 1; TNF-α, Tumor Necrosis Factor Alpha; TNOS, Total Nitric Oxide Synthase; TOS, Total Oxidant Status; TSH, Thyroid Stimulating Hormone; T3, Tri-iodothyronine; T4, Thyroxin; UCP2, Uncoupling Protein 2; XBP1s, X-Box-Binding Protein 1 splicing; XRCC1, X-Ray Repair Cross Complementing 1; VAP, Average Path Velocity; VCL, Curvilinear Velocity; VSL, Straight Line Velocity; 3β-KSD, 3β-hydroxysteroid dehydrogenase; 8-OhdG, 8-hydroxydeoxyguanosine; 17-KSR, 17-Ketosteroid Reductase; 17β-HSD, 17β-hydroxysteroid dehydrogenase; γ-GT, γ-glutamyl-transpeptidase.

Table 2 clearly shows that animal models used for the in vivo experiments were mice and rats of different strains. Most of the studies listed have addressed the toxicity of MONPs at concentrations that are far from real-life conditions, even though there is no information available on the concentration of MONPs to which humans are exposed. Lauvås et al. used a lower and more realistic intratracheal dose of TiO_2 NPs (63 µg/week for seven weeks), based on the estimated lung deposition of titanium at the Danish occupational exposure limit [137].

The exposure times used for the studies were highly variable. In some studies, male mammals received MONPs for very short periods, like 4 days [126], and, in other studies, the MONPs were used for much longer periods, namely six months [131]. These studies with these differences in exposure times are crucial since they help to create a better understanding of the acute and long-term effects of MONP administration. Additionally, many experiments have established the duration of treatment at around four weeks, to accomplish the duration of complete spermatogenesis in mice and rats [149].

Different routes of MONPS administration were used in animal experiments, namely, oral, intragastric, intratracheal, intraperitoneal, intravenous, and subcutaneous administration. It has been previously reported that there is very low absorption of MONPs through inhalation or oral administration in animals [62]. This aspect was confirmed by Lauvås et al. , which was the only study included in Table 2, which administered MONPs intratracheally, and found that sperm cells are not susceptible to MONP exposure via the airways, at low doses [137]. On the other hand, in oral exposure, MONPs release more ions in the stomach due to the acidic environment. Therefore, this dissolution may be a reason for the cytotoxicity reported in the studies that used this administration approach, although fewer amounts of NPs are absorbed [145]. In contrast, intraperitoneal injections ensure proper absorption of the tested MONPs due to the highly vascularized peritoneal cavity [140]. The intravenous administration of nanomaterials ensures a much higher direct testicular exposure since NPs are administered directly into the bloodstream.

Only Tang et al. , Yousef et al. , and Radhi et al. reported the increase of reproductive organs' weight after the oral administration of NPs, which may be attributed to the inflammation and hypertrophy or even accumulation of NPs in those tissues [90,123,147]. In fact, all studies that evaluated the content of MONPs in the testis and epididymis confirmed their presence in these organs. This was the case for cerium [124], iron [97], manganese [110], titanium [131,134,138], and zinc [90] NPs. The only exception was reported by Miura et al. studies, in which TiO_2 NPs administered intravenously were found in the testis, but not in significant amounts [134,138]. This deposition of NPs in the reproductive tissues triggers the harmful events that will be described throughout this section. In fact, the damage has been reported in the testis and epididymis. Al_2O_3 [123], F_2O_3 [125], Fe_3O_4 [126], Mn_3O_4 [110,128], MnO_2 [129], TiO_2 [131,132,135,136,139,140], and ZnO [123,140,141,143,144,146] NPs all caused histopathological changes in the testis, mainly due to degeneration of the seminiferous tubules. Furthermore, Morgan et al. studied the histopathological changes induced by TiO_2 NPs in the prostate and seminal vesicle, and reported that these reproductive organs were also affected by NPs, since they caused congestion, hyperplasia, and

desquamation of the prostate's epithelial, lining, and congestion in the seminal vesicle [133]. Salman also reported that ZnO NPs caused mild damage in seminal vesicles but severe damage to the prostate [148]. The reduction in the testis cell population has also been commonly reported, which is an indicator of a lack of active spermatogenesis in the testis [150].

The translocation of MONPs from their site of administration to the testicular tissue confirms that these NPs can cross and enter the BTB, where they interfere with normal physiological processes. Then, when in contact with reproductive tissues, these NPs can permeate cell membranes, inducing the overproduction of ROS, which leads to oxidative stress (Figure 4). This interferes with the balance between the oxidant and antioxidant systems, which causes oxidative damage in biomolecules, such as lipids, proteins, and nucleic acids [97]. To confirm the oxidative damage caused by MONPs, different studies evaluated ROS production and the levels of other oxidant markers, such as Malondialdehyde (MDA), Nitric Oxide (NO), Protein Carbonyl Content (PC), Lipid Peroxidation (LPO), and Total Oxidant Status (TOS). Antioxidant parameters such as Superoxide Dismutase (SOD), Glutathione Peroxidase (GPx), Reduced Glutathione (GSH), Catalase (CAT), and Total Antioxidant Capacity (TAC), were also evaluated. These parameters of oxidative stress were assessed on all types of MONPs, except CeO_2 NPs [124]. The results reported an increase in oxidant markers and a decrease in intracellular antioxidant defenses and TAC. This confirms that MONPs suppress the antioxidant machinery and induce oxidative stress, which can lead to various cellular damages and, consequently, interfere with male fertility. In fact, according to previous studies, 30–80% of male infertility cases can be attributed to oxidative stress-mediated injury to the male reproductive system [110,151,152]. Persistent oxidative stress leads to the downregulation of Bcl-2 and upregulation of Bax, which results in the leakage of cytochrome c from dysfunctional mitochondria, ultimately resulting in apoptosis (Figure 4), through the activation of caspase molecules, as confirmed by Sundarraj et al. , Meena et al. , Shen et al. , and Morgan et al. [97,118,132,135]. MONPs not only induce apoptosis, but some have also proven to be autophagy activators and inducers of autophagic cell death [118].

The levels of endocrine and reproductive hormones were also evaluated, and the results also suggest an imbalance in reproductive hormones (Testosterone, FSH, LH, GnRH, E2) and thyroid hormones (TSH, T3, T4) that can be attributed to the increase of ROS and the concomitant reduction of antioxidant enzymes. The exceptions were Lauvås et al. and Ogunsuyi et al. , who reported that TiO_2 NPs did not trigger alterations in testosterone levels [137,140]. Contrarily, Miura et al. reported that TiO_2 NPs affected testosterone levels, but not FSH, LH, and GnRH [134].

Additionally, some authors explored the influence of MONPs on the expression of genes related to steroidogenesis. Testosterone is produced mainly in Leydig cells by a series of enzymatic reactions. First, the StAR protein transfers cholesterol to mitochondria. Then, the mitochondrial cytochrome P450scc transforms cholesterol into pregnenolone. Subsequently, other enzymes (3β-HSD, P450c17, 17β-HSD) convert the pregnenolone into testosterone [124]. Interestingly, Nr5A1, a transcription factor that regulates the expression of steroidogenic genes in Leydig cells (such as 3β-HSD), was downregulated after exposure to ZnO NP [144]. The StAR protein was also

downregulated by CeO_2 [124] and ZnO NPs [90], which can manifest in their inability to transfer cholesterol to the inner mitochondrial membrane, which stops steroidogenesis and justifies the decline in testosterone levels in most of the results listed. However, Bara and Kaul reported the conflicting results of increased testosterone production and StAR upregulation, but this was only related to small concentrations of ZnO NPs [117]. Ogunsuyi et al. did not report alterations in testosterone levels after intraperitoneal administration of TiO_2 NPs; however, these levels were increased in the same study, under the same conditions, by ZnO NPs [140]. Likewise, Lauvås et al. found no significant alterations in testosterone levels after intratracheal administration of TiO_2 NPs [137].

Sperm parameters, such as sperm number, viability, abnormalities, and motility, have been extensively studied. All studies that analyzed sperm count observed its decline with increasing concentrations of NPs, except for Varzeghani et al. , Lauvås et al. , and Song et al. , who did not report significant alterations [126,136,137]. The results listed in Table 2 also indicate a reduction in motile spermatozoa, which affects their fertilizing potential. This decrease in sperm motility may have been a result of lipid peroxidation [140] (Figure 4). In addition, Morgan et al. , Hussein et al. , Srivastav et al. , and Abbasalipourkabir et al. were the only research teams that evaluated sperm viability, having reported its decline [133,135,142,144,145]. An increase in sperm abnormalities, such as small head, double head, formless head, and double tails, has also been reported, which may be the result of oxidative damage [140] (Figure 4). These results are in agreement with those reported under in vitro conditions (Table 1).

Hong et al. evaluated the activity of metabolism-related enzymes — LDH, SDH, and SODH —t hat play key roles in the growth and development of testicular cells [130]. The results suggest that there was a decline in their activity, which may be associated with the disturbance of energy metabolism in germ cells. It was also the only study to evaluate the testicular activity of G-6PD, testis-marker enzymes ACP and AKP, and the activity of Ca^{2+}-ATPase, Ca^{2+}/Mg^{2+}-ATPase and Na^{+}/K^{+}-ATPase. G-6PD is associated with androgen biogenesis, and its reduction implies that TiO_2 NPs interfered with androgen secretion. In this study, ACP and AKP were used as markers of impaired spermatogenesis. Since ACP is related to the degeneration of the seminiferous epithelium and AKP is related to the activity of division of germ cells, their increase suggests testicular degeneration. Reductions in ATPases suggest an imbalance in the concentrations of intracellular ions, which could promote spermatogenesis dysfunctions [130].

Due to their small size, MONPs can reach the nucleus and interact directly with DNA, which causes the generation of ROS that further damages DNA (Figure 4) [146]. Not all studies tested the genotoxicity of NPs, but all studies that evaluated DNA damage later confirmed it. Mesallam et al. detected DNA fragmentation in the testis and prostate of rats treated with 422 mg/kg ZnO NPs daily for four weeks [146]. Meena et al. also found DNA strand breaks in spermatozoa of rats treated with 25 and 50 mg/kg TiO_2 NPs weekly for 30 days [132].

Results also indicate elevated levels of TNF-α [123,146], and pro-inflammatory IL-6 cytokine [123], and a decrease in anti-inflammatory IL-4 cytokine [146] in reproductive tissues, which indicates a cellular inflammatory response to the NP exposure.

Zhang et al. evaluated male fertility by assessing the offspring of rats treated with Mn_3O_4 NPs [110]. The obtained results confirmed that this treatment decreased rats' fertility and reduced the survival rate of their offspring in a time-dependent manner. For these authors, these results are attributed to changes in reproductive hormones and the decline in sperm quality [110].

In summary, most biochemical and molecular results were concomitant with histological findings. Therefore, despite the many benefits of MONPs, the results of the listed in vivo studies confirm the in vitro studies, emphasizing the possibility that exposure to these NPs could have a detrimental impact on male fertility.

4.3. MONPs in Human Reproductive Medicine

The recent approval of MONPs-based technologies in clinical medicine allowed an increase in human living standards and an improvement in mankind's healthcare conditions through the prevention, early detection, diagnosis, treatment, and follow-up of multiple diseases [153]. However, their usefulness in human reproductive medicine has yet to be proved.

Considering that 50% of infertile couples, the male partner is affected by aberrations in sperm properties, number, vitality, and morphology [154], there is a clear need to develop novel methodologies for the early identification of infertility causes and its treatment. Some research teams have already developed MONP-based approaches that were tested in vitro and in vivo, with promising results. These include methods to reduce oxidative stress induced by cryopreservation [155], improve the proportion of healthy spermatozoa in semen prior to insemination [156], provide movement to sperm with motility deficit [157], protect the fertility of men who are exposed to fertility disrupters [158], and even treat other male associated disorders, such as erectile dysfunction [159].

Although these and other approaches have shown promising results, most of the literature still suggests uncertainty regarding the risk of MONPs in fertility, which may be one of the main reasons why, to date, there are no trials involving this type of engineered NPs for fertility regulation and treatment of male reproductive diseases. Another limiting factor is that only a few studies tried to identify the exact mechanism and pathways induced by MONPs. Current animal experiments also fail to assess pregnancy rates, and the health of offspring, which is the most relevant outcome parameter of fertility [160]. This gap in literature allows the speculation around the hazard posed by MONPs, which could prevent the translation of the results from the lab to the clinical applications [161]. NPs represent a valuable tool to alleviate much of the suffering arising from many reproductive difficulties and disorders, but further work is required to determine if these NPs can fulfill the needs in reproductive health. Human clinical reproductive trials may help accelerate the commercial availability of these new alternatives.

5. Conclusions and Future Perspectives

The increased application of MONPs in many industries and scientific fields has made these materials highly present in the environment, resulting in an increased risk of human exposure. Additionally, evidence that keeps emerging suggests that MONPs interfere with the male reproductive system at many biological levels.

The results presented in this review from both in vitro and in vivo studies prove that MONPs can interfere with the male reproductive system, and these results should not be ignored. The collected data show that this reproductive toxicity is achieved due to the MONPs' ability to interfere with cell molecules and reproductive hormones, which often results in DNA damage and altered gene expression. It was also reported that MONPs induce oxidative stress in germ cells, which affects their number, quality, morphology, and activity. At the organ level, MONPs can cross the BTB and accumulate in the testis, resulting in many histological alterations in tissues of the reproductive system. Since the normal physiological processes that occur in the male reproductive system are highly complex and vulnerable, the interference of MONPs at any level can be deleterious and impair male fertility. Whether these harmful effects are reversible or not is still unclear and should be investigated in further research. How these alterations affect pregnancy and offspring is still an unresolved issue and should be addressed in future studies.

In the studies presented, the only conditions considered to evaluate the reproductive toxicity of MONPs were concentration and duration of exposure. However, the size and surface area are two crucial physical properties that affect how MONPs interact with cells and thus greatly determine the cytotoxicity of NPs. In addition, current studies generally focus on individual alterations but fail to establish a relationship between them. This may be partly the reason why the exact mechanism of nanotoxicity is not yet fully elucidated. Therefore, future studies should make a more in-depth examination of the molecular mechanisms of NPs and MONPs, in particular in reproductive toxicity and the interaction between each reported alteration. In addition, the in vivo studies are of significant heterogeneity, mainly due to the difference in the route of administration and the highly variable administered doses and exposure times. All of these factors can potentially be a source of toxicity that may influence the outcome of the studies. In some cases, unrealistically high concentrations of MONPs were used in cell culture and animal studies, which obviously results in cytotoxicity. Those studies lead to discouraging results that affect the accurate estimation of the reproductive health risks and hinder clinical translation.

It is reasonable to conclude that there are still difficulties in evaluating the reproductive toxicity of MONPs and in understanding exactly how they interact with the male reproductive system. The results summarized in this review reinforce the need for further studies with uniform protocols to obtain solid results with real implications in humans.

References:

1. McNeil, S.E. Nanotechnology for the biologist. *J. Leukoc. Biol.* **2005**, *78*, 585–594, doi:10.1189/jlb.0205074.

2. Lövestam, G.; Rauscher, H.; Roebben, G.; Klüttgen, B.; Gibson, N.; Putaud, J.-P.; Stamm, H. *Considerations on a Definition of Nanomaterial for Regulatory Purposes*; JRC Reference Reports, 2010;

3. Khan, I.; Saeed, K.; Khan, I. Nanoparticles: Properties, applications and toxicities. *Arab. J. Chem.* **2019**, *12*, 908–931, doi:10.1016/j.arabjc.2017.05.011.

4. Singla, R.; Guliani, A.; Kumari, A.; Yadav, S.K. *Metallic Nanoparticles, Toxicity Issues and Applications in Medicine*; 2016; ISBN 9789811008184.

5. Nikolova, M.P.; Chavali, M.S. Metal oxide nanoparticles as biomedical materials. *Biomimetics* **2020**, *5*, doi:10.3390/BIOMIMETICS5020027.

6. Sengupta, J.; Ghosh, S.; Datta, P.; Gomes, A.; Gomes, A. Physiologically important metal nanoparticles and their toxicity. *J. Nanosci. Nanotechnol.* **2014**, *14*, 990–1006, doi:10.1166/jnn.2014.9078.

7. Zoroddu, M.A.; Aaseth, J.; Crisponi, G.; Medici, S.; Peana, M.; Nurchi, V.M. The essential metals for humans: a brief overview. *J. Inorg. Biochem.* **2019**, *195*, 120–129, doi:10.1016/j.jinorgbio.2019.03.013.

8. Das, R.K.; Brar, S.K.; Verma, M. Checking the Biocompatibility of Plant-Derived Metallic Nanoparticles : Molecular Perspectives. *Trends Biotechnol.* **2016**, *xx*, 1–10, doi:10.1016/j.tibtech.2016.02.005.

9. Zhao, J.; Dong, X.; Hu, X.; Long, Z.; Wang, L.; Liu, Q.; Sun, B.; Wang, Q.; Wu, Q.; Li, L. Zinc levels in seminal plasma and their correlation with male infertility: A systematic review and meta-analysis. *Sci. Rep.* **2016**, *6*, 1–10, doi:10.1038/srep22386.

10. Fallah, A.; Mohammad-Hasani, A.; Colagar, A. Zinc is an Essential Element for Male Fertility: A Review of Zn Roles in Men's Health, Germination, Sperm Quality, and Fertilization. *J. Reprod. Infertil.* **2018**, *19*, 69–81.

11. Rezaeian, Z.; Yazdekhasti, H.; Nasri, S.; Rajabi, Z.; Fallahi, P.; Amidi, F. Effect of selenium on human sperm parameters after freezing and thawing procedures. *Asian Pacific J. Reprod.* **2016**, *5*, 462–466, doi:10.1016/j.apjr.2016.11.001.

12. Herman, S.; Lipinski, P.; Ogórek, M.; Starzynski, R.; Grzmil, P.; Bednarz, A.; Lenartowicz, M. Molecular Regulation of Copper Homeostasis in the Male Gonad during the Process of Spermatogenesis. *Int. J. Mol. Sci.* **2020**, *21*, 1–16, doi:10.3390/ijms21239053.

13. Taylor, U.; Barchanski, A.; Kues, W.; Barcikowski, S.; Rath, D. Impact of Metal Nanoparticles on Germ Cell Viability and Functionality Production of Metal Nanoparticles. *Reprod. Domest. Anim.* **2012**, *47*, 359–368, doi:10.1111/j.1439-0531.2012.02099.x.

14. Umrani, R.D.; Paknikar, K.M. Zinc oxide nanoparticles show antidiabetic activity in streptozotocin- induced Type 1 and 2 diabetic rats. *Nanomedicine* **2014**, *9*, 89–104, doi:10.2217/nnm.12.205.

15. Falchi, L.; Khalil, W.A.; Hassan, M.; Marei, W.F.A. Perspectives of nanotechnology in male fertility and sperm function. *Int. J. Vet. Sci. Med.* **2018**, *6*, 265–269, doi:10.1016/j.ijvsm.2018.09.001.

16. Yoshikawa, A.H.; Possebon, L.; Costa, S.D.S.; Souza, H.; Girol, A.; Pereira, M. de L. Adverse effects of Metal-based Nanoparticles on Male Reproductive Cells. In *Top 10 Contributions on Environmental Healt*; Avid Science: Berlin, Germany, 2018; pp. 1–19.

17. Matsumoto, A.M.; Bremner, W.J. *Testicular Disorders*; Thirteenth.; Elsevier Inc., 2016;

18. Zhou, Q.; Yue, Z.; Li, Q.; Zhou, R.; Liu, L. Exposure to PbSe Nanoparticles and Male Reproductive Damage in a Rat Model. *Environ. Sci. Technol.* **2019**, *53*, 13408–13416, doi:10.1021/acs.est.9b03581.

19. Ijaz, I.; Gilani, E.; Nazir, A.; Bukhari, A. Detail review on chemical, physical and green synthesis, classification, characterizations and applications of nanoparticles. *Green Chem. Lett. Rev.* **2020**, *13*, 59–81, doi:10.1080/17518253.2020.1802517.

20. Vaseem, M.; Umar, A.; Hahn, Y. *ZnO Nanoparticles : Growth, Properties, and Applications*; 2010; Vol. 5; ISBN 1588831701.

21. Reverberi, A.P.; Kuznetsov, N.T.; Meshalkin, V.P.; Salerno, M.; Fabiano, B. Systematical analysis of chemical methods in metal nanoparticles synthesis. *Theor. Found. Chem. Eng.* **2016**, *50*, 59–66, doi:10.1134/S0040579516010127.

22. Ealias, A.M.; Saravanakumar, M.P. A review on the classification, characterisation, synthesis of nanoparticles and their application. *IOP Conf. Ser. Mater. Sci. Eng.* **2017**, *263*, doi:10.1088/1757-899X/263/3/032019.

23. Cormode, D.; Naha, P.; Fayad, Z. Nanoparticle contrast agents for computed tomography : a focus on micelles. *Contrast Media Mol. Imaging* **2014**, *9*, 37–52, doi:10.1002/cmmi.1551.

24. Jeevanandam, J.; Barhoum, A.; Chan, Y.S.; Dufresne, A.; Danquah, M.K. Review on nanoparticles and nanostructured materials: History, sources, toxicity and regulations. *Beilstein J. Nanotechnol.* **2018**, *9*, 1050–1074, doi:10.3762/bjnano.9.98.

25. Moreno-Vega, A.I.; Gómez-Quintero, T.; Nuñez-Anita, R.E.; Acosta-Torres, L.S.; Castaño, V. Polymeric and ceramic nanoparticles in biomedical applications. *J. Nanotechnol.* **2012**, *2012*, doi:10.1155/2012/936041.

26. Chavali, M.S.; Nikolova, M.P. Metal oxide nanoparticles and their applications in nanotechnology. *SN Appl. Sci.* **2019**, *1*, 1–30, doi:10.1007/s42452-019-0592-3.

27. Ahmad, F.; Ashraf, N.; Ashraf, T.; Zhou, R. Bin; Yin, D.C. Biological synthesis of metallic nanoparticles (MNPs) by plants and microbes: their cellular uptake, biocompatibility, and biomedical applications. *Appl. Microbiol. Biotechnol.* **2019**, *103*, 2913–2935, doi:10.1007/s00253-019-09675-5.

28. Das, R.K.; Laxman, V.; Linson, P. Biological synthesis of metallic nanoparticles : plants , animals and microbial aspects. *Nanotechnol. Environ. Eng.* **2017**, *2*, 1–21, doi:10.1007/s41204-017-0029-4.

29. Stankic, S.; Suman, S.; Haque, F.; Vidic, J. Pure and multi metal oxide nanoparticles: Synthesis, antibacterial and cytotoxic properties. *J. Nanobiotechnology* **2016**, *14*, 1–20, doi:10.1186/s12951-016-0225-6.

30. Sharma, D.; Rajput, J.; Kaith, B.S.; Kaur, M.; Sharma, S. Synthesis of ZnO nanoparticles and

study of their antibacterial and antifungal properties. *Thin Solid Films* **2010**, *519*, 1224–1229, doi:10.1016/j.tsf.2010.08.073.

31. Pinho, A.; Rebelo, S.; Pereira, M. The Impact of Zinc Oxide Nanoparticles on Male (In)Fertility. *Materials (Basel).* **2020**, *13*, 1–18, doi:https://doi.org/10.3390/ma13040849.

32. Augustine, R.; Mathew, A.P.; Sosnik, A. Metal Oxide Nanoparticles as Versatile Therapeutic Agents Modulating Cell Signaling Pathways: Linking Nanotechnology with Molecular Medicine. *Appl. Mater. Today* **2017**, *7*, 91–103, doi:10.1016/j.apmt.2017.01.010.

33. Al-fartusie, F.S.; Mohssan, S.N. Trace Elements and Their Vital Roles in Human Body. *Indian J. Adv. Chem. Sci.* **2017**, *5*, 127–136, doi:10.22607/IJACS.2017.503003.

34. Huxford, R.C.; Della Rocca, J.; Lin, W. Metal-organic frameworks as potential drug carriers. *Curr. Opin. Chem. Biol.* **2010**, *14*, 262–268, doi:10.1016/j.cbpa.2009.12.012.

35. Raven, E.; Le Brun, N.E.; McMaster, J.; Reedijk, J.; Robinson, N.J. *Bioinorganic chemistry*; 2013; Vol. 42; ISBN 0935702571.

36. Bost, M.; Houdart, S.; Oberli, M.; Kalonji, E.; Huneau, J.F.; Margaritis, I. Dietary copper and human health: Current evidence and unresolved issues. *J. Trace Elem. Med. Biol.* **2016**, *35*, 107–115, doi:10.1016/j.jtemb.2016.02.006.

37. Venkatachalam, M.; Govindaraju, K.; Mohamed Sadiq, A.; Tamilselvan, S.; Ganesh Kumar, V.; Singaravelu, G. Functionalization of gold nanoparticles as antidiabetic nanomaterial. *Spectrochim. Acta - Part A Mol. Biomol. Spectrosc.* **2013**, *116*, 331–338, doi:10.1016/j.saa.2013.07.038.

38. Gold, K.; Slay, B.; Knackstedt, M.; Gaharwar, A.K. Antimicrobial Activity of Metal and Metal-Oxide Based Nanoparticles. *Adv. Ther.* **2018**, *1*, 1700033, doi:10.1002/adtp.201700033.

39. Lemire, J.A.; Harrison, J.J.; Turner, R.J. Antimicrobial activity of metals: Mechanisms, molecular targets and applications. *Nat. Rev. Microbiol.* **2013**, *11*, 371–384, doi:10.1038/nrmicro3028.

40. Shahzadi, S.; Zafar, N.; Sharif, R. Antibacterial Activity of Metallic Nanoparticles. *Bact. Pathog. Antibact. Control* **2018**, doi:10.5772/intechopen.72526.

41. Beyth, N.; Houri-Haddad, Y.; Domb, A.; Khan, W.; Hazan, R. Alternative antimicrobial approach: Nano-antimicrobial materials. *Evidence-based Complement. Altern. Med.* **2015**, doi:10.1155/2015/246012.

42. Wang, L.; Hu, C.; Shao, L. The-antimicrobial-activity-of-nanoparticles--present-situati. *Int. J. Nanomedicine* **2017**, *12*, 1227–1249.

43. Talebian, N.; Amininezhad, S.M.; Doudi, M. Controllable synthesis of ZnO nanoparticles and their morphology-dependent antibacterial and optical properties. *J. Photochem. Photobiol. B Biol.* **2013**, *120*, 66–73, doi:10.1016/j.jphotobiol.2013.01.004.

44. Jesline, A.; John, N.P.; Narayanan, P.M.; Vani, C.; Murugan, S. Antimicrobial activity of zinc and titanium dioxide nanoparticles against biofilm-producing methicillin-resistant Staphylococcus aureus. *Appl. Nanosci.* **2015**, *5*, 157–162, doi:10.1007/s13204-014-0301-x.

45. Nguyen, N.Y.T.; Grelling, N.; Wetteland, C.L.; Rosario, R.; Liu, H. Antimicrobial Activities and Mechanisms of Magnesium Oxide Nanoparticles (nMgO) against Pathogenic Bacteria, Yeasts, and Biofilms. *Sci. Rep.* **2018**, *8*, 1–23, doi:10.1038/s41598-018-34567-5.

46. Navale, G.R.; Thripuranthaka, M.; Late, Dattatray J Shinde, S.S. Antimicrobial Activity of ZnO Nanoparticles against Pathogenic Bacteria and Fungi. *JSM Nanotechnol. Nanomedicine* **2015**, *3*, 1033.

47. Mageshwari, K.; Sathyamoorthy, R. Flower-shaped CuO Nanostructures: Synthesis, Characterization andAntimicrobial Activity. *J. Mater. Sci. Technol.* **2013**, *29*, 909–914, doi:10.1016/j.jmst.2013.04.020.

48. Anghel, I.; Grumezescu, A.M.; Holban, A.M.; Ficai, A.; Anghel, A.G.; Chifiriuc, M.C. Biohybrid nanostructured iron oxide nanoparticles and Satureja hortensis to prevent fungal biofilm development. *Int. J. Mol. Sci.* **2013**, *14*, 18110–18123, doi:10.3390/ijms140918110.

49. Farias, I.; Santos, C.; Sampaio, F. Antimicrobial Activity of Cerium Oxide Nanoparticles on Opportunistic Microorganisms : A Systematic Review. *Biomed Res. Int.* **2018**, *2018*, doi:https://doi.org/10.1155/2018/1923606.

50. Allahverdiyev, A.M.; Abamor, E.S.; Bagirova, M.; Rafailovich, M. Antimicrobial effects of TiO 2 and Ag 2 O nanoparticles against drug-resistant bacteria and. **2011**, 933–940.

51. Parveen, S.; Wani, A.H.; Shah, M.A.; Devi, H.S.; Bhat, M.Y.; Koka, J.A. Preparation, characterization and antifungal activity of iron oxide nanoparticles. *Microb. Pathog.* **2018**, *115*, 287–292, doi:10.1016/j.micpath.2017.12.068.

52. Mazurkova, N.A.; Spitsyna, Y.E.; Shikina, N. V.; Ismagilov, Z.R.; Zagrebel'nyi, S.N.; Ryabchikova, E.I. Interaction of titanium dioxide nanoparticles with influenza virus. *Nanotechnologies Russ.* **2010**, *5*, 417–420, doi:10.1134/S1995078010050174.

53. Brandelli, A.; Ritter, A.C.; Veras, F. Antimicrobial Activities of Metal Nanoparticles. In *Metal Nanoparticles in Pharma*; Springer, Ed.; 2017 ISBN 9783319637907.

54. Meléndez-Villanueva, M.A.; Morán-Santibañez, K.; Martínez-Sanmiguel, J.J.; Rangel-López, R.; Garza-Navarro, M.A.; Rodríguez-Padilla, C.; Zarate-Triviño, D.G.; Trejo-Ávila, L.M. Virucidal activity of gold nanoparticles synthesized by green chemistry using garlic extract. *Viruses* **2019**, *11*, 1–13, doi:10.3390/v11121111.

55. Hang, X.; Peng, H.; Song, H.; Qi, Z.; Miao, X.; Xu, W. Antiviral activity of cuprous oxide nanoparticles against Hepatitis C Virus in vitro. *J. Virol. Methods* **2015**, *222*, 150–157, doi:10.1016/j.jviromet.2015.06.010.

56. Rasmussen, J.W.; Martinez, E.; Louka, P.; Wingett, D.G. Zinc oxide nanoparticles for selective destruction of tumor cells and potential for drug delivery applications. *Expert Opin. Drug Deliv.* **2010**, *7*, 1063–1077, doi:10.1517/17425247.2010.502560.

57. Loutfy, S.A.; Al-Ansary, N.A.; Abdel-Ghani, N.T.; Hamed, A.R.; Mohamed, M.B.; Craik, J.D.; Salah Eldin, T.A.; Abdellah, A.M.; Hussein, Y.; Hasanin, M.T.M.; et al. Anti-proliferative activities of metallic nanoparticles in an in vitro breast cancer model. *Asian Pacific J. Cancer Prev.* **2015**, *16*, 6039–6046, doi:10.7314/APJCP.2015.16.14.6039.

58. Vinardell, M.P.; Mitjans, M. Antitumor activities of metal oxide nanoparticles. *Nanomaterials* **2015**, *5*, 1004–1021, doi:10.3390/nano5021004.

59. Alphandéry, E. Natural metallic nanoparticles for application in nano-oncology. *Int. J. Mol. Sci.* **2020**, *21*, 1–12, doi:10.3390/ijms21124412.

60. Bai Aswathanarayan, J.; Rai Vittal, R.; Muddegowda, U. Anticancer activity of metal nanoparticles and their peptide conjugates against human colon adenorectal carcinoma cells. *Artif. Cells, Nanomedicine Biotechnol.* **2018**, *46*, 1444–1451,

doi:10.1080/21691401.2017.1373655.

61. Shaukat, A.; Anwar, H.; Mahmood, A.; Hussain, G.; Rasul, A.; Umar, M.; Naeem, M.; Ibrahim, M.; Ali, A. Synthesis cum characterization of MgO and MnO nanoparticles and their assessment as antidiabetic and antioxidative agents in diabetic rat model. *Phys. B Phys. Condens. Matter* **2020**, *602*, doi:10.1016/j.physb.2020.412570.

62. Artimani, T.; Asl, S.; Saidijam, M.; Hasanvand, D.; Afshar, S. Amelioration of diabetes-induced testicular and sperm damage in rats by cerium oxide nanoparticle treatment. *Andrologia* **2018**, *50*, doi:https://doi.org/10.1111/and.13089.

63. El-gharbawy, R.M.; Mahmoud, A.; Abu-risha, S.E. Zinc oxide nanoparticles and a standard antidiabetic drug restore the function and structure of beta cells in Type-2 diabetes. *Biomed. Pharmacother.* **2016**, *84*, 810–820, doi:10.1016/j.biopha.2016.09.068.

64. Alkaladi, A.; Abdelazim, A.M.; Afifi, M. Antidiabetic activity of zinc oxide and silver nanoparticles on streptozotocin-induced diabetic rats. *Int. J. Mol. Sci.* **2014**, *15*, 2015–2023, doi:10.3390/ijms15022015.

65. Ali, L.; Shaker, S.; Pinol, R.; Millan, A.; Hanafy, M.; Helmy, M.; Kamel, M.; Mahmoud, S. Effect of superparamagnetic iron oxide nanoparticles on glucose homeostasis on type 2 diabetes experimental model. *Life Sci.* **2020**, *245*, 117361, doi:10.1016/j.lfs.2020.117361.

66. Prabhu, S.; Vinodhini, S.; Elanchezhiyan, C.; Rajeswari, D. Evaluation of antidiabetic activity of biologically synthesized silver nanoparticles using Pouteria sapota in streptozotocin-induced diabetic rats. *J. Diabetes* **2018**, *10*, 28–42, doi:10.1111/1753-0407.12554.

67. Anderson, D.; Anderson, T.; Fahmi, F. Advances in Applications of Metal Oxide Nanomaterials as Imaging Contrast Agents. *Phys. Status Solidi* **2019**, 1–16, doi:10.1002/pssa.201801008.

68. Thurn, K.T.; Brown, E.M.B.; Wu, A.; Vogt, S.; Lai, B.; Maser, J.; Paunesku, T.; Woloschak, G.E. Nanoparticles for applications in cellular imaging. *Nanoscale Res. Lett.* **2007**, *2*, 430–441, doi:10.1007/s11671-007-9081-5.

69. Huang, H.C.; Barua, S.; Sharma, G.; Dey, S.K.; Rege, K. Inorganic nanoparticles for cancer imaging and therapy. *J. Control. Release* **2011**, *155*, 344–357, doi:10.1016/j.jconrel.2011.06.004.

70. Wolfbeis, O.S. An overview of nanoparticles commonly used in fluorescent bioimaging. *Chem. Soc. Rev.* **2015**, *44*, 4743–4768, doi:10.1039/c4cs00392f.

71. Naseri, N.; Ajorlou, E.; Asghari, F.; Pilehvar-Soltanahmadi, Y. An update on nanoparticle-based contrast agents in medical imaging. *Artif. Cells, Nanomedicine Biotechnol.* **2018**, *46*, 1111–1121, doi:10.1080/21691401.2017.1379014.

72. Arifin, D.; Long, C.; Gilad, A.; Alric, C.; Roux, S.; Tillement, O.; Link, T.; Arepally, A.; Bulte, J. Trimodal Gadolinium-Gold Pancreatic Islet Cells Restore Normoglycemia in Diabetic Mice and Can Be Tracked by Using US , Purpose : Methods : Results : *Radiology* **2011**, *260*, 790–798, doi:10.1148/radiol.11101608/-/DC1.

73. Forte, E.; Fiorenza, D.; Torino, E.; Costagliola di Polidoro, A.; Cavaliere, C.; Netti, P.A.; Salvatore, M.; Aiello, M. Radiolabeled PET/MRI Nanoparticles for Tumor Imaging. *J. Clin. Med.* **2019**, *9*, 89, doi:10.3390/jcm9010089.

74. Jeon, M.; Halbert, M. V.; Stephen, Z.R.; Zhang, M. Iron Oxide Nanoparticles as T1 Contrast Agents for Magnetic Resonance Imaging: Fundamentals, Challenges, Applications, and

Prospectives. *Adv. Mater.* **2020**, *1906539*, 1–18, doi:10.1002/adma.201906539.

75. Guo, W.; Wang, F.; Ding, D.; Song, C.; Guo, C.; Liu, S. TiO 2-x Based Nano-platform for Bimodal Cancer Imaging and NIR-Triggered Chem / Photodynamic / Photothermal Combination Therapy. *Chem. Mater.* **2017**, *29*, 9262–9274, doi:10.1021/acs.chemmater.7b03241.

76. Zhan, Y.; Shi, S.; Ehlerding, E.B.; Graves, S.A.; Goel, S.; Engle, J.W.; Liang, J.; Tian, J.; Cai, W. Radiolabeled , Antibody-Conjugated Manganese Oxide Nanoparticles for Tumor Vasculature Targeted Positron Emission Tomography and Magnetic Resonance Imaging. *ACS Appl. Mater. Interfaces* **2017**, *9*, 38304–38312, doi:10.1021/acsami.7b12216.

77. Xue, S.; Wang, Y.; Wang, M.; Du, X.; Gu, H.; Zhang, C. Iodinated oil-loaded , fluorescent mesoporous silica-coated iron oxide nanoparticles for magnetic resonance imaging / computed tomography / fluorescence trimodal imaging. *Int. J. Nanomedicine* **2014**, *9*, 2527–2538.

78. Guo, Z.; Zhang, P.; Luo, Y.; Xie, H.Q.; Chakraborty, S.; Monikh, F.A.; Bu, L.; Liu, Y.; Ma, Y.; Zhang, Z.; et al. Intranasal exposure to ZnO nanoparticles induces alterations in cholinergic neurotransmission in rat brain. *Nano Today* **2020**, *35*, doi:10.1016/j.nantod.2020.100977.

79. Falchi, L.; Galleri, G.; Dore, G.M.; Zedda, M.T.; Pau, S.; Bogliolo, L.; Ariu, F.; Pinna, A.; Nieddu, S.; Innocenzi, P.; et al. Effect of exposure to CeO 2 nanoparticles on ram spermatozoa during storage at 4 ° C for 96 hours. *Reprod. Biol. Endocrinol.* **2018**, 1–10.

80. Odhiambo, J.; Dejarnette, J.; Geary, T.; Kennedy, C.; Susan, S.; Sutovsky, M.; Sutovsky, P. Increased Conception Rates in Beef Cattle Inseminated with Nanopurified Bull Semen. *Biol. Reprod.* **2014**, *91*, doi:10.1095/biolreprod.114.121897.

81. Makhluf, S.; Qasem, R.; Rubinstein, S.; Gedanken, A. Loading Magnetic Nanoparticles into Sperm Cells Does Not Affect Their Functionality. *Langmuir* **2006**, *22*, 9480–9482.

82. Stern, S.T.; McNeil, S.E. Nanotechnology safety concerns revisited. *Toxicol. Sci.* **2008**, *101*, 4–21, doi:10.1093/toxsci/kfm169.

83. Chenthamara, D.; Subramaniam, S.; Ramakrishnan, S.G.; Krishnaswamy, S.; Essa, M.M.; Lin, F.H.; Qoronfleh, M.W. Therapeutic efficacy of nanoparticles and routes of administration. *Biomater. Res.* **2019**, *23*, 1–29, doi:10.1186/s40824-019-0166-x.

84. Song, B.; Zhang, Y.L.; Liu, J.; Feng, X.L.; Zhou, T.; Shao, L.Q. Is Neurotoxicity of Metallic Nanoparticles the Cascades of Oxidative Stress? *Nanoscale Res. Lett.* **2016**, *11*, doi:10.1186/s11671-016-1508-4.

85. Jørgensen, N.; Asklund, C.; Carlsen, E.; Skakkebæk, N.E. Coordinated European investigations of semen quality : results from studies of Scandinavian young men is a matter of concern. *Int. J. Androl.* **2006**, *29*, 54–61, doi:10.1111/j.1365-2605.2005.00635.x.

86. Levine, H.; Jørgensen, N.; Martino-, A.; Mendiola, J.; Weksler-derri, D.; Mindlis, I.; Pinotti, R.; Swan, S.H. Temporal trends in sperm count: a systematic review and meta-regression analysis. *Hum. Reprod. Update* **2017**, *23*, 646–659, doi:10.1093/humupd/dmx022.

87. Agarwal, A.; Mulgund, A.; Hamada, A.; Chyatte, M.R. A unique view on male infertility around the globe. *Reprod. Biol. Endocrinol.* **2015**, 1–9, doi:10.1186/s12958-015-0032-1.

88. Chandel, M.; Jain, G. Toxic effects of transition metals on male reproductive system: A review. *J. Environ. Occup. Sci.* **2014**, *3*, 204, doi:10.5455/jeos.20140929042630.

89. Benatta, M.; Kettache, R.; Buchholz, N.; Trinchieri, A. The impact of nutrition and lifestyle on male fertility. *Arch. Ital. di Urol. e Androl.* **2020**, *92*, 121–131, doi:https://doi.org/10.4081/aiua.2020.2.121.

90. Tang, Y.; Chen, B.; Hong, W.; Chen, L.; Yao, L.; Zhao, Y.; Aguilar, Z.P.; Xu, H. ZnO nanoparticles induced male reproductive toxicity based on the effects on the endoplasmic reticulum stress signaling pathway. *Int. J. Nanomedicine* **2019**, *14*, 9563–9576, doi:10.2147/IJN.S223318.

91. Afifi, M.; Almaghrabi, O.A.; Kadasa, N.M. Ameliorative Effect of Zinc Oxide Nanoparticles on Antioxidants and Sperm Characteristics in Streptozotocin-Induced Diabetic Rat Testes. *Biomed Res. Int.* **2015**, *2015*, doi:10.1155/2015/153573.

92. Pinho, A.R.; Martins, F.; Costa, M.E. V.; Senos, A.M.R.; Silva, O.A.B. d. C.E.; Pereira, M. de L.; Rebelo, S. In Vitro Cytotoxicity Effects of Zinc Oxide Nanoparticles on Spermatogonia Cells. *Cells* **2020**, *9*, doi:10.3390/cells9051081.

93. Mäkelä, J.-A.; Toppari, J. Spermatogenesis. In *Endocrinology*; Simoni, M., Huhtaniemi, I.T., Eds.; Springer International Publishing, 2017; pp. 417–455 ISBN 9783319444413.

94. Kretser, D.M. De; Loveland, K.L.; Meinhardt, A.; Simorangkir, D.; Wreford, N. Spermatogenesis. *Hum. Reprod.* **1998**, *13*.

95. Yan Cheng, C.; Mruk, D.D. *Biochemistry of Sertoli cell/germ cell junctions, germ cell transport, and spermiation in the seminiferous epithelium*; Elsevier Inc., 2015; ISBN 9780124170476.

96. Gao, G.; Ze, Y.; Zhao, X.; Sang, X.; Zheng, L.; Ze, X.; Gui, S.; Sheng, L.; Sun, Q.; Hong, J.; et al. Titanium dioxide nanoparticle-induced testicular damage , spermatogenesis suppression , and gene expression alterations in male mice. *J. Hazard. Mater.* **2013**, *258–259*, 133–143, doi:10.1016/j.jhazmat.2013.04.046.

97. Sundarraj, K.; Manickam, V.; Raghunath, A.; Periyasamy, M.; Viswanathan, M.; Perumal, E. Repeated Exposure to Iron Oxide Nanoparticles Causes Testicular Toxicity in Mice. *Environ. Toxicol.* **2016**, 594–608, doi:10.1002/tox.22262.

98. Takeda, K.; Suzuki, K.I.; Ishihara, A.; Kubo-Irie, M.; Fujimoto, R.; Tabata, M.; Oshio, S.; Nihei, Y.; Ihara, T.; Sugamata, M. Nanoparticles transferred from pregnant mice to their offspring can damage the genital and cranial nerve systems. *J. Heal. Sci.* **2009**, *55*, 95–102, doi:10.1248/jhs.55.95.

99. McAuliffe, M.E.; Perry, M.J. Are nanoparticles potential male reproductive toxicants? A literature review. *Nanotoxicology* **2007**, *1*, 204–210, doi:10.1080/17435390701675914.

100. Gallo, A.; Boni, R.; Buttino, I.; Tosti, E. Spermiotoxicity of nickel nanoparticles in the marine invertebrate Ciona intestinalis (ascidians). *Nanotoxicology* **2016**, *10*, 1096–1104, doi:10.1080/17435390.2016.1177743.

101. Liu, Y.; Li, X.; Xiao, S.; Liu, X.; Chen, X.; Xia, Q.; Lei, S.; Li, H.; Zhong, Z.; Xiao, K. The Effects of Gold Nanoparticles on Leydig Cells and Male Reproductive Function in Mice . *Int. J. Nanomedicine* **2020**, *Volume 15*, 9499–9514, doi:10.2147/ijn.s276606.

102. Sharma, R.; Agarwal, A. *Sperm Chromatin: Biological and Clinical Applications in Male Infertility and Assisted Reproduction*; Zini, A., Agarwal, A., Eds.; 1st ed.; Springer, 2011; ISBN 9781441968579.

103. Manku, G.; Culty, M. Mammalian gonocyte and spermatogonia differentiation: Recent advances and remaining challenges. *Reproduction* **2015**, *149*, R139–R157,

doi:10.1530/REP-14-0431.

104. Hess, R.A.; De Franca, L.R. Spermatogenesis and cycle of the seminiferous epithelium. *Adv. Exp. Med. Biol.* **2008**, *636*, 1–15, doi:10.1007/978-0-387-09597-4_1.

105. Pereira, C.; Serrano, J.; Martins, F.; Silva, O.; Rebelo, S. Nuclear envelope dynamics during mammalian spermatogenesis: new insights on male fertility. *Biol. Rev.* **2019**, *94*, 1195–1219, doi:10.1111/brv.12498.

106. Donnell, L.; Nicholls, P.; Bryan, M.; Mclachlan, R.; Stanton, P. Spermiation: the process of sperm release. *Spermatogenesis* **2011**, *1*, 14–35, doi:10.4161/spmg.1.1.14525.

107. Tapia, J.; Peña, F. *Apoptotic Events in Male Germ Cells and in Mature Mammalian Spermatozoa*; Salido G.M., R.J.A., Ed.; Springer, Dordrecht, 2009; ISBN 9781402098734.

108. Préaubert, L.; Tassistro, V.; Au, M.; Sari-minodier, I.; Rose, J.; Courbiere, B.; Perrin, J. Very low concentration of cerium dioxide nanoparticles induce DNA damage, but no loss of vitality, in human spermatozoa. *Toxicol. Vitr.* **2018**, *50*, 236–241, doi:10.1016/j.tiv.2018.03.013.

109. Basioura, A.; Michos, I.; Ntemka, A.; Karagiannis, I.; Boscos, M. Effect of iron oxide and silver nanoparticles on boar semen CASA motility and kinetics. *J. Hell. Vet. Med. Soc.* **2020**, *71*, 2331–2338.

110. Zhang, X.; Yue, Z.; Zhang, H.; Liu, L.; Zhou, X. Repeated administrations of Mn3O4 nanoparticles cause testis damage and fertility decrease through PPAR-signaling pathway. *Nanotoxicology* **2020**, *14*, 326–340, doi:10.1080/17435390.2019.1695976.

111. Pawar, K.; Kaul, G. Toxicity of titanium oxide nanoparticles causes functionality and DNA damage in buffalo (Bubalus bubalis) sperm in vitro. *Toxicol. Ind. Health* **2014**, *30*, 520–533, doi:10.1177/0748233712462475.

112. Mao, Z.; Yao, M.; Xu, B.; Ji, X.; Jiang, H.; Han, X.; Tang, Q.; Zhou, Z.; Chen, R.; Li, X.; et al. Cytoskeletons of two reproductive germ cell lines response differently to titanium dioxide nanoparticles mediating vary reproductive toxicity. *J. Biomed. Nanotechnol.* **2017**, *13*, 409–416, doi:10.1166/jbn.2017.2360.

113. Santonastaso, M.; Mottola, F.; Colacurci, N.; Iovine, C.; Pacifico, S.; Cammarota, M.; Cesaroni, F.; Rocco, L. In vitro genotoxic effects of titanium dioxide nanoparticles (n-TiO2) in human sperm cells. *Mol. Reprod. Dev.* **2019**, *86*, 1369–1377, doi:10.1002/mrd.23134.

114. Barkhoradi, A.; Hekmatimoghaddam, S.; Jebali, A.; Khalili, M.; Talebi, A.; Noorani, M. Effect of zinc oxide nanoparticles on viability of human spermatozoa. *Iran. J. Reprod. Med.* **2013**, *11*, 767–771.

115. Han, Z.; Yan, Q.; Ge, W.; Liu, Z.-G.; Gurunathan, S.; Felici, M.; Shen, W.; Zang, X.-F. Cytotoxic effects of ZnO nanoparticles on mouse testicular cells. *Int. J. Nanomedicine* **2016**, *11*, 5187–5203.

116. Liu, Q.; Xu, C.; Ji, G.; Liu, H.; Mo, Y.; Tollerud, D.J.; Gu, A.; Zhang, Q. Sublethal effects of zinc oxide nanoparticles on male reproductive cells. *Toxicol. Vitr.* **2016**, *35*, 131–138, doi:10.1016/j.tiv.2016.05.017.

117. Bara, N.; Kaul, G. Enhanced steroidogenic and altered antioxidant response by ZnO nanoparticles in mouse testis Leydig cells. *Toxicol. Ind. Health* **2018**, *34*, 571–588, doi:10.1177/0748233718774220.

118. Shen, J.; Yang, D.; Zhou, X.; Wang, Y.; Tang, S.; Yin, H. Role of Autophagy in Zinc Oxide

Nanoparticles-Induced Apoptosis of Mouse LEYDIG Cells. *Int. J. Mol.* **2019**, *20*.

119. Pan, Y.; Neuss, S.; Leifert, A.; Fischler, M.; Wen, F.; Simon, U.; Schmid, G.; Brandau, W.; Jahnen-dechent, W. Size-Dependent Cytotoxicity of Gold Nanoparticles. *Small* **2007**, *3*, 1941–1949, doi:10.1002/smll.200700378.

120. Gromadzka-ostrowska, J.; Dziendzikowska, K.; Lankoff, A.; Radzikowska, J.; Wojewódzka, M.; Kruszewski, M. Silver nanoparticles effects on epididymal sperm in rats. *Toxicol. Lett.* **2012**, *214*, 251–258, doi:10.1016/j.toxlet.2012.08.028.

121. Valko, M.; Leibfritz, D.; Moncol, J.; Cronin, M.; Mazur, M.; Telser, J. Free radicals and antioxidants in normal physiological functions and human disease. *Int. J. Biochem. Cell Biol.* **2007**, *39*, 44–84, doi:10.1016/j.biocel.2006.07.001.

122. Castellini, C.; Ruggeri, S.; Mattioli, S.; Bernardini, G.; Macchioni, L.; Moretti, E.; Collodel, G. Long-term effects of silver nanoparticles on reproductive activity of rabbit buck. *Syst. Biol. Reprod. Med.* **2014**, *60*, 143–150, doi:10.3109/19396368.2014.891163.

123. Yousef, M.; Al-hamadani, M.; Kamel, M. Reproductive Toxicity of Aluminum Oxide Nanoparticles and Zinc Oxide Nanoparticles in Male Rats. *Nanoparticle* **2019**, *1*, 1–10, doi:10.35702/nano.10002.

124. Qin, F.; Shen, T.; Li, J.; Qian, J.; Zhang, J.; Zhou, G.; Tong, J. SF-1 mediates reproductive toxicity induced by Cerium oxide nanoparticles in male mice. *J. Nanobiotechnology* **2019**, *17*, 1–13, doi:10.1186/s12951-019-0474-2.

125. Nasri, S.; Rezai-zarchi, S.; Kerishchi, P.; Sadeghi, S. The Effect of Iron Oxide Nanoparticles on Sperm Numbers and Mobility in Male Mice. *Zahedan J. Res. Med. Sci.* **2015**, *17*, 10–12, doi:10.17795/zjrms-2185.

126. Varzeghani, S.M.; Parivar, K.; Abdollahifar, M.-A.; Karamian, A. Effects of Iron Oxide Nanoparticles on Mouse Sperm Parameters and Testicular Tissue. *Iran. J. Toxicol.* **2018**, *12*, 39–44.

127. Ahmed Ibrahim Younus; Mokhtar Ibrahim Yousef; Maher Abdel-NabiKamel; Rakhad Alrawi; Jubran Mohammed Abdulrahman Changes in semen characteristics and sex hormones of rats treated with iron oxide nanoparticles, silver nanoparticles and their mixture. *GSC Biol. Pharm. Sci.* **2020**, *12*, 229–237, doi:10.30574/gscbps.2020.12.2.0272.

128. Negahdary, M.; Arefian, Z.; Dastjerdi, H.A.; Ajdary, M. Toxic effects of Mn2O3 nanoparticles on rat testis and sex hormone. *J. Nat. Sci. Biol. Med.* **2015**, *6*, 335–339, doi:10.4103/0976-9668.159998.

129. Yousefalizadegan, N.; Mousavi, Z.; Rastegar, T.; Razavi, Y.; Najafizadeh, P. Reproductive toxicity of manganese dioxide in forms of micro-and nanoparticles in male rats. *Int. J. Reprod. Biomed.* **2019**, *17*, 361–370, doi:10.18502/ijrm.v17i5.4603.

130. Hong, F.; Si, W.; Zhao, X.; Wang, L.; Zhou, Y.; Chen, M.; Ge, Y.; Zhang, Q.; Wang, Y.; Zhang, J. TiO2 Nanoparticle Exposure Decreases Spermatogenesis via Biochemical Dysfunctions in the Testis of Male Mice. *J. Agric. Food Chem.* **2015**, *63*, 7084–7092, doi:10.1021/acs.jafc.5b02652.

131. Hong, F.; Zhao, X.; Si, W.; Ze, Y.; Wang, L. Decreased spermatogenesis led to alterations of testis-specific gene expression in male mice following nano-TiO 2 exposure. *J. Hazard. Mater.* **2015**, *300*, 718–728, doi:10.1016/j.jhazmat.2015.08.010.

132. Meena, R.; Kajal, K.; Paulraj, R. Cytotoxic and Genotoxic Effects of Titanium Dioxide

Nanoparticles in Testicular Cells of Male Wistar Rat. *Appl. Biochem. Biotechnol.* **2015**, *175*, 825–840, doi:10.1007/s12010-014-1299-y.

133. Morgan, A.; El-hamid, M.; Noshy, P. Reproductive Toxicity Investigation of Titanium Dioxide Nanoparticles in Male Albino Rats. *World J. Pharm. Pharm. Sci.* **2015**, *4*, 34–49.

134. Miura, N.; Ohtani, K.; Hasegawa, T.; Yoshioka, H.; Hwang, G.W. High sensitivity of testicular function to titanium nanoparticles. *J. Toxicol. Sci.* **2017**, *42*, 359–366, doi:10.2131/jts.42.359.

135. Morgan, A.M.; Ibrahim, M.A.; Noshy, P.A. Reproductive toxicity provoked by titanium dioxide nanoparticles and the ameliorative role of Tiron in adult male rats. *Biochem. Biophys. Res. Commun.* **2017**, *486*, 595–600, doi:10.1016/j.bbrc.2017.03.098.

136. Song, G.; Lin, L.; Liu, L.; Wang, K.; Ding, Y.; Niu, Q.; Mu, L.; Wang, H.; Shen, H.; Guo, S. Toxic effects of anatase titanium dioxide nanoparticles on spermatogenesis and testicles in male mice. *Polish J. Environ. Stud.* **2017**, *26*, 2739–2746, doi:10.15244/pjoes/70807.

137. Lauvås, A.J.; Skovmand, A.; Poulsen, M.S.; Kyjovska, Z.O.; Roursgaard, M.; Goericke-Pesch, S.; Vogel, U.; Hougaard, K.S. Airway exposure to TiO2 nanoparticles and quartz and effects on sperm counts and testosterone levels in male mice. *Reprod. Toxicol.* **2019**, *90*, 134–140, doi:10.1016/j.reprotox.2019.07.023.

138. Miura, N.; Ohtani, K.; Hasegawa, T.; Yoshioka, H.; Hwang, G.W. Biphasic adverse effect of titanium nanoparticles on testicular function in mice. *Sci. Rep.* **2019**, *9*, 81–85, doi:10.1038/s41598-019-50741-9.

139. Jafari, A.; Karimipour, M.; Khaksar, M.R.; Ghasemnejad-Berenji, M. Protective effects of orally administered thymol against titanium dioxide nanoparticle–induced testicular damage. *Environ. Sci. Pollut. Res.* **2020**, *27*, 2353–2360, doi:10.1007/s11356-019-06937-7.

140. Ogunsuyi, O.M.; Ogunsuyi, O.I.; Akanni, O.; Alabi, O.A.; Alimba, C.G.; Adaramoye, O.A.; Cambier, S.; Eswara, S.; Gutleb, A.C.; Bakare, A.A. Alteration of sperm parameters and reproductive hormones in Swiss mice via oxidative stress after co-exposure to titanium dioxide and zinc oxide nanoparticles. *Andrologia* **2020**, *52*, 1–17, doi:10.1111/and.13758.

141. Talebi, A.R.; Khorsandi, L.; Moridian, M. The effect of zinc oxide nanoparticles on mouse spermatogenesis. *J. Assist. Reprod. Genet.* **2013**, *30*, 1203–1209, doi:10.1007/s10815-013-0078-y.

142. Abbasalipourkabir, R.; Moradi, H.; Zarei, S.; Asadi, S.; Salehzadeh, A.; Ghafourikhosroshahi, A.; Mortazavi, M.; Ziamajidi, N. Toxicity of zinc oxide nanoparticles on adult male Wistar rats. *Food Chem. Toxicol.* **2015**, *84*, 154–160, doi:10.1016/j.fct.2015.08.019.

143. Mozaffari, Z.; Parivar, K.; Roodbari, N.H.; Irani, S. Histopathological Evaluation of the Toxic Effects of Zinc Oxide (ZnO) Nanoparticles on Testicular Tissue of NMRI Adult Mice. *Adv. Stud. Biol.* **2015**, *7*, 275–291, doi:http://dx.doi.org/10.12988/asb.2015.5425.

144. Hussein, M.; Ali, H.; Saadeldin, I.; Ahmed, M. Querectin Alleviates Zinc Oxide Nanoreprotoxicity in Male Albino Rats. *J. Biochem. Mol. Toxicol.* **2016**, *30*, 489–496, doi:10.1002/jbt.

145. Srivastav, A.K.; Kumar, A.; Prakash, J.; Singh, D.; Jagdale, P.; Shankar, J.; Kumar, M. Genotoxicity evaluation of zinc oxide nanoparticles in Swiss mice after oral administration using chromosomal aberration, micronuclei, semen analysis, and RAPD profile. *Toxicol. Ind. Health* **2017**, *33*, 821–834, doi:10.1177/0748233717717842.

146. Mesallam, D.; Deraz, R.; Abdel Aal, S.; Ahmed, S. Toxicity of Subacute Oral Zinc Oxide

Nanoparticles on Testes and Prostate of Adult Albino Rats and Role of Recovery. *J. Histol. Histopathol.* **2019**, *6*, 2, doi:10.7243/2055-091x-6-2.

147. Radhi, M.J.; Adnan, G.; Latef, A. Effect of Zinc oxide nanoparticles (ZnO-NPs) on weights of some reproductive organs and sperm abnormalities in the tail of epididymis of albino mice. *J. Pharm. Sci. Res.* **2019**, *11*, 243–246.

148. Salman, R.A. The Influence of ZnO NPs on Reproductive System Tissues of Albino Male Mice . Histopathological Study. *Int. J. Sci. Res.* **2021**, *6*, 2021–2025, doi:10.21275/ART20175455.

149. Hess, R.; Chen, P. Computer tracking of germ cells in the cycle of the seminiferous epithelium and prediction of changes in cycle duration in animals commonly used in reproductive biology and toxicology. *J. Androl.* **1992**, *13*.

150. Millaku, L.; Imeri, R.; Trebicka, A. Histopathological changes in testes of house sparrow (Passer domesticus). *J. Mater. Environ. Sci.* **2015**, *6*, 1292–1296.

151. Saleh, R.; Agarwal, A. Oxidative Stress and Male Infertility: From Research Bench to Clinical Practice. *J. Androl.* **2002**, *23*.

152. Tremellen, K. Oxidative stress and male infertility — a clinical perspective. *Hum. Reprod. Updat.* **2008**, *14*, 243–258.

153. Huang, H.; Feng, W.; Chen, Y.; Shi, J. Inorganic nanoparticles in clinical trials and translations. *Nano Today* **2020**, *35*, 100972, doi:10.1016/j.nantod.2020.100972.

154. Shandilya, R.; Mishra, P.K.; Pathak, N.; Lohiya, N.K.; Sharma, R.S. Nanotechnology in reproductive medicine: Opportunities for clinical translation. *Clin. Exp. Reprod. Med.* **2020**, *47*, 245–262, doi:10.5653/cerm.2020.03650.

155. Isaac, A. V.; Kumari, S.; Nair, R.; Urs, D.R.; Salian, S.R.; Kalthur, G.; Adiga, S.K.; Manikkath, J.; Mutalik, S.; Sachdev, D.; et al. Supplementing zinc oxide nanoparticles to cryopreservation medium minimizes the freeze-thaw-induced damage to spermatozoa. *Biochem. Biophys. Res. Commun.* **2017**, *494*, 656–662, doi:10.1016/j.bbrc.2017.10.112.

156. Durfey, C.L.; Swistek, S.E.; Liao, S.F.; Crenshaw, M.A.; Clemente, H.J.; Thirumalai, R.V.K.G.; Steadman, C.S.; Ryan, P.L.; Willard, S.T.; Feugang, J.M. Nanotechnology-based approach for safer enrichment of semen with best spermatozoa. *J. Anim. Sci. Biotechnol.* **2019**, *10*, 1–12, doi:10.1186/s40104-018-0307-4.

157. Chang, M.; Chang, Y.-J.; Wang, T.-Y.; Yu, Q. Sperm Movement Control Utilizing Surface Charged Magnetic Nanoparticles. *J. Nanosci. Nanotechnol.* **2019**, *19*, 5713–5722, doi:10.1166/jnn.2019.16551.

158. Moridi, H.; Hosseini, S.A.; Shateri, H.; Kheiripour, N.; Kaki, A.; Hatami, M.; Ranjbar, A. Protective effect of cerium oxide nanoparticle on sperm quality and oxidative damage in malathioninduced testicular toxicity in rats: An experimental study. *Int. J. Reprod. Biomed.* **2018**, *16*, 261–266, doi:10.29252/ijrm.16.4.261.

159. Kim, J.H.; Lee, H.J.; Doo, S.H.; Yang, W.J.; Choi, D.; Kim, J.H.; Won, J.H.; Song, Y.S. Use of nanoparticles to monitor human mesenchymal stem cells transplanted into penile cavernosum of rats with erectile dysfunction. *Korean J. Urol.* **2015**, *56*, 280–287, doi:10.4111/kju.2015.56.4.280.

160. Kobyliak, N.M.; Falalyeyeva, T.M.; Kuryk, O.G.; Beregova, T. V.; Bodnar, P.M.; Zholobak, N.M.; Shcherbakov, O.B.; Bubnov, R. V.; Spivak, Y.M. Antioxidative effects of cerium dioxide

nanoparticles ameliorate age-related male infertility: Optimistic results in rats and the review of clinical clues for integrative concept of men health and fertility. *EPMA J.* **2015**, *6*, 1–22, doi:10.1186/s13167-015-0034-2.

161. Bitounis, D.; Klein, J.P.; Mery, L.; El-Merhie, A.; Forest, V.; Boudard, D.; Pourchez, J.; Cottier, M. Ex vivo detection and quantification of gold nanoparticles in human seminal and follicular fluids. *Analyst* **2018**, *143*, 475–486, doi:10.1039/c7an01641g.

Chapter 2

Aims

A growing amount of evidence has demonstrated that ZnO NPs can interfere with all types of male reproductive cells in a dose and time-dependent manner [1–3]. Due to their widespread use, exposure is almost inevitable.

In this context, it is essential to evaluate not only the immediate effects of ZnO NPs on reproductive cells but also how these effects evolve over time. To date, there are no studies on the reversibility of the cytotoxic effects of ZnO NPs in a male reproductive GC-1 spg cell line. But what happens to cells upon the removal of the NPs must be considered when assessing the reproductive toxicity of nanomaterials. While there is no consensus about the effects of NPs on the male reproductive system, the search for approaches that can protect male reproductive health must continue.

There is a growing interest in antioxidants as preventive or therapeutic agents against NPs-mediated injuries [4–6]. However, few studies have described the toxicity and the protective effects of antioxidants against ZnO NPs on cells from the early stages of spermatogenesis. Some studies have indicated that chalcones may have antioxidant properties due to their free radical scavenging activities [7], but no data are available on their effects on the cytotoxicity induced by NPs in reproductive cells. Therefore, the purpose to the specific aims of this dissertation are the following:

- Compare the effects of ZnO NPs on cells of the first stage of spermatogenesis (GC-1) at two different timepoints: immediately after the exposure to ZnO NPs and after a recovery period;
- Understand whether short exposures to a cytotoxic concentration of ZnO NPs permanently affect GC-1 cells;
- Determine the viability of the GC-1 cells upon exposure with different chalcone VS3 concentrations;
- Evaluate whether synthetic chalcone VS3 can prevent or alleviate the cytotoxic effects induced by NPs on spermatogonia cells;
- Understand if the potential protective effect of VS3 is related to antioxidant activity.

References:

1. Pinho, A.R.; Martins, F.; Costa, M.E. V.; Senos, A.M.R.; Silva, O.A.B. d. C.E.; Pereira, M. de L.; Rebelo, S. In Vitro Cytotoxicity Effects of Zinc Oxide Nanoparticles on Spermatogonia Cells. *Cells* **2020**, *9*, doi:10.3390/cells9051081.

2. Barkhoradi, A.; Hekmatimoghaddam, S.; Jebali, A.; Khalili, M.; Talebi, A.; Noorani, M. Effect of zinc oxide nanoparticles on viability of human spermatozoa. *Iran. J. Reprod. Med.* **2013**, *11*, 767–771.

3. Shen, J.; Yang, D.; Zhou, X.; Wang, Y.; Tang, S.; Yin, H. Role of Autophagy in Zinc Oxide Nanoparticles-Induced Apoptosis of Mouse LEYDIG Cells. *Int. J. Mol.* **2019**, *20*.

4. Özgür, M.E. The protective effects of Vitamin C and Trolox on kinematic and oxidative stress indices in rainbow trout sperm cells against flower-like ZnO nanoparticles. *Aquac. Res.* **2019**, *50*, 2838–2845, doi:10.1111/are.14236.

5. Özgür, M.E.; Ulu, A.; Noma, S.A.A.; Özcan, İ.; Balcıoğlu, S.; Ateş, B.; Köytepe, S. Melatonin protects sperm cells of Capoeta trutta from toxicity of titanium dioxide nanoparticles. *Environ. Sci. Pollut. Res.* **2020**, *27*, 17843–17853, doi:10.1007/s11356-020-08273-7.

6. Hussein, M.M.A.; Ali, H.A.; Saadeldin, I.M.; Ahmed, M.M. Querectin Alleviates Zinc Oxide Nanoreprotoxicity in Male Albino Rats. *J. Biochem. Mol. Toxicol.* **2016**, *30*, 489–496, doi:10.1002/jbt.21812.

7. Martins, T.; Silva, V.L.M.; Silva, A.M.S.; Lima, J.L.F.C.; Fernandes, E.; Ribeiro, D. Chalcones as Scavengers of HOCl and Inhibitors of Oxidative Burst: Structure-Activity Relationship Studies. *Med. Chem. (Los. Angeles).* **2020**, *17*, 1–9.

Chapter 3

Recovery of cytotoxicity in spermatogonia cells upon Zinc Oxide Nanoparticles treatment

Abstract

Exposure to ZnO NPs induces several cellular alterations in male reproductive cells. Herein, a spermatogonia cell line (GC-1 spg) was incubated with a cytotoxic concentration of ZnO NPs (20 µg/mL) for two different short periods, 6h and 12 h. Exposure to ZnO NPs induced a viability decrease of 25% and 41%, after 6h and 12h of incubation periods, respectively. Then, cells were allowed to recover in an NPs-free environment for four days. At the end of the recovery period (4 days), cells that were exposed to ZnO NPs for 6 and 12h had a viability increase of 16% and 25%, respectively. Additionally, light microscopy images revealed that cells were able to divide despite the damage caused by NPs.

In conclusion, although the results obtained in the viability assay performed on the fourth day without ZnO NPs suggest a trend towards recovery, the fact is that GC-1 cells were not able to fully recover. As a result, other treatment strategies should be investigated to alleviate the reproductive toxicity of ZnO NPs.

Keywords: zinc oxide nanoparticles, spermatogonia cells, recovery, fertility, reproductive toxicity

1. Introduction

Due to the widespread use of nanoparticles, the question of whether these nanomaterials have a negative impact on human health, especially on the reproductive system, remains a matter of concern. The male reproductive toxicology caused by nanoparticles has drawn more attention because testis is known to be more sensitive to exogenous materials than other organs [1]. In fact, male infertility is a rising global problem that affects an estimated 70 million people worldwide, with the highest incidence in industrialized countries [2]. In general, most NPs induce adverse effects on spermatogenesis at many levels, but some NPs, show no adverse effects at all. Reproductive toxicity of nanoparticles was reported in 82% and 72% of *in vitro* and *in vivo* studies with male mammals, respectively. Of note, in 19% of these studies, NPs did not interfere with male reproductive cells [2]. However, we should keep in mind that these negative results may be attributed to the use of NPs with different characteristics and also huge variability of experimental conditions.

Although the male reproductive system is known to be vulnerable to many exogenous materials, it has previously been recognized that the testis itself can recover from some injuries [3,4], meaning that the lesions induced by NPs can be reversible, and male fertility may remain unaffected [5]. This may be related to the fact that mammalian cells have many active and efficient defense mechanisms.

The antioxidant defense system is the most important defense mechanism against oxidative stress-induced cell damage [6]. It consists of enzymatic components, such as peroxide dismutase (SOD), catalase (CAT), and glutathione peroxidase (GPx) [7]. These enzymes scavenge free

radicals and their by-products transforming them into less reactive species to protect proteins and other biomolecules. For example, the SOD enzyme converts superoxide radicals into hydrogen peroxide, which is then broken down by catalysis into water and oxygen [8]. Free radicals, commonly known as reactive oxygen species (ROS), are unstable molecules produced predominantly in organelles such as the endoplasmic reticulum, peroxisomes, but mainly, at mitochondria [9]. These molecules have unpaired electrons in their upper electron layer, which explains their tendency to react with almost every type of molecule in the body, oxidizing them. Among them, lipids, proteins, and DNA are the main targets [10]. Under physiological conditions, there is a pro-oxidant-antioxidant balance. However, NPs can create ROS bursts in cells and/or inhibit the activity of the cells' antioxidants. This starts a sequence of reactions, which leads to an imbalance between ROS production and the antioxidant system, resulting in oxidative stress [11].

NPs can induce DNA damage by binding directly to DNA or through ROS overproduction. Excessive ROS can directly attack DNA by oxidizing nucleoside bases, producing modified nucleotides (8-hydroxy-2'-deoxyguanosine, 8-OHdG), which ultimately may result in DNA strand breaks [10]. In response to DNA disruption, a defense biological response is triggered to maintain genomic integrity. In that case, the cell triggers repair mechanisms, such as regulation of the cell cycle through checkpoints, DNA repair regulators, and cell death mechanisms to prevent the loss of genetic information and mutations [12]. Cell cycle checkpoints are important players in cell repair mechanisms providing time for cells to analyze and overcome any disruption before proceeding into the next phase of the cell cycle [13]. DNA repair pathways include the nucleotide repair (NR), base excision repair (BER), mismatch repair (MMR), and double strand break repair, including homologous recombination repair (HR), and non-homologous end joining (NHEJ) repair [14]. However, at some points, NPs can also repress those DNA damage repair mechanisms, which can result in genome instability, that may ultimately contribute to cell death or cancer [15].

The cell defense mechanisms mentioned above may be the reason why *in vitro* and *in vivo* studies are starting to emerge, suggesting that the male reproductive system can recover from the damage induced by different types of NPs. Previous studies co-exposed human sperm cells to TiO_2 and $CdCl_2$ NPs and it was found that sperm DNA fragmentation decreased with increasing exposure time, suggesting that sperm activated DNA repair mechanisms [16]. Additionally, the removal of ZnO NPs for two weeks, after prolonged treatment (four-week treatment) of male albino rats with 422 mg/kg/day, significantly improved the lesions previously identified in both testis and prostate, indicating that the injuries inflicted by these NPs were temporary and were recovered [17].

In another study, Ag NPs were administered intravenously to New Zealand rabbits at 0.6 mg/kg for 126 days and it was reported a partial recovery of semen traits after 7 weeks [18]. SiO_2 NPs were also intravenously administered to Institute of Cancer Research (ICR) mice, five times for 13 days at doses of 20 mg/kg and it was found that the dysfunction of energy metabolism in the testis induced by these particles was recovered by day 60. The authors propose that with NPs excreted from the body or encapsulated by organelles, oxidative stress disappears, and the damage is repaired [19].

Given the previously reported results indicating that there is an improvement in male reproductive health, the aim of the present study was to determine whether a spermatogonia cell line (GC-1) is able to recover from the damage induced by exposure to a cytotoxic concentration of ZnO NPs previously reported [20].

2. Materials and methods

2.1. Characterization of ZnO NPs for cell culture

A commercial ZnO nanopowder (<100 nm particle size) (Sigma-Aldrich) was provided by Professor Ana Maria Senos and Professor Elisabete Costa from the Department of Materials and Ceramics Engineering and CICECO-Aveiro Institute of Materials, University of Aveiro. The structure, morphology and surface charge of these nanoparticles were already described in detail elsewhere [20].

ZnO NPs stock of 2000 µg/mL was prepared in sterile 1x PBS (Phosphate Buffered Saline, Thermo Scientific). To reduce agglomeration, the nanoparticle suspension was sonicated for 3 minutes, at 60% amplitude and 1 second cycles, using a probe sonicator (U 200 S control, IKA-WERKE). This suspension was diluted in GC-1 cell culture medium to create a 200 µg/mL stock solution, which underwent another sonication cycle and a 20 minutes ultraviolet (UV) light sterilization process. Prior to cell culture, the latter stock solution was further diluted into GC-1 culture medium to create a final concentration of 20 µg/mL. This concentration was used as previously described by our group [20]. Prior to use, the suspension was homogenized by vortexing.

Briefly, when GC-1 cells were treated with ZnO NPs at concentrations ranging from 0-20 µg/mL for 6 and 12h, it was observed that the 20 µg/mL concentration impacted the viability of the cells, inducing cell damage and the cytoskeleton and nucleoskeleton dynamics alterations. Therefore, in the present study, 20 µg/mL concentration was used to induce damage on GC-1 cells.

2.2. Cell culture

The biological effect of ZnO NPs was studied in the mouse-derived spermatogonia cell line, GC-1 spg cells (ATCC®, CRL2053™), a cell line that exhibits phenotypic features of mouse type B spermatogonia and early spermatocytes [21]. GC-1 cells were cultured in Dulbecco's Modified Eagle's Medium (DMEM, Sigma-Aldrich) containing 10% (v/v) of Fetal Bovine Serum (FBS, bioWest) and 1% (v/v) penicillin-streptomycin solution (PenStrep, bioWest) at standard cell culture conditions (humidified incubator under 5% CO2, at 37ºC). After reaching 80% of confluence, cells are split using trypsin-EDTA (Gibco) into 100 mm new plates (cell culture maintenance) or were seeded in 6-well plates (experiments) and allowed to adhere for 16 hours before any treatment.

2.3. Experimental design

To investigate if GC-1 cells could recover from the damage induced by ZnO NPs, cells were seeded at a density of 30,000 cells/well and upon 16 hours were exposed to 20 µg/mL of ZnO NPs for 6 and 12 hours. Then, cells were extensively washed with 1x PBS and maintained in NPs-free

GC-1 culture medium for the following 4 days to evaluate if the cells were able to repair and restore themselves. Essentially, a cell viability assay was performed at two different timepoints: at the end of the exposure times to ZnO NPs and after the 4-day recovery period (Figure 1). At least 3 replicates were performed independently.

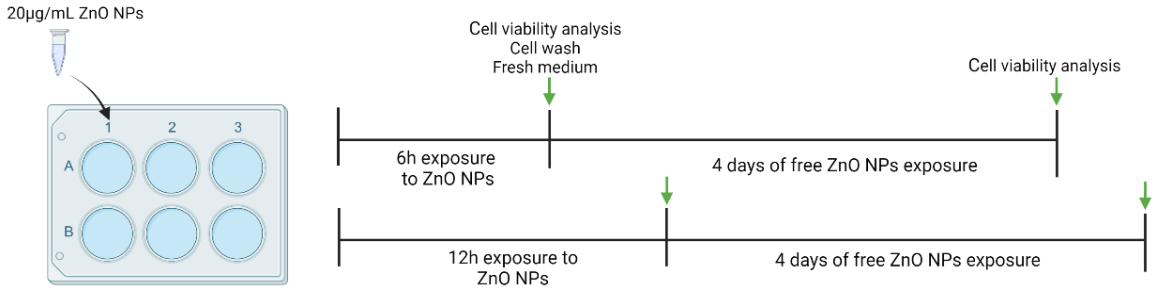

Figure 1. Schematic diagram of experimental design used. The exposure times used for the present study as well as the recovery period. The time points where the cell viability was monitored are indicated with a green arrow.

2.4. Cell viability analysis

The GC-1 cells viability was measured using a resazurin reduction assay. Viable cells with active metabolism have coenzymes, such as NADH, which are used by diaphorases to reduce resazurin (blue, non-fluorescent) to resorufin (pink, fluorescent) (Figure 2) [22]. The level of reduction is proportional to the number of viable cells. Resazurin was chosen to perform a cell viability assay because it is not toxic and, therefore, cells exposed to it can remain in culture and further be used for other experimental purposes [23].

Cells were incubated with 10% of the culture volume with a resazurin (Sigma-Aldrich) solution (0.1 mg/mL) resazurin in 1x PBS [24], 4 hours before the end of the 6h and 12h incubation timepoints and 4 hours before the end of the 4-day recovery period. After 4 hours of incubation, 100 µL of the supernatant from each condition was transferred to a 96-well plate, and the resazurin viability signal was measured spectrophotometrically at 570 and 600nm (Infinite M200, PRO, Tecan). A cell-free culture medium with ZnO NPs was also incubated with resazurin for 4 hours, to normalize the results. The final resazurin value was obtained by subtracting the 570/600 nm ratio of the cell-free conditions to the 570/600 nm ratio of the different cell culture conditions.

Cells were visualized every day, under an inverted light microscope (EVOS™ M5000 Imaging System), to check confluence and morphology.

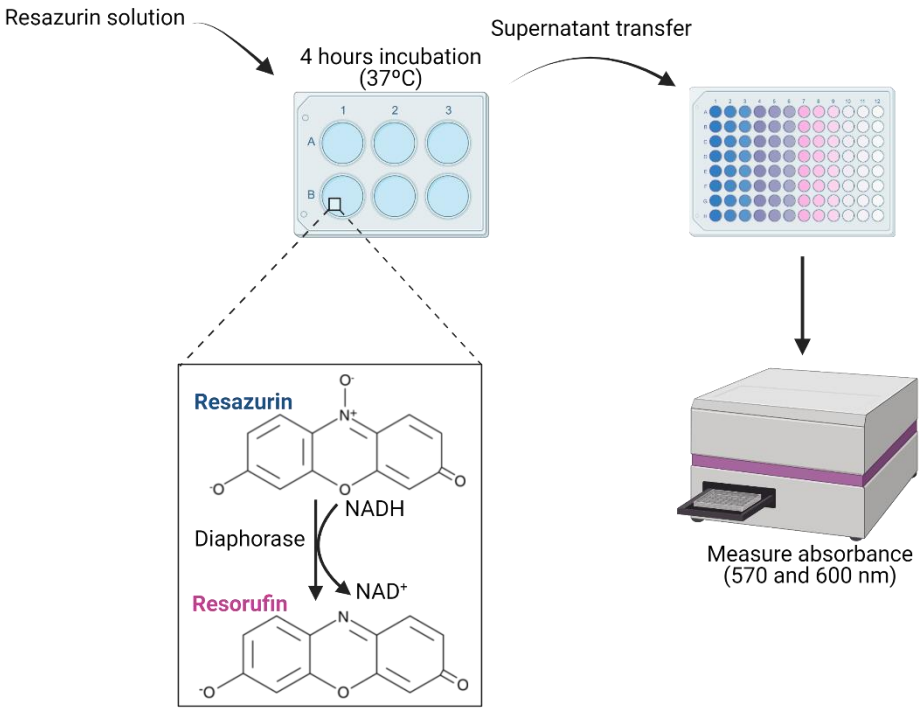

Figure 2. Overview of the resazurin assay and its principle for the cell viability analysis. In the presence of metabolically active cells, resazurin is reduced to resorufin through the oxidation of NADH to NAD^+, which results in a color change to fluorescent pink, that can be quantified.

2.5. Statistical analysis

Statistical analysis was performed by GraphPad Prism software (GraphPad Prism version 8.0.1 for Windows), using one-way ANOVA followed by Tukey's multiple comparisons test with a statistical confidence coefficient of 0.95. A minimum of three independent experiments were performed, using duplicate samples per condition. All data was expressed as mean ± standard error of the mean (SEM).

3. Results

GC-1 cells were exposed to 20 µg/Ml of ZnO NPs, for 6 and 12h. This dose ensures strong effects on cells, keeping cellular mortality at an acceptable level to evaluate cell recovery [20]. The viability of GC-1 cells was determined at the end of these timepoints by the resazurin assay. This assay is based on the reduction of resazurin to highly fluorescent resorufin, which is proportional to the number of metabolically active cells [25]. From the results reported in Figure 3, it is clear that the viability of GC-1 cells was negatively affected by ZnO NPs, although to different degrees. Upon 6 hours of exposure, there was a viability decrease of 25%, compared to control. However, this difference was not statistically significant. After 12 hours, there was a significant decrease of 41% in

the cell viability ($p<0.01$). At the end of these timepoints, the treatment solution was removed, cells were washed three times with 1x PBS and a new culture medium was added. Cells were allowed to recover from stress in an NPs-free condition, for 4 days. After that period, new viability assays were performed. Cells that were exposed to ZnO NPs for 6 hours had a viability increase of 16%. Those that were exposed for 12 hours recovered more readily, with an increase of 25%. Although no statistical difference was measured between the treatment and recovery conditions, there is a clear improvement in cell viability, which are very close to 100%.

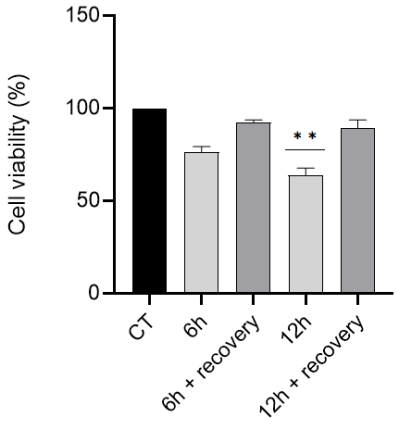

Figure 3. GC-1 cells recovery upon NPs exposure. Results from viability assays analysis of GC-1 cells after their incubation with 20 µg/mL of ZnO NPs, for 6 hours and 12 hours and after a recovery period of 4 days. The percentage of viable cells was plotted as mean ± SEM of four independent experiments. * was used to compare the treatment conditions and control, using one-way ANOVA. ** p<0,01. CT; control.

Figure 4 shows light microscopy images regarding the morphology of unexposed cells (Figures 4 and 5, A-E) and exposed (Figures 4 and 5, F-J) to ZnO NPs. In detail, at the end of both incubation times with ZnO NPs, there was a decrease in the number of adherent cells. When evaluating the amount of space available between cells, the confluence was much lower relative to the control, from the end of the exposure times until the third day of recovery (Figures 4 and 5, F-I). Dark dots can be seen adhered onto the cell surface and the bottom of the cell culture plates. These dark dots are ZnO NPs, which remained strongly adhered even after the washing steps with PBS, which can be confirmed by their presence in the images captured for the 24h recovery day (Figures 4 and 5, G). Over the recovery period, ZnO NPs became less visible in the available space between cells and their surface. However, at the end of the 4-day recovery period (Figures 4 and 5, J), due to the high confluency, it is clear that cells were able to proliferate, despite the presence of ZnO NPs.

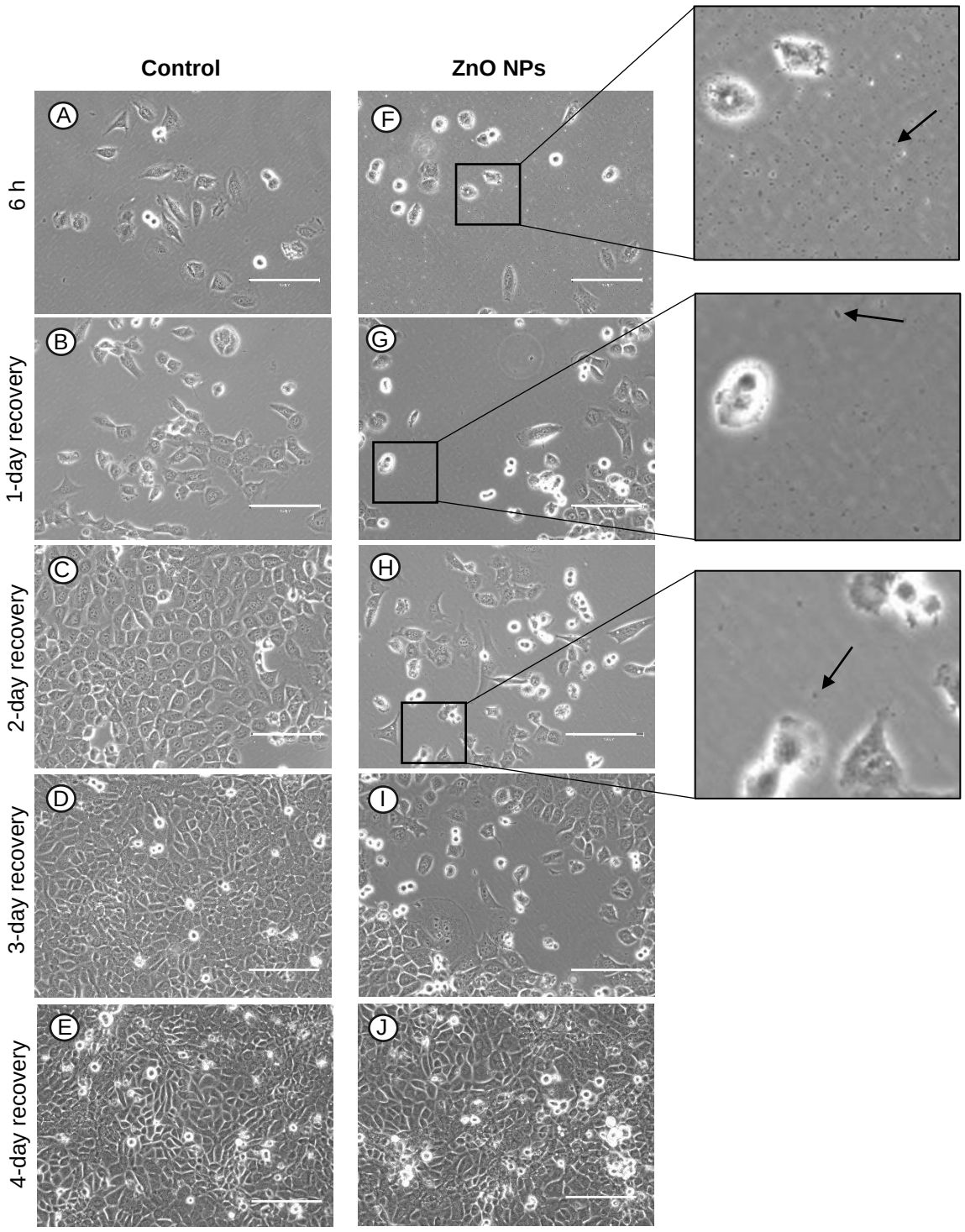

Figure 4. GC-1 cells monitoring by microscopy. Light microscopy images of GC-1 cells at different time points; (A-E) unexposed cells, (F-J) cells exposed to 20 μg/mL of ZnO NPs for 6 hours. Black arrows are pointing into visible aggregates of ZnO NPs. Photos were taken at 20x magnification. Bar corresponds to 150 μm.

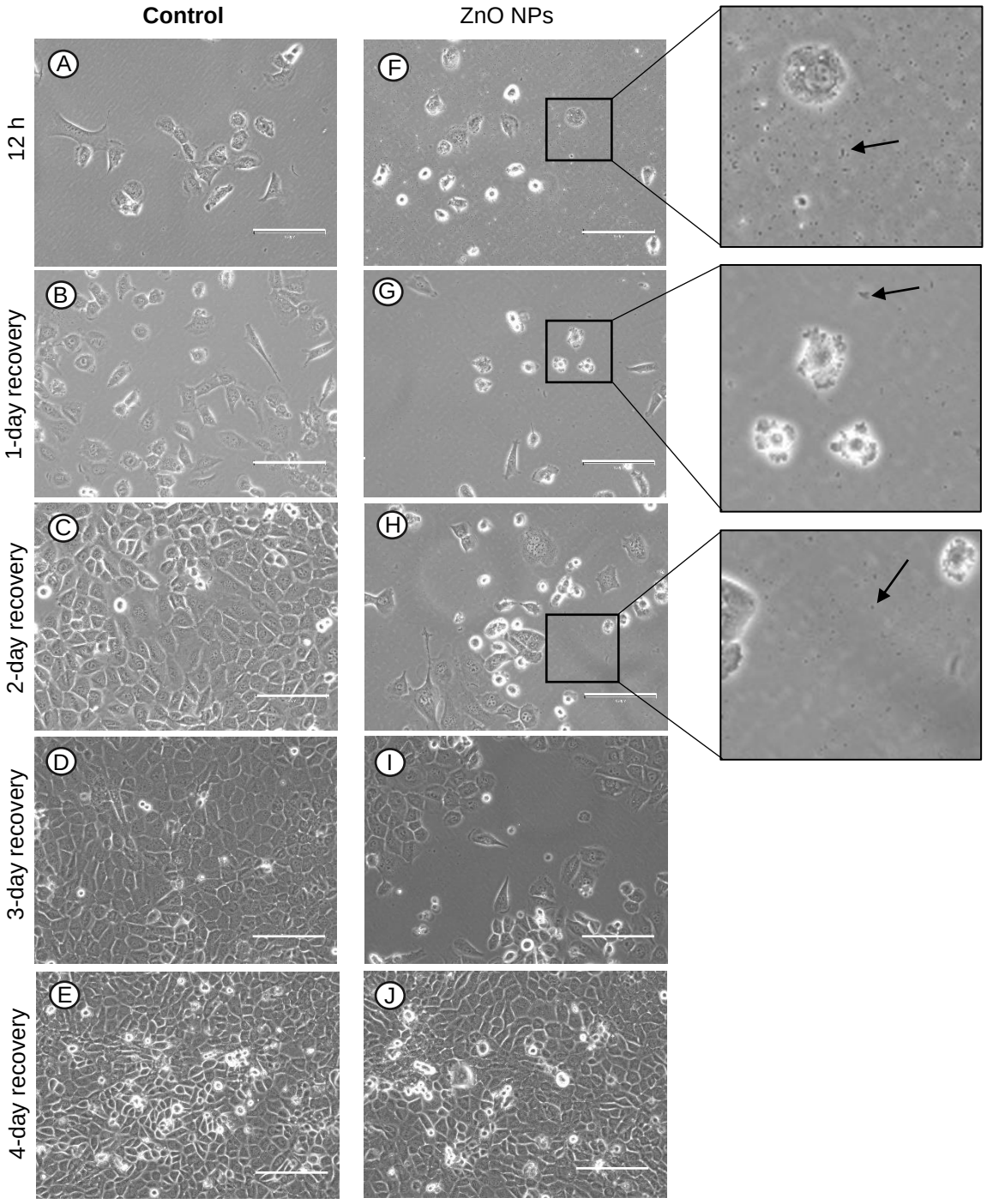

Figure 5. GC-1 cells monitoring by microscopy. Light microscopy images of GC-1 cells at different time points; (A-E) unexposed cells, (F-J) cells exposed to 20 μg/mL of ZnO NPs for 12 hours. Black arrows are pointing into visible aggregates of ZnO NPs. Photos were taken at 20x magnification. Bar corresponds to 150 μm.

4. Discussion

Many studies on the reproductive toxicity of NPs focus on the consequences of their exposure over time. However, uninterrupted exposure to NPs seems unrealistic under real-life conditions. Therefore, it is crucial to investigate the cell recoverability and potential consequences of NPs removal. Changes in sperm number, quality and DNA damage induced by NPs can be reversed, after removal of NPs treatment (e.g., SiO_2 and Ag NPs, carbon nanotubes) [5,18,19]. This can be attributed to the fact that the toxicity of NPs causes cells to activate molecular responses to deal with the generation of oxidative stress, genetic damage, inhibition of cell division, and so on [12]. However, studies pointing towards the recovery of reproductive cells after their exposure to NPs are still very scarce.

Several studies have reported the adverse effects of ZnO NPs on the male reproductive system [17,20,26,27]. In fact, the present study is an extension of previous work that found ZnO NPs had dose and time-dependent cytotoxic effects on spermatogonia cells (GC-1) [20]. With this in mind and considering that cells have a range of defense mechanisms, this work intended to determine to extent to which GC-1 cells recover after cytotoxic exposure to ZnO NPs.

GC-1 cells were exposed to 20 µg/mL of ZnO NPs for short periods (6h and 12h). Then, cells were allowed to recover from stress in a NPs-free condition for 4 days. Different recovery periods were tested (data not shown); however, it was concluded that 4 days was the required time for cells to proliferate and reach maximum confluence. Ultimately, a comparison was made between cells immediately after treatment with ZnO NPs and cells at the end of the recovery period (figure 3, 4 e 5).

Light microscopy images, obtained every day throughout the 4-day period, suggest gradual recovery of cells, since they were able to divide and grow with normal epithelial morphology. On day 4, cells are at maximum confluency, which is a good indication of the healthy state of cells. A cell viability assay was also performed since it provides information about the overall health of cells. From the results reported in Figure 3, there is a clear increase in cell viability at the end of the recovery phase. In fact, cells exposed to ZnO NPs for 6 hours had a viability of 96%, very close to the control condition. Those that were exposed for 12 hours only reached viability values of 89%. Although this percentage is lower than that achieved by the 6-hour condition, there was a 25% increase in viability, higher than the 16% increase reported by the previously mentioned condition.

Full recovery was not possible, probably due to the NPs firmly attached onto cell surfaces and to the bottom of the cell culture plate, even after several washing steps with PBS. Since the insult is still present, the cells' defense system may become overburdened. However, this exposure beyond the stipulated 6h and 12h does not seem to have resulted in further cell damage, since cell viability increased over time. This means that cells may have adapted to the presence of NPs, which was the case for fibroblasts that were continuously exposed to 0.1 nM of gold NPs for 20 weeks. This long-term exposure changed fibroblasts at the molecular level to reach an adapted state (new homeostasis) to the continuous stress induced by NPs, in order to ensure survival [28].

From the close-ups of Figures 4 and 5 (F-H), it is possible to observe a decrease in the number of nanoparticles adsorbed at the bottom of the culture plate. Since in the present study NPs internalization assays were not performed, one can only hypothesize about what might have caused this decrease. Over time, NPs may have detached from the bottom of the culture plates and were left floating in the culture medium. However, it was previously reported that NPs are removed from the culture environment because cells internalize them through endocytosis. One study suggested that after their uptake, cells pass NPs to daughter cells and, if no more NPs are added into the cell culture, the ZnO NPs concentration inside the cell becomes increasingly diluted [29]. Other studies have reported that, after their uptake, NPs are partially degraded by the acidic pH of lysosomes and then released by exocytosis [30–32]. This may explain not only the decrease in NPs in cell culture but also the cell's ability to return to its near normal status.

5. Conclusions and future perspectives

In this study, ZnO NPs at 20 µg/mL affected the viability of GC-1 cells, especially for longer incubation times (12 hours). After this exposure, it was intended to evaluate whether the adverse effects caused by ZnO NPs in GC-1 cells were reversible. At this point, to allow cells to recover in a NPs-free environment, an attempt was made to remove the NPs from the cell culture. However, the ZnO NPs remained strongly adhered onto the cells surface and the bottom of the culture plates, even after multiple washing steps. Despite this drawback in the experimental design, the cells showed a good recoverability within the recovery period that was initially stipulated. By day 4, cell viability was close to the control conditions. Additionally, cells were closely observed under light microscopy and the images obtained lead to conclude that the cells maintained their proliferation capacity, reaching maximum confluency by the end of the experiment. However, results from the viability assays showed that although cell viability increased after 4 days, they also show that cells were not able to fully recover. As a result, other approaches that could mitigate NPs-mediated toxicity should be studied, such as treatments with antioxidants.

References:

1. Yang, Q.; Li, F.; Miao, Y. CdSe/ZnS quantum dots induced spermatogenesis dysfunction via autophagy activation. *J. Hazard. Mater.* **2020**, *398*, doi:doi.org/10.1016/j.jhazmat.2020.122327.

2. Souza, M.; Mazaro-costa, R.; Rocha, T. Can nanomaterials induce reproductive toxicity in male mammals? A historical and critical review. *Sci. Total Environ.* **2021**, *769*, doi:doi.org/10.1016/j.scitotenv.2020.144354.

3. Mandal, T.K.; Das, N.S. Testicular toxicity in cannabis extract treated mice : association with oxidative stress and role of antioxidant enzyme systems. *Toxicol. Ind. Health* **2015**, *26*, 11–23, doi:10.1177/0748233709354553.

4. Meistrich, B.M.L.; Wilson, G.; Mathur, K.; Fuller, L.M.; Rodriguez, M.A.; Mclaughlin, P.; Romaguera, J.E.; Cabanillas, F.F.; Ha, C.S.; Lipshultz, L.I.; et al. Rapid Recovery of Spermatogenesis After Mitoxantrone, Vincristine, Vinblastine, and Prednisone Chemotherapy for Hodgkin's Disease. *J. Clin. Oncol.* **1997**, *15*, 3488–3495, doi:doi: 10.1200/JCO.1997.15.12.3488.

5. Bai, Y.; Zhang, Y.; Zhang, J.; Mu, Q.; Zhang, W.; Elizabeth, R.; Snyder, S.E.; Yan, B.; Chemistry, I. Repeated carbon nanotube administrations in male mice cause reversible testis damage without affecting fertility. *Nat. Nanotechnol.* **2011**, *5*, 683–689, doi:10.1038/nnano.2010.153.Repeated.

6. Ighodaro, O.M.; Akinloye, O.A. First line defence antioxidants-superoxide dismutase (SOD), catalase (CAT) and glutathione peroxidase (GPX): Their fundamental role in the entire antioxidant defence grid. *Alexandria J. Med.* **2018**, *54*, 287–293, doi:10.1016/j.ajme.2017.09.001.

7. Pizzino, G.; Irrera, N.; Cucinotta, M.; Pallio, G.; Mannino, F.; Arcoraci, V.; Squadrito, F.; Altavilla, D.; Bitto, A. Oxidative Stress: Harms and Benefits for Human Health. *Oxid. Med. Cell. Longev.* **2017**, *2017*, doi:10.1155/2017/8416763.

8. Wang, Y.; Branicky, R.; Noë, A.; Hekimi, S. Superoxide dismutases: Dual roles in controlling ROS damage and regulating ROS signaling. *J. Cell Biol.* **2014**, *217*.

9. Yu, Z.; Li, Q.; Wang, J.; Yu, Y.; Wang, Y. Reactive Oxygen Species-Related Nanoparticle Toxicity in the Biomedical Field. *Nanoscale Res. Lett.* **2020**, *15*, doi:doi.org/10.1186/s11671-020-03344-7.

10. Lobo, V.; Patil, A.; Phatak, A.; Chandra, N. Free radicals , antioxidants and functional foods : Impact on human health. **2010**, doi:10.4103/0973-7847.70902.

11. Capek, J. Detection of Oxidative Stress Induced by Nanomaterials in Cells — The Roles of Reactive Oxygen Species and Glutathione. *Molecules* **2021**, *26*.

12. Quevedo, A.; Lynch, I.; Valsami-Jones, E. Cellular repair mechanisms triggered by exposure to silver nanoparticles to ionic silver in embryonic zebrafish cells. *Environ. Sci. Nano* **2021**, *8*, 2507–2522, doi:10.1039/d1en00422k.

13. Lett, R.; Wang, D.; Dan, M.; Ji, Y.; Wu, X.; Wang, X.; Wen, H. Roles of ROS and cell cycle arrest in the genotoxicity induced by gold nanorod core / silver shell nanostructure. *Nanoscale Res. Lett.* **2020**, *15*, 1–13, doi:10.1186/s11671-020-03455-1.

14. García-Rodríguez; Gos, J.; Agarwal, A.; Roy, R. DNA Damage and Repair in Human Reproductive Cells. *Int. J. Mol. Sci.* **2019**, 1–22, doi:10.3390/ijms20010031.

15. Surova, O.; Zhivotovsky, B. Various modes of cell death induced by DNA damage. *Oncogene* **2013**, 3789–3797, doi:10.1038/onc.2012.556.

16. Santonastaso, M.; Mottola, F.; Iovine, C.; Cesaroni, F. In Vitro E ff ects of Titanium Dioxide Nanoparticles (TiO 2 NPs) on Cadmium Chloride (CdCl 2) Genotoxicity in Human Sperm Cells. *Nanomaterials* **2020**, *10*, 1–16.

17. Mesallam, D.; Deraz, R.; Abdel Aal, S.; Ahmed, S. Toxicity of Subacute Oral Zinc Oxide Nanoparticles on Testes and Prostate of Adult Albino Rats and Role of Recovery. *J. Histol. Histopathol.* **2019**, *6*, 2, doi:10.7243/2055-091x-6-2.

18. Castellini, C.; Ruggeri, S.; Mattioli, S.; Bernardini, G.; Macchioni, L.; Moretti, E.; Collodel, G. Long-term effects of silver nanoparticles on reproductive activity of rabbit buck. *Syst. Biol. Reprod. Med.* **2014**, *60*, 143–150, doi:10.3109/19396368.2014.891163.

19. Xu, Y.; Wang, N.; Yu, Y.; Li, Y.; Li, Y.; Yu, Y.; Zhou, X. Exposure to Silica Nanoparticles Causes Reversible Damage of the Spermatogenic Process in Mice. *PLoS One* **2014**, *9*, 1–11, doi:10.1371/journal.pone.0101572.

20. Pinho, A.R.; Martins, F.; Costa, M.E. V.; Senos, A.M.R.; Silva, O.A.B. d. C.E.; Pereira, M. de L.; Rebelo, S. In Vitro Cytotoxicity Effects of Zinc Oxide Nanoparticles on Spermatogonia Cells. *Cells* **2020**, *9*, doi:10.3390/cells9051081.

21. Verma, P.; Parte, P. Revisiting the Characteristics of Testicular Germ Cell Lines GC - 1 (spg) and GC - 2 (spd)ts. *Mol. Biotechnol.* **2021**, *1*, doi:10.1007/s12033-021-00352-5.

22. Breznan, D.; Das, D.; Mackinnon-roy, C.; Simard, B.; Kumarathasan, P.; Vincent, R. Non-specific interaction of carbon nanotubes with the resazurin assay reagent: Impact on in vitro assessment of nanoparticle cytotoxicity. *Toxicol. Vitr.* **2015**, *29*, 142–147, doi:10.1016/j.tiv.2014.09.009.

23. Pereira, A.; Monteiro, P.; Oliveira, F.; Santos, S.; Fontes, A.; Cabral, E. Resazurin-Based Assay to Evaluate Cell Viability After Quantum Dot Interaction. *Quantum Dots. Methods Mol. Biol.* **2020**, *2135*, doi:https://doi.org/10.1007/978-1-0716-0463-2_12.

24. Pina, S.; Vieira, S.; Rego, P.; Torres, P. Biological responses of brushite-forming Zn-and ZnSr-substituted- Tricalcium phosphate bone cements. **2010**, doi:10.22203/eCM.v020a14.

25. Divito, M.; Miller, W.; Uzarski, J.; Wertheim, J. Essential Design Considerations for the Resazurin Reduction Assay to Noninvasively Quantify Cell Expansion within Perfused Extracellular Matrix Scaffolds. *Biomaterials* **2017**, *129*, 163–175, doi:10.1016/j.biomaterials.2017.02.015.Essential.

26. Barkhoradi, A.; Hekmatimoghaddam, S.; Jebali, A.; Khalili, M.; Talebi, A.; Noorani, M. Effect of zinc oxide nanoparticles on viability of human spermatozoa. *Iran. J. Reprod. Med.* **2013**, *11*, 767–771.

27. Han, Z.; Yan, Q.; Ge, W.; Liu, Z.-G.; Gurunathan, S.; Felici, M.; Shen, W.; Zang, X.-F. Cytotoxic effects of ZnO nanoparticles on mouse testicular cells. *Int. J. Nanomedicine* **2016**, *11*, 5187–5203.

28. Falagan-lotsch, P.; Grzincic, E.M.; Murphy, C.J. One low-dose exposure of gold nanoparticles induces long-term changes in human cells. *PNAS* **2016**, *113*, 13318–13323, doi:10.1073/pnas.1616400113.

29. Mironava, T.; Hadjiargyrou, M.; Simon, M.; Jurukovski, V.; Rafailovich, M.H. Gold nanoparticles cellular toxicity and recovery : Effect of size , concentration and exposure time.

Nanotoxi **2010**, *4*, 120–137, doi:10.3109/17435390903471463.

30. Oh, N.; Park, J.-H. Endocytosis and exocytosis of nanoparticles in mammalian cells. *Int. J. Nanomedicine* **2014**, *9*, 51–63.

31. Fröhlich, E. Cellular Screening Methods for the Study of Nanoparticle-Induced Lysosomal Damage. *Lysosomes - Assoc. Dis. Methods to Study their Funct.* **2017**, doi:10.5772/intechopen.69306.

32. Borgese, M.; Rossi, F.; Bonfanti, P.; Colombo, A.; Mantecca, P.; Valdatta, L.; Bernardini, G.; Gornati, R. Recovery ability of human adipose stem cells exposed to cobalt nanoparticles : outcome of dissolution. *Nanomedicine* **2020**, *15*, 453–465.

Chapter 4

Evaluation of the protective effects of a synthetic chalcone against the reproductive toxicity induced by Zinc Oxide Nanoparticles

Abstract

A previous study from our group demonstrated that ZnO NPs compromise the viability of GC-1 cells, elicit oxidative stress, DNA damage, interfere with the cytoskeleton and nucleoskeleton dynamics, which ultimately results in cell death. In the present study, the protective effects of a synthetic chalcone named VS3 against the reproductive toxicity of ZnO NPs were investigated in the same cell line.

GC-1 cells were simultaneously exposed to VS3 (0-12.5 µM) and ZnO NPs (20 µg/mL) for 6 and 12 hours. After 6 hours of co-exposure, 3.1 µM of VS3 was the dose that resulted in the highest cell survival. However, after 12 hours, 12.5 µM of VS3 resulted in significantly higher cell viability than cells that were treated with only ZnO NPs only ($p<0.001$). The levels of DNA damage elicited by ZnO NPs were reversed by VS3 supplementation after 6h of exposure, but not upon 12h treatment. VS3 also stabilized cytoskeleton proteins levels (β-tubulin, acetylated α-tubulin) upon ZnO NPs exposure, in a dose-dependent manner.

Taken together, the present study demonstrated that some of the adverse effects induced by ZnO NPs can be partially rescued by combined exposure with VS3. These results may provide insights into the effect of therapeutic agents on male infertility.

Keywords: chalcone, antioxidant, zinc oxide nanoparticles, oxidative stress, cytoskeleton, DNA damage, male infertility

1. Introduction

Chalcones (1,3-diarylprop-2-en-1-one) are natural products with widespread distribution in different plant families belonging to the flavonoids group [1,2]. Chalcones are often referred as ‘open chain flavonoids’ since they lack the heterocyclic C ring [3]. These compounds have two aromatic rings (rings A and B) that are connected by a three-carbon α,β-unsaturated carbonyl system (Figure 1). Due to their structural simplicity, these molecules can be easily synthesized to present different structures, since their geometry can be decorated with side chains, so that the resulting products bind to different biomolecules and present distinct properties [1,4]. In fact, chalcones are so versatile and abundant that there are several thousand naturally occurring chalcones reported in the literature [5,6]. These molecules have been explored for thousands of years through the use of plants and herbs for the treatment of different pathologies, such as cancer, inflammation, and diabetes [6]. Researchers are often inspired by the structure of naturally occurring chalcones to synthesize derivatives with enhanced bioactivities and/or reduced toxicity [5]. Within the broad spectrum of therapeutic applications that natural and synthetic chalcones display, their antioxidant potential is the most explored [7].

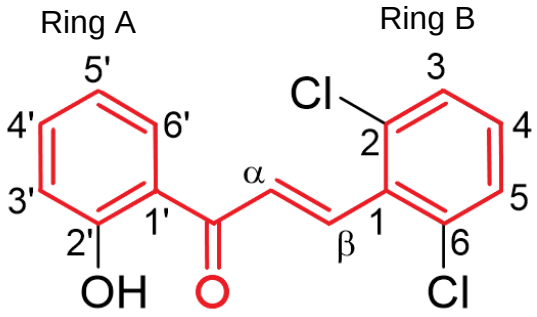

Figure 1. Structure of the synthesized chalcone VS3 [(E)-3-(2,6-dichlorophenyl)-1-(2-hydroxyphenyl)prop-2-en-1-one)]. The 1,3-diaryprop-2-en-1-one fragment is marked in red.

Antioxidants are substances that are able to protect cells from oxidative damage caused by free radicals and their derivates. Free radicals, such as superoxide radicals ($O_2^{\bullet-}$), hydrogen peroxide (H_2O_2), hydroxyl radicals (●OH), and singlet oxygen ($^1O_2$), are commonly referred to as reactive oxygen species (ROS). These are generated as metabolic by-products, mainly in the mitochondria [8]. Although they are important components in cell respiration and other vital cellular processes, they are unstable and highly reactive molecules. They can easily start a cascade of chain reactions, leading to oxidative stress, which can seriously alter cell membranes and structures [9].

Several *in vitro* and *in vivo* studies have demonstrated that ZnO NPs induce substantial cytotoxicity, mainly through the overproduction of ROS [10–14]. These NPs, being one of the most synthesized type of metal oxide NPs, have been used in various commercial products including medicine, agriculture, pharmaceuticals, cosmetics [15]. However, their widespread applications result in higher human exposure and new biological interactions [16].

To a certain degree, cells antioxidant defense system can minimize the levels of ROS, compensate for the oxidative stress, and even repair the DNA damage if necessary. However, when the intracellular antioxidant system is not able to maintain the proper balance of free radicals due to their chronic production, several health problems may occur [8,14]. In fact, oxidative stress is related to many reproductive disorders [17]. It is an emerging risk factor for male infertility since it can interfere with sperm quality mainly by inducing DNA and protein oxidation, and lipid peroxidation [18]. Therefore, antioxidant therapies have been considered viable treatment options for male infertility, since they are able to restore the proper balance between free radicals and antioxidants in the reproductive cells [19].

Some chalcones have been reported to have antioxidant properties [1,5,20–22]. This activity is highly influenced by the structure of the two aromatic rings in the backbone [23], and by the number and position of the hydroxy group, methoxy group, and other groups in the A and B rings [24]. Although the antioxidant potential of many chalcone analogs has been found in many cell lines, the protective effects of this compound on male reproductive cells have not been previously studied. Consequently, the present study aimed to evaluate the protective effects of different doses of the synthesized chalcone named VS3 [(E)-3-(2,6-dichlorophenyl)-1-(2-hydroxyphenyl)prop-2-en-1-one)]

on GC-1 cells, when combined with a cytotoxic concentration of ZnO NPs. The following outcomes will be monitored, namely, cell viability, oxidative stress, DNA damage, and alterations of cytoskeleton dynamics.

2. Materials and Methods

2.1. Characterization of ZnO NPs for cell culture

A commercial ZnO nanopowder (<100 nm) (Sigma-Aldrich, Saint Louis, MO, USA) was provided by Professor Ana Maria Senos and Professor Elisabete Costa from the Department of Materials and Ceramics Engineering and CICECO-Aveiro Institute of Materials, University of Aveiro. ZnO NPs were diluted in a cell culture medium to obtain a final concentration of 20 µg/mL, as described in the section 2.1 of Chapter 3.

2.2. Synthesis and characterization of chalcone VS3 for cell culture

Chalcone VS3 ((E)-3-(2,6-dichlorophenyl)-1-(2-hydroxyphenyl)prop-2-en-1-one) was kindly provided and characterized by Professor Vera Silva from the Chemistry Department, University of Aveiro, according to established methods [25–27]. Chalcone VS3 was dissolved in dimethylsulfoxide (DMSO; Panerac AplliChem) and stored at 4ºC in the dark. Prior to use, it was diluted in a cell culture medium to create the final concentrations (1.6, 3.1, 6.25, 12.5, and 25 µM). DMSO final concentration did not exceed 0.25% (v/v).

2.3. Cell culture

The mouse-derived spermatogonial cell line GC-1 spg cells (ATCC®, CRL2053™) was cultured under the conditions previously described in section 2.2 of Chapter 3. Before the experiments, cells were seeded in 6-well plates (Corning Inc. Costar) and left for 16 hours for cell adhesion. Then, cells were then treated as described in Figure 2.

2.4. Experimental design

For the treatment conditions, cells were plated with a density of 250,000 cells/well in 6-well plates, and pretreated with various concentrations of VS3 (1.6, 3.1, 6.25, and 12.5 µM) for 1h prior to ZnO NPs exposure (20 µg/mL) and both VS3 and ZnONPs were left for 6 and 12 hours. However, to determine the ROS intracellular content, 96-well plates were used and thus, a lower cell density of 10,000 cells/well was adopted for that assay.

GC-1 cells were also cultured with VS3 (0-25 µM for 7 and 13 hours) and ZnO NPs (20 µg/mL for 6 and 12 hours) independently to understand how each treatment affects cells (Figure 2). The control group included cells without any treatment. At least 3 replicates from each group were performed independently.

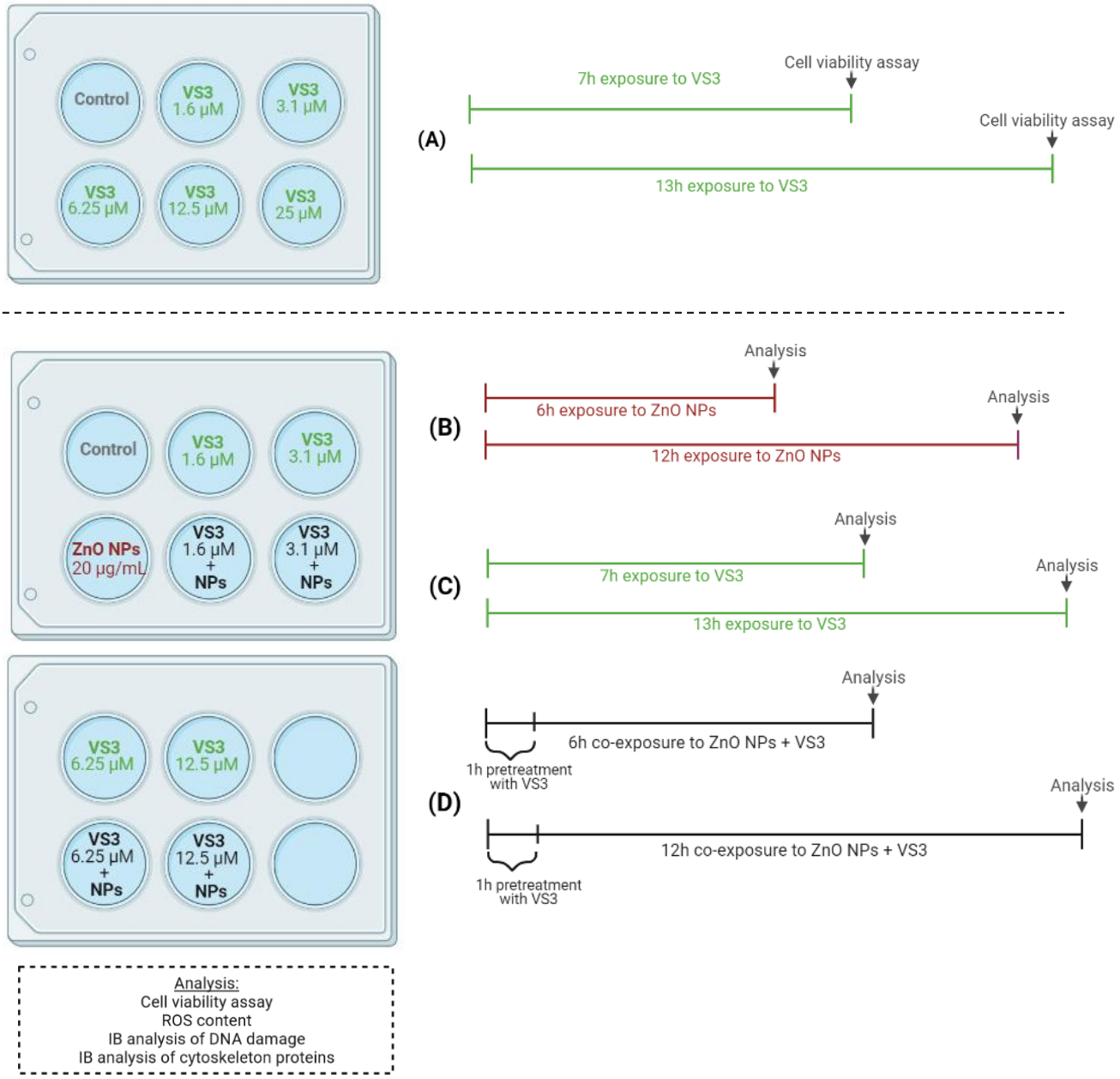

Figure 2. Schematic diagram of the experimental design. First, **(A)** cells were incubated only with VS3 (0-25 µM) for 7 and 13 hours to test the cytotoxicity of the compound. Then, cells were exposed to **(B)** VS3 (0-12.5 µM) and **(C)** 20 µg/mL of ZnO NPs independently to understand how each treatment affects cells. **(D)** Cell pretreatment with VS3 for 1 hour and co-exposure to ZnO NPs and VS3 to evaluate the protective effects of VS3 against ZnO NPs toxicity. IB, immunoblotting; ROS, reactive oxygen species; NPs, nanoparticles

2.5. Cell viability assay

The viability of GC-1 cells was measured using resazurin reduction assay, as described in section 2.4 of Chapter 3. In this case, GC-1 cells were seeded in 6-well plates at 250,000 cells/well and treated with ZnO NPs and VS3, as described above. All absorbance values were corrected against blank wells which contained cell-free culture medium with ZnO NPs and different concentrations of chalcone VS3. The final resazurin value was obtained by subtracting the 570/600 nm ratio of the cell-free conditions to the 570/600 nm ratio of the different cell culture conditions.

2.6. Preparation of cell lysates

GC-1 cells were exposed as described in section 2.4 (Figure 2) and at the end of the experiment, protein lysates were prepared by harvesting cells with 1% boiling Sodium Dodecyl Sulfate (SDS) and boiling them at 95ºC for 10 minutes. Then, lysates were sonicated with a probe sonicator for 10 seconds (60% amplitude, 0.5 seconds cycles) before SDS-polyacrylamide gel electrophoresis (SDS-PAGE) and immunoblotting analysis [28,29]. The total protein concentration from cell lysates was determined by Pierce's bicinchoninic acid (BCA) protein assay kit (Thermo Fisher Scientific), which was performed according to the manufacturer's instructions and quantified by an absorbance reader (Infinite M200, PRO, Tecan).

2.7. SDS-PAGE and Immunoblotting

After protein collection and quantification, 30 µg of protein samples were further denatured by boiling for 5 minutes in the presence of 1% SDS and loading buffer with β-mercaptoethanol. Protein samples were then run by a 5%-20% gradient SDS-PAGE, using a 90 mA electrical current and electrotransferred for 18 hours at 200 mA onto nitrocellulose membranes (0.2 µm pore size; GE Healthcare) [29]. These membranes were then stained with Ponceau-S red (Sigma-Aldrich) to assure equal loading of proteins. Membranes were scanned in a GS-800 calibrated image densitometer (Bio-Rad) and the red staining was removed by washing membranes with 1x Tris-buffered saline with 0.1% Tween-20 (TBST-T). Blots were incubated for 2 hours with a blocking solution (3% bovine serum albumin (BSA)/1x TBST-T), which prevents antibodies from binding to the membrane nonspecifically, which reduces the background. After the blocking step, blots were incubated overnight at 4ºC and 2 hours at room temperature with the following: anti-γ-H2AX, anti-α-tubulin-acetylated, anti-β-tubulin, and anti-β-actin (Table 3). The primary antibody incubation was followed by three washes of 10 minutes each with TBS-T. Then, all blots were further incubated with horseradish peroxidase-conjugated secondary antibodies (Cell Signalling Technology, 1:10000) for 1 hour at room temperature. Following three washes with TBS-T, the membrane was incubated for 5 minutes with the ECL Select WB detection reagent (GE-Healthcare) and protein bands were detected by chemiluminescence on the Chemi-Doc Imaging System, using Quantity One densitometry software (Bio-Rad). For reprobing, blots were stripped in a mild stripping solution, followed by several washes with TBS-T.

Table 1. Primary antibodies used for immunoblotting analysis. BSA, Bovine Serum Albumin; TBS-T, Tris-buffered saline-Tween

Primary Antibody	Host	Type	Working Dilution	Supplier	Blocking Solution	Target
Anti-γ-H2AX (S139)	Mouse	Monoclonal	1:500	Millipore	3% BSA / 1x TBS-T	γ-H2AX (S139)
Anti-α-tubulin-acetylated	Mouse	Monoclonal	1:2000	Sigma-Aldrich	3% BSA / 1x TBS-T	α-tubulin-acetylated
Anti-β-tubulin	Mouse	Monoclonal	1:1000	Invitrogen	3% BSA / 1x TBS-T	β-tubulin
Anti-β-actin	Mouse	Monoclonal	1:75000	Sigma-Aldrich	1% BSA / 1x TBS-T	β-actin

2.8. Detection of intracellular ROS content

Intracellular ROS production was measured using Total ROS detection kit (Enzo Life Sciences) according to the manufacturer's protocol. This assay uses the reagent 2'-7'-dichlorodihydrofluorescein-diacetate (DCFH-DA) which enters cells and is hydrolysed by intracellular esterases, resulting in non-fluorescent dichlorodihydrofluorescein (DCFH). DCFH reacts with ROS to form the highly fluorescent dichlorofluorescein (DCF) which can be measured [30,31].

Briefly, GC-1 cells were seeded at a density of 10,000 cells/well in a 96-well plate with a black bottom and they were allowed to adhere for 16 hours before being treated according to the experimental design presented in Figure 2. Right before the end of the treatments, cells were stained with ROS detection solution for 1h at 37ºC. For negative control, N-acetyl-L-cysteine (NAC) was added to cells, 30 minutes before the ROS detection solution, to scavenge ROS. For positive control, pyocyanin was added 30 minutes after the ROS detection solution, to induce ROS production. Then, cells were analysed by using a fluorescence microplate reader (Infinite M200 PRO, Tecan) at an excitation wavelength of 488 nm and an emission wavelength of 520 nm. The fluorescence intensity is proportional to the ROS levels within the cell cytoplasm.

2.9. Statistical treatment

Statistical analysis was performed by GraphPad Prism software (GraphPad Prism version 8.0.1 for Windows), using common one-way ANOVA followed by Tukey's multiple comparisons test with a statistical confidence coefficient of 0.95. However, when data did not meet the assumption of normality or homogeneity of variance, the nonparametric Kruskal-Wallis one-way ANOVA was performed, followed by Dunn's multiple comparisons test. A minimum of three independent experiments were performed, with two replicates per condition. All data was expressed as mean ± standard error of the mean (SEM).

3. Results

3.1. Effect of VS3 on GC-1 cells survival

In previous studies, the effect of 20 µg/mL of ZnO NPs on GC-1 cells was assessed and a dose- and time-dependent decrease in cell viability was found. This concentration induced more cell damage, namely increased oxidative stress and DNA damage, as well as cytoskeleton and nucleoskeleton changes and even cell death [32]. Therefore, this dose was chosen to induce injuries in GC-1 cells for subsequent experiments.

Before assessing the protective potential of chalcone VS3 against the damage induced by ZnO NPs, the effect of this compound on cell viability was assessed, by incubating GC-1 cells with different concentrations of VS3 (0-25 µM) for 7 and 13 hours. These two exposure periods were selected according to the total time that GC-1 cells will be incubated with VS3 (1 hour of pretreatment followed by 6 and 12 hours of co-exposure with ZnO NPs).

Results presented in Figure 3 show that the tested concentrations of VS3 are not toxic to GC-1 cells. Compared to the control, cells that were incubated with 3.1 µM of VS3 for 7 hours showed a significant viability increase of 21.8% ($p<0.01$). After 13 hours of incubation, 3.1 µM and 12.5 µM of VS3 presented similar results, with a viability increase of 20.7% and 20%, respectively.

In fact, all the tested concentrations resulted in higher viability levels than the control condition, except for the highest concentration (25 µM). Since 25 µM of VS3 presented a tendency to decrease the viability of GC-1 cells, especially for longer incubation periods (13h), this concentration was not considered in the next assays.

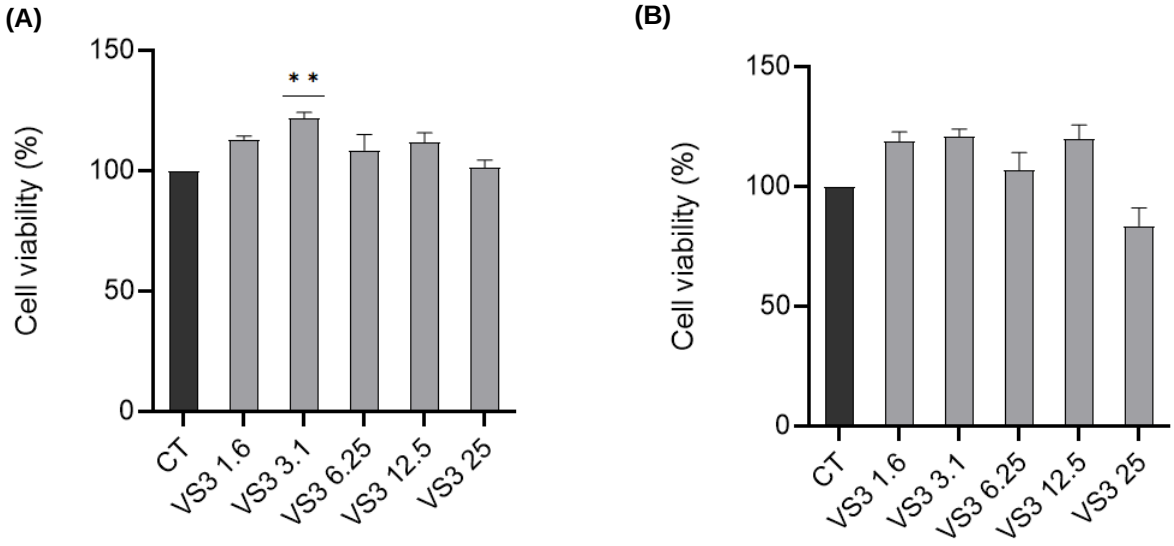

Figure 3. Cell viability assay of cells treated with VS3. Changes in the viability of GC-1 cells after being treated with different concentrations of chalcone VS3 (0-25 µM) for **(A)** 7 hours and **(B)** 13 hours. All data were expressed as mean ± SEM of five independent experiments performed in duplicate. ** $p<0.01$ compared to the control group, using nonparametric Kruskal-Wallis one-way ANOVA test. CT, control.

Next, to examine the potential of chalcone VS3 in reducing the cytotoxicity caused by ZnO NPs, GC-1 cells were pretreated with various concentrations (1.6, 3.1, 6.25, and 12.5 µM) of this chalcone for 1 hour. Then, the treatment solution with VS3 was removed and a new culture medium containing both VS3 and ZnO NPs was added.

As shown in Figure 4, the viability of GC-1 cells was 85.7% and 69.6% when exposed to ZnO NPs for 6h and 12h, respectively. However, the survival rate of cells pretreated for 1h with different concentrations of VS3 before exposure to ZnO NPs seems to increase. In fact, under the 6 hour-exposure conditions, all cells pretreated with VS3 had cell viability higher than 90%, very close to the control condition. The highest cell viability value for cells co-exposed with ZnO NPs and VS3 for 6h was 96.5% (VS3 3.1 + NPs group), but this value was not significantly higher than the group of cells treated only with ZnO NPs. However, under 12h treatment conditions, cell viability of 91.3% in cells co-exposed to ZnO NPs and 12.5 µM of VS3 was significantly higher than in the ZnO NPs treated group ($p<0.001$).

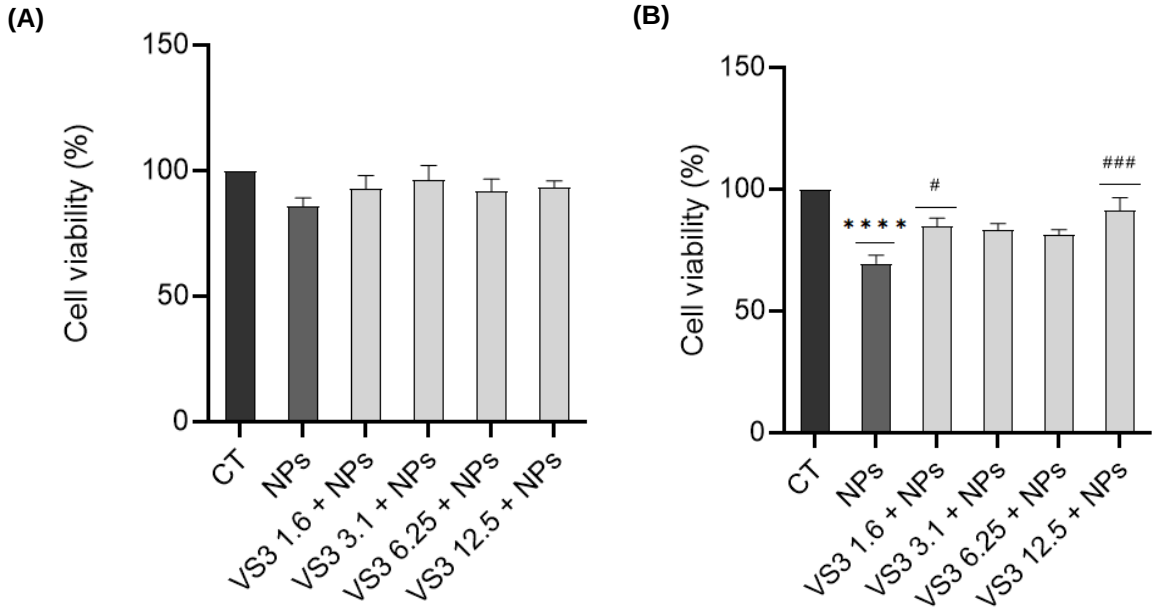

Figure 4. Cell viability assay of cells co-exposed with VS3 and ZnO NPs. Changes in the viability of GC-1 cells treated with 20 µg/Ml of ZnO NPs in the absence and presence of different concentrations of VS3 (0-12.5 µM) after **(A)** 6 and **(B)** 12 hours of exposure. All data were expressed as mean ± SEM of five independent experiments performed in duplicate. **** $p<0.0001$ compared to the control group, # $p<0.05$ and ### $p<0.001$ compared to the group treated with ZnO NPs, using one-way ANOVA. CT, control; NPs, nanoparticles.

3.2. Determination of intracellular ROS levels

The ability of VS3 to protect GC-1 cells against oxidative stress was assessed by measuring the levels of intracellular ROS. For the 6h timepoint, ROS intracellular content remained relatively constant and close to the control group, without significant changes (Figure 5, A). For the 12h timepoint, all tested conditions resulted in higher ROS levels than the control group (Figure 5, B). However, supplementation with VS3 appears to attenuate the levels of ROS produced by NPs exposure. The exception was the group of cells treated with ZnO NPs and 12.5 µM of VS3. This group had slightly higher ROS levels than the ZnO NPs-treated group. Furthermore, while the group of cells treated with only 1.6 and 3.1 µM of VS3 presented similar ROS content to the control, higher concentrations of VS3 (6.25 and 12.5 µM) clearly resulted in an increase in ROS levels, which were very close to the groups treated with ZnO NPs. However, none of the reported changes were statistically significant.

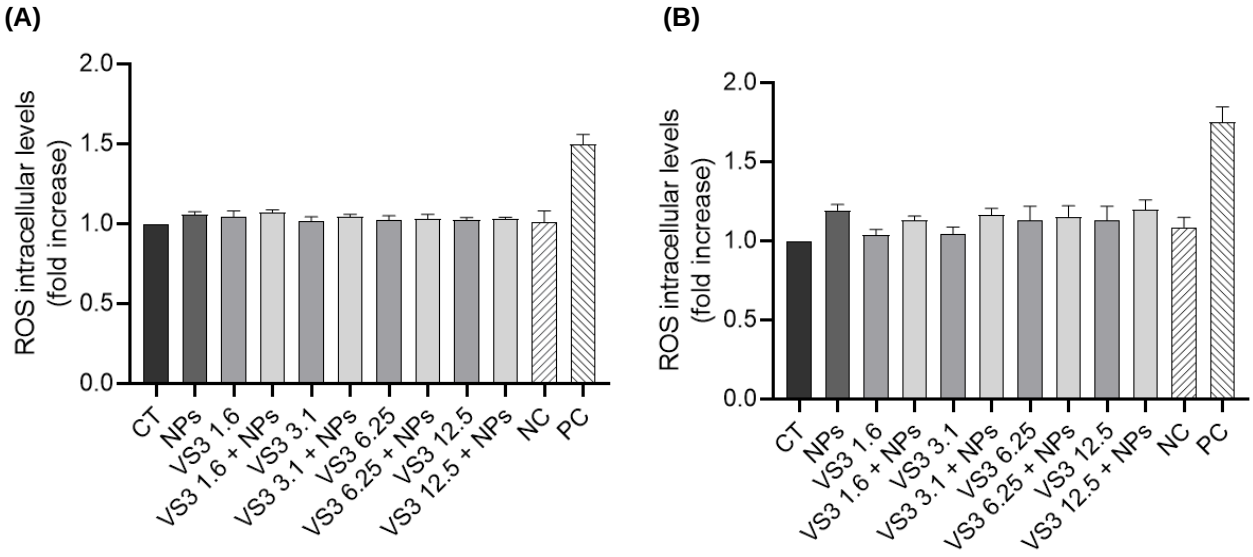

Figure 5. Oxidative stress assay. ROS intracellular levels following treatment with ZnO NPs and VS3 independently, and co-exposure of ZnO NPs + VS3 was analysed by the Total ROS Detection Kit. No significant differences were detected between groups when analysed by one-way ANOVA. All data were expressed as mean ± SEM of four independent experiments. CT, control; NPs, nanoparticles; NC, negative control; PC, positive control.

3.3. Influence of VS3 on DNA damage

To assess the potential mechanisms underlying the effect of chalcone VS3 on ZnO NPs-induced genotoxicity, the presence of DNA damage was determined by measuring the intracellular levels of γ-H2AX (Ser139) by immunoblotting, which is a marker that reveals the occurrence of double-stranded breaks (DSBs) [33].

The effect of different concentrations of chalcone VS3 (0-12.5 µM) on DNA integrity was tested for 7 and 13 hours to assess the impact of this compound on the DNA, without the interference of

NPs. After 7 hours of exposure, none of the tested concentrations induced DNA damage, since the levels of γ-H2AX remained below the control group levels (Figure 6, A). However, after 13 hours of incubation, higher concentrations of VS3 (6.25 and 12.5 µM) seem to have interfered with the DNA integrity (Figure 6, B), but these results were not statistically significant.

Compared to the control group, DNA damage increased in both timepoints after the exposure to 20 µg/mL of ZnO NPs (Figure 6). When GC-1 cells were incubated with ZnO NPs in the presence of different concentrations of VS3 for 6 hours, the levels of DNA damage remained higher than the control group, but lower than the ZnO NPs-treated group. This was not the case for the 12h timepoint, since the levels of DNA damage of the co-exposed groups were higher than the group treated with ZnO NPs only.

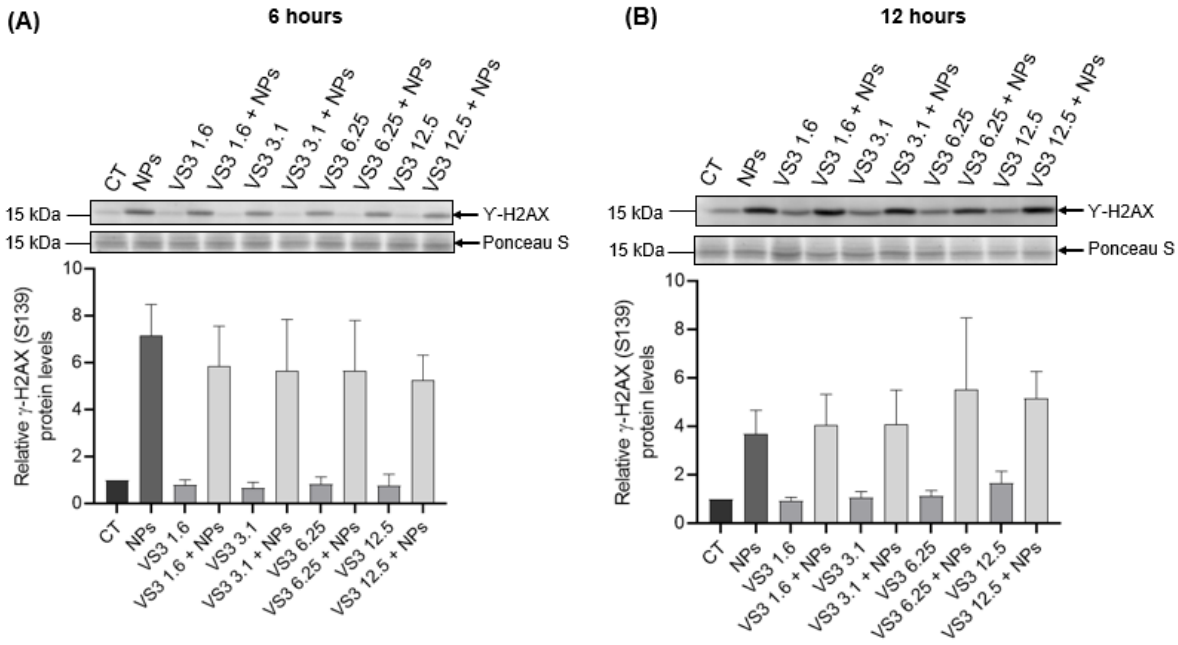

Figure 6. **Immunobloting analysis of γ-H2AX (Ser139) levels**. This assay allows to assess the DNA damage after the incubation of GC-1 cells with 20 µg/mL of ZnO NPs and different concentrations of VS3 (0-12.5 µM) *per se*, and the protective effects of VS3 against the genotoxicity induced by the NPs after **(A)** 6h and **(B)** 12h of co-exposure with ZnO NPs. No significant differences were detected between groups when analysed by one-way ANOVA. All data were expressed as mean ± SEM of four independent experiments. CT, control; NPs, nanoparticles

3.4. Analysis of cytoskeleton proteins

Many key spermatogenic processes, such as mitotic and meiotic divisions, rely on cytoskeleton dynamics. However, previous studies reported that ZnO NPs lead to alterations in the cytoskeletal protein of keratinocytes, epithelial cells [34], and spermatogonia [32]. ZnO NPs lead to the overproduction of ROS, which can influence the cytoskeleton through the oxidation of

cytoskeletal proteins [35]. Therefore, immunoblotting analysis was performed to understand if a compound with antioxidant activity could protect cytoskeletal proteins from oxidative stress during exposure to ZnO NPs.

Exposure of GC-1 cells to ZnO NPs for 6h and 12h resulted in an increase of acetylated α-tubulin, which was significantly higher than the control ($p<0.05$, $p<0.01$). However, increasing concentrations of VS3 resulted in lower levels of this protein at both timepoints (Figure 7, A). Co-exposure of ZnO NPs and 12.5 µM of VS3 for 12h significantly decreased acetylated α-tubulin levels, approaching those of the control group levels ($p<0.01$).

Intracellular β-tubulin levels after 6h of exposure to ZnO NPs significantly increased ($p<0.05$) but, as was the case for acetylated α-tubulin, the highest dose of VS3 (12.5 µM) resulted in protein levels close to the control condition (Figure 7, B). However, this was not the case for the 12h timepoint. After 12h of exposure, β-tubulin levels remained relatively stable and close to the control condition.

β-actin levels remained unaffected by ZnO NPs exposure and VS3 supplementation. There were some slight variations in intracellular levels of this protein but no clear trend and nostatistical significance (Figure 7, C).

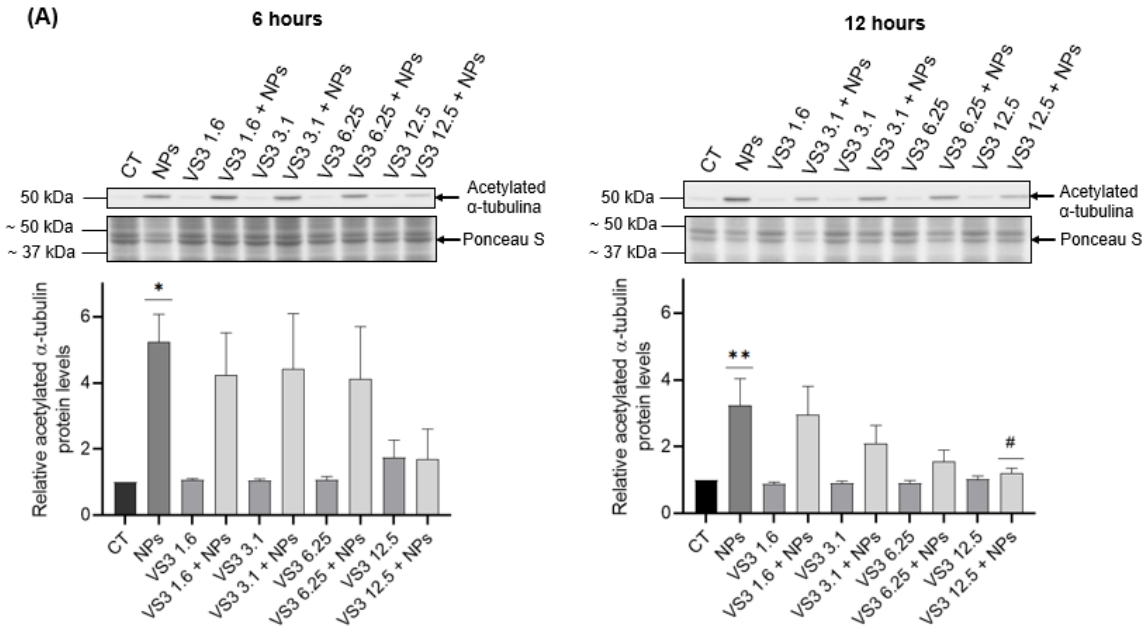

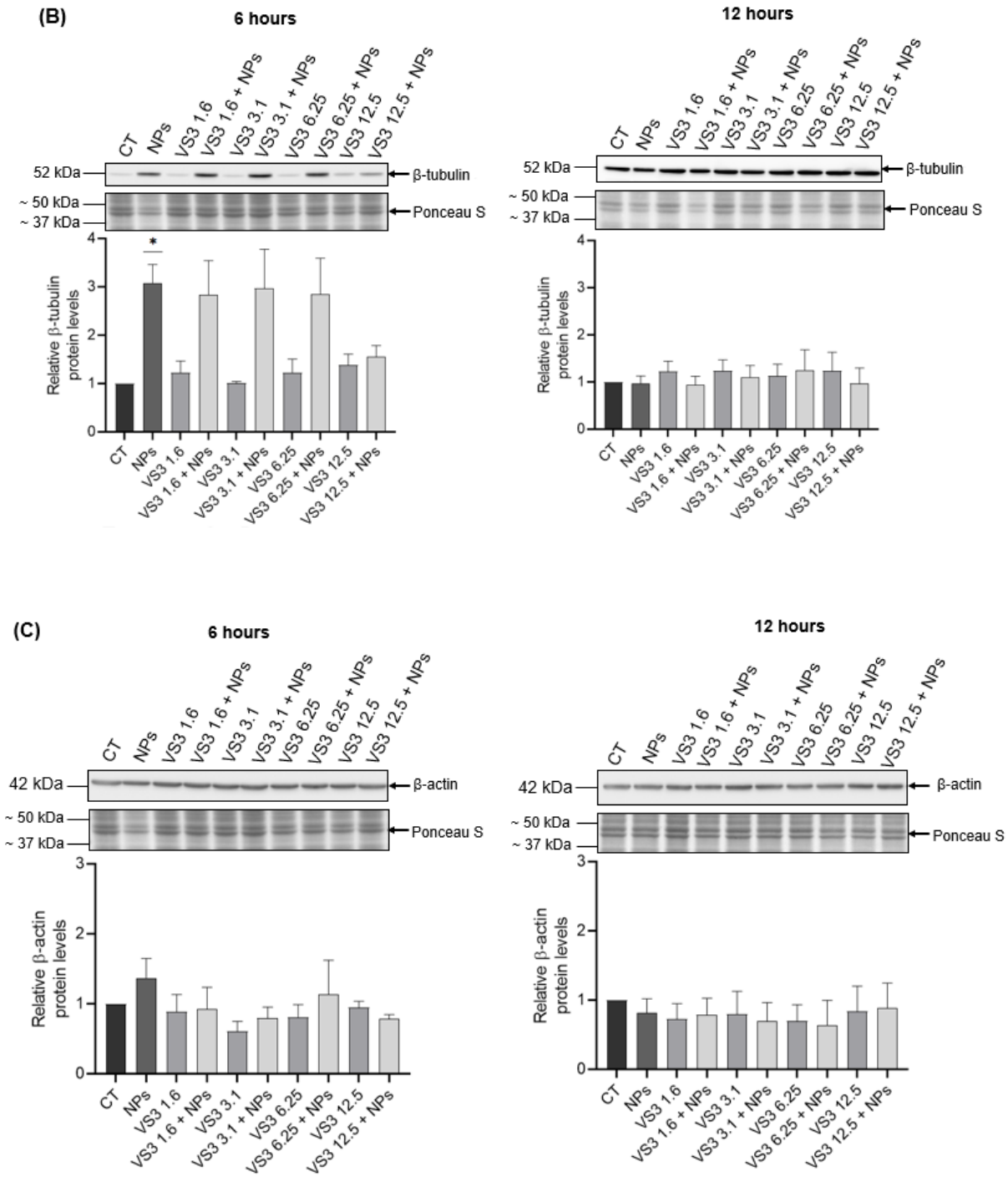

Figure 7. Immunoblotting analysis of cytoskeleton proteins. (A) acetylated α-tubulin, **(B)** β-tubulin and **(C)** β-actin of GC-1 cells treated with ZnO NPs (20 µg/mL) and VS3 (0-12.5 µM) for 6 and 12 hours. All data were expressed as mean ± SEM of four independent experiments. * p<0.05, **p<0.01 compared to the control group, # p<0.05 compared to the group treated with ZnO NPs, using one-way ANOVA. CT, control; NPs, nanoparticles

4. Discussion

Several studies have already confirmed the toxic effects of different doses, sizes, and exposure times of ZnO NPs in many model systems: different cell lines, organs, and animals. However, little research has been made on how to neutralize or decrease the negative effects that ZnO NPs have on male reproductive health.

The reproductive toxicity of ZnO NPs is mainly mediated through oxidative stress and oxidative-triggered DNA damage. Hence, antioxidant treatment should help combat reproductive toxicity. Previous research has shown that treatment with agents with antioxidant properties can reduce adverse reproductive health effects [36–38]. As a result, the current study focuses on the potential ameliorating effect of synthetic chalcone VS3 against ZnO NPs-induced cytotoxicity in a spermatogonia cell line, GC-1.

In previous work, among many other synthetic chalcones that were studied, chalcone VS3 (compound 4b) was one of the most active chalcones in modulating the exacerbated production of ROS during neutrophils oxidative burst [25]. This activity was attributed to the lipophilicity of this chalcone, which facilitates membrane transport and the binding of this compound to intracellular targets. Since VS3 showed promising results in neutrophils, in the present study, its antioxidant activity was assessed in a different cell type, in a mouse spermatogonia cell line.

Human lung epithelial cells were pretreated with resveratrol (1, 5 and 10 µM) for 1 hour before being exposed to 25 µg/mL of carbon black NPs for 24 hours. This pretreatment was enough to attenuate the oxidative stress induced by these NPs [39]. Mice kidney cells were also incubated with antioxidant N-acetylcysteine (0, 250, 500 µmol/L and 2, 3 mmol/L) for 1 hour before being treated with 450 µmol/L of cobalt NPs for 24 hours, and this pretreatment decreased the ROS-induced cell death caused by the NPs [40]. Similar results were reported in rat neuronal cells that were pretreated with Vitamin E (0.01-2 mM) for 1 hour, before being exposed to single-walled carbon nanotubes (50 µg/mL) for 24h and 48h [41]. Hence, in the current study, a pretreatment duration of 1 hour was selected in accordance with the mentioned studies since exposure to antioxidant agents for 1 hour seems to be enough to protect cells from NP toxicity.

Therefore, GC-1 cells were pretreated with different concentrations of VS3 (0-12.5 µM), 1 hour before being co-exposed to ZnO NPs and VS3 for 6 and 12 hours. Data from the viability assay confirmed the results obtained from other studies which indicate that the cytotoxicity of ZnO NPs is time dependent [32,42,43]. Resazurin assay revealed that incubation with ZnO NPs for 6 and 12 hours resulted in cell viabilities of 85.7% and 69.6%, respectively. Results also suggest that treating cells with VS3 for 1 hour before the co-exposure of ZnO NPs with VS3 could effectively attenuate the cytotoxicity of NPs. VS3 pretreatment and the combined exposure of ZnO NPs with 3.1 µM VS3 increased cell viability to 96.5% at the 6h timepoint (Figure 4, A). This means that VS3 supplementation resulted in a remarkable cell viability increase of 10.8%. For the 12h timepoint, supplementation with 12.5 µM of VS3 resulted in maximum cell viability of 91.3%, which translates into a 21.7% increase when compared to cells treated with ZnO NPs alone ($p<0.001$) (Figure 4, B).

It was hypothesized that, since oxidative stress is the main mechanism of NPs-mediated reproductive toxicity, by adding compounds with antioxidant activity into the cell culture, the oxidative stress would be ameliorated. In this study, cells exposed to ZnO NPs for 6 hours slightly increased ROS production (Figure 5, A). However, this increase was more evident at the 12h timepoint (Figure 5, B). At the 6h timepoint the ROS content of ZnO NPs + VS3 groups remained relatively constant and with values below the ZnO NPs-treated group, indicating that for shorter exposure times, VS3 is able to decrease the ROS production triggered by ZnO NPs. In the 12h timepoint, supplementation with VS3 also resulted in lower ROS levels than the group of cells treated with NPs only. However, for longer exposure times, higher doses of VS3 (6.25 and 12.5 µM) showed a tendency to trigger ROS production. This might explain the fact that the group of cells co-exposed to ZnO NPs + 12.5 µM of VS3 presented slightly higher values of ROS than the group of cells treated with only ZnO NPs. Therefore, longer incubation periods with VS3 may have a negative impact on GC-1 cells, and fuel oxidative stress. However, these were small alterations with no statistical relevance.

As expected, DNA damage levels increased in both timepoints when cells were exposed to ZnO NPs alone. Co-exposure with VS3 reduced the damage at the 6 hour timepoint, for all tested VS3 concentrations. However, VS3 seems unable to protect cells from NPs-induced genotoxicity for longer exposure times since the levels of DNA damage elicited by ZnO NPs were not reversed by VS3 supplementation at the 12h timepoint.

By now it is well established that oxidative stress is an important source of DNA damage, since the overproduction of ROS results in strand breaks and base oxidation [44]. In fact, at the 12h timepoint, ZnO NPs + VS3 (6.25 and 12.5 µM) and VS3 alone (6.25 and 12.5 µM) resulted in higher ROS production and, consequently, higher DNA damage. From these results, it can also be speculated that for longer exposure periods and higher VS3 concentrations, this compound may damage cells. This would account for the fact that more DNA damage occurs when cells are co-exposed to ZnO NPs + VS3 (6.25 and 12.5 µM), than when cells are exposed to ZnO NPs alone. Perhaps, for longer exposure times, higher concentrations of VS3 contributes to cell damage.

In fact, the induced DNA damage and ROS content did not always correspond to the viability of GC-1 cells. At the 12h timepoint, the cytotoxic results were in contrast to the genotoxic profile and oxidative stress of the investigated NPs with VS3. Even though all tested concentrations of VS3 with ZnO NPs resulted in higher cell viability than when cells were incubated with ZnO NPs only; all the tested conditions presented more DNA damage and more ROS content than the ZnO NPs group. In support of these data, Calarco et al. also reported that Polyethylenimine-PLGA NPs triggered oxidative stress and DNA damage without affecting the viability of human primary cells [45]. Human endothelial cells exposed to different concentrations of four different types of modified NPs, maintained their viability even though with high levels of DNA damage and oxidative stress [46]. Therefore, it can be concluded that NPs can reveal cytotoxic properties, even though they do not always reduce cell viability.

The spermatogonial cytoskeleton is fundamental for the initial establishment of spermatogenesis [47]. Cells can remodel their cytoskeleton in response to internal and external cues, and this ability

is required for dynamic processes, such as spermatogenesis because it requires extensive changes in cell shape, size, and germ cell movement [48].

The cytoskeleton comprises microfilaments, intermediate filaments, and microtubule networks. Since the role of intermediate filaments in spermatogenesis is less understood [49], in this study, only microfilaments and microtubules proteins were studied. Microfilaments are solid rods made of actin. Microtubules are cylindrical polymers formed by α- and β-tubulin heterodimers, but α-tubulin undergoes acetylation in the cytoplasm, which provides flexibility, mechanical resistance, and overall stability to microtubules [50]. However, NPs can interfere with this dynamic and lead to the breakdown and reorganization of the cytoskeleton [34,51], which can affect many cellular processes essential for spermatogenesis.

Immunobloting analysis reveals a clear increase of acetylated α-tubulin levels after GC-1 cells exposure to ZnO NPs for 6 and 12 hours (Figure 7, A). Alterations in the microtubule network in the presence of NPs are not always related to lower levels of α-tubulin acetylation [52]. Instead, this increase may be a cell coping mechanism to make microtubules softer and thus more resistant to damage induced by mechanical bending [53]. However, these levels decreased and approached normal values as VS3 concentration increased, suggesting that VS3 may have exerted protective effects. The reported alterations in the cytoskeleton could have been a result of the increased levels of ROS, a product of mechanical stress from ZnO NPs direct interaction with the cytoskeleton [54] or else, the result of the dissolution of zinc ions [34]. Tubulin molecules have many zinc-binding sites and act as zinc scavengers. Therefore, it is possible that zinc ions released from ZnO NPs may have triggered tubulin polymerization and the formation of large, aberrant macrotubules [34], which could explain the significant increase of β-tubulin levels after 6 hours of ZnO NPs exposure ($p<0.05$) (Figure 7, B). As was the case for acetylated α-tubulin, β-tubulin levels also decreased with increasing concentrations of VS3, but this decrease was more evident for the highest concentration of VS3. In fact, when cells were co-exposed to ZnO NPs and 12.5 μM of VS3, β-tubulin intracellular levels returned to normal. However, the intracellular levels of this protein did not follow the same pattern for longer incubation periods. After 12h of exposure, VS3 alone slightly increased β-tubulin levels, and the groups treated with NPs presented lower values. But in all tested conditions, these levels remained close to the control group. Therefore, it is reasonable to conclude that β-tubulin disruption is temporary and can stabilize after some time of exposure.

Most studies that assessed the impact of NPs on cytoskeletal integrity found a destabilization and degradation of actin filaments [34,52,55]. However, in the present work, β-actin levels remained unaltered in every treatment condition in both timepoints. There were only slight variations, with no statistical significance (Figure 7, C), which suggests that β-actin remained unaffected.

5. Conclusions

This study aimed to provide a potential strategy for reducing the adverse reproductive consequences of ZnO NPs by evaluating the potential protective effects of a synthetic chalcone on GC-1 cells. Overall, results suggest that chalcone VS3 can partially recover the viability of GC-1 cells and may have some protective effects on the cytoskeleton. Additionally, this compound attenuates the NPs-induced genotoxicity and ROS production for shorter exposure times. However, more research is needed to explain the precise mechanisms by which this compound behaves in the presence of ZnO NPs.

References:

1. Sousa, A.; Lucas, M.; Ribeiro, D.; Correia, C.M.; Silva, V.L.M.; Silva, A.M.S.; Fernandes, E.; Freitas, M. Chalcones as Modulators of Neutrophil Oxidative Burst under Physiological and High Glucose Conditions. **2020**, doi:10.1021/acs.jnatprod.0c00728.

2. Horvat, T.; Verbanac, D.; Kuˇ, M. Antioxidant Activities of Alkyl Substituted Pyrazine Derivatives of Chalcones — In Vitro and In Silico Study. **2019**.

3. Gacche, R.N.; Dhole, N.A.; Kamble, S.G.; Bandgar, B.P.; Dhole, N.A.; Kamble, S.G.; In-vitro, B.P.B. In-vitro evaluation of selected chalcones for antioxidant activity. *J. Enzyme Inhib. Med. Chem.* **2008**, *23*, 28–31, doi:10.1080/14756360701306370.

4. Santos, C.M.M.; Silva, A.M.S. Chalcones as Versatile Synthons for the Synthesis of 5- and 6-membered Nitrogen Heterocycles. *Curr. Org. Chem.* **2014**.

5. Jasim, H.A.; Nahar, L.; Jasim, M.A.; Moore, S.A.; Ritchie, K.J.; Sarker, S.D. Chalcones : Synthetic Chemistry Follows Where Nature Leads. *Biomolecules* **2021**.

6. Zhuang, C.; Zhang, W.; Sheng, C.; Zhang, W.; Xing, C.; Miao, Z.; States, U. Chalcone: A Privileged Structure in Medicinal Chemistry. *Chem Rev.* **2018**, *117*, 7762–7810, doi:10.1021/acs.chemrev.7b00020.Chalcone.

7. Wang, J.; Huang, L.; Cheng, C.; Li, G.; Qiu, P.; Wu, J. Design, synthesis and biological evaluation of chalcone analogues with novel dual antioxidant mechanisms as potential anti-ischemic stroke agents. *Acta Pharm. Sin. B* **2019**, *9*, 335–350, doi:10.1016/j.apsb.2019.01.003.

8. Pizzino, G.; Irrera, N.; Cucinotta, M.; Pallio, G.; Mannino, F.; Arcoraci, V.; Squadrito, F.; Altavilla, D.; Bitto, A. Oxidative Stress: Harms and Benefits for Human Health. *Oxid. Med. Cell. Longev.* **2017**, *2017*, doi:10.1155/2017/8416763.

9. Phaniendra, A.; Babu, D. Free Radicals : Properties , Sources , Targets , and Their Implication in Various Diseases. *Ind J Clin Biochem* **2015**, *30*, 11–26, doi:10.1007/s12291-014-0446-0.

10. Shen, J.; Yang, D.; Zhou, X.; Wang, Y.; Tang, S.; Yin, H. Role of Autophagy in Zinc Oxide Nanoparticles-Induced Apoptosis of Mouse LEYDIG Cells. *Int. J. Mol.* **2019**, *20*.

11. Talebi, A.R.; Khorsandi, L.; Moridian, M. The effect of zinc oxide nanoparticles on mouse spermatogenesis. *J. Assist. Reprod. Genet.* **2013**, *30*, 1203–1209, doi:10.1007/s10815-013-0078-y.

12. Abbasalipourkabir, R.; Moradi, H.; Zarei, S.; Asadi, S.; Salehzadeh, A.; Ghafourikhosroshahi, A.; Mortazavi, M.; Ziamajidi, N. Toxicity of zinc oxide nanoparticles on adult male Wistar rats. *Food Chem. Toxicol.* **2015**, *84*, 154–160, doi:10.1016/j.fct.2015.08.019.

13. Donnell, B.O.; Huo, L.; Polli, J.R.; Qiu, L.; Collier, D.N.; Zhang, B.; Pan, X.; Carolina, N.; Services, W.P.; Carolina, N. ZnO Nanoparticles Enhanced Germ Cell Apoptosis in Caenorhabditis elegans , in Comparison with ZnCl 2. *Toxicol. Sci.* **2017**, *156*, 336–343, doi:10.1093/toxsci/kfw258.

14. Simko, M.; Gazso, A.; Fiedeler, U.; Nentwich, M. Nanoparticles, free radicals and oxidative stress. *NanoTrust Dossiers* **2011**, *12*, 1–3.

15. Lakshmipriya, T.; Gopinath, S. Introduction to nanoparticles and analytical devices. In *Nanoparticles in Analytical and Medical Devices*; 2021; pp. 1–29.

16. Pinho, A.; Rebelo, S.; Pereira, M. The Impact of Zinc Oxide Nanoparticles on Male (In)Fertility. *Materials (Basel).* **2020**, *13*, 1–18, doi:https://doi.org/10.3390/ma13040849.

17. Bisht, S.; Faiq, M.; Tolahunase, M.; Dada, R. Oxidative stress and male infertility. *Nat. Rev. Urol.* **2017**, *14*, 470–485, doi:10.1038/nrurol.2017.69.

18. Alahmar, A.T. Role of Oxidative Stress in Male Infertility: An Updated Review. *J. Hum. Reprod. Sci.* **2019**, *12*, 4–18, doi:10.4103/jhrs.JHRS.

19. Agarwal, A.; Leisegang, K.; Majzoub, A.; Henkel, R.; Finelli, R.; Selvam, M.K.P.; Tadros, N.; Parekh, N.; Ko, E.Y.; Cho, C.L.; et al. Utility of antioxidants in the treatment of male infertility: Clinical guidelines based on a systematic review and analysis of evidence. *World J. Mens. Health* **2021**, *39*, 1–58, doi:10.5534/WJMH.200196.

20. Wu, J.Z.; Cheng, C.C.; Shen, L.L.; Wang, Z.K.; Wu, S.B.; Li, W.L.; Chen, S.H.; Zhou, R.P.; Qiu, P.H. Synthetic chalcones with potent antioxidant ability on H2O2-induced apoptosis in PC12 cells. *Int. J. Mol. Sci.* **2014**, *15*, 18525–18539, doi:10.3390/ijms151018525.

21. Janković, T.; Turković, N.; Kotur-Stevuljević, J.; Vujić, Z.; Ivković, B. Differences in antioxidant potential of chalcones in human serum: In vitro study. *Chem. Biol. Interact.* **2020**, *324*, doi:10.1016/j.cbi.2020.109084.

22. Wang, L.; Chen, H.C.; Yang, X.; Tao, J.J.; Liang, G.; Wu, J.Z.; Wu, W.C.; Wang, Y.; Song, Z.M.; Zhang, X. The novel chalcone analog L2H17 protects retinal ganglion cells from oxidative stress-induced apoptosis. *Neural Regen. Res.* **2018**, *13*, 1665–1672, doi:10.4103/1673-5374.237140.

23. Lahsasni, S.A.; Hamad, F.; Korbi, A.; Aljaber, N.A. Synthesis , characterization and evaluation of antioxidant activities of some novel chalcones analogues. *Chem. Cent. J.* **2014**, *8*, 1–10.

24. Series, I.O.P.C.; Science, M. A Green Synthesis of Chalcones As an Antioxidant and Anticancer A Green Synthesis of Chalcones As an Antioxidant and Anticancer. *Int. Conf. Chem. Mater. Sci.* **2018**, doi:10.1088/1757-899X/299/1/012077.

25. Martins, T.; Silva, V.L.M.; Silva, A.M.S.; Lima, J.L.F.C.; Fernandes, E.; Ribeiro, D. Chalcones as Scavengers of HOCl and Inhibitors of Oxidative Burst: Structure-Activity Relationship Studies. *Med. Chem. (Los. Angeles).* **2020**, *17*, 1–9.

26. Barros, A.I.R.N.A.; Nunes, F.M.; Barros, C.; Silva, A.M.S.; Domingues, M.R.M. Structural characterization of - nitrated 2 ¢ -hydroxychalcones by electrospray ionization tandem mass spectrometry. **2009**, *616*, 605–616, doi:10.1255/ejms.1020.

27. Barros, A.I.R.N.A. Reductive Coupling Reactions of 2-Nitrochalcones and their b -Hydroxy-analogues : New Syntheses of 2-Arylquinoline and 2-Aryl-4-hydroxyquinoline Derivatives. **2007**, *594*, 585–594, doi:10.1007/s00706-007-0647-9.

28. Martins, F.; Serrano, J.B.; Müller, T.; da Cruz e Silva, O.A.B.; Rebelo, S. BRI2 Processing and Its Neuritogenic Role Are Modulated by Protein Phosphatase 1 Complexing. *J. Cell. Biochem.* **2017**, *118*, 2752–2763, doi:10.1002/jcb.25925.

29. Pereira, C.D.; Martins, F.; Santos, M.; Müeller, T.; da Cruz E Silva, O.A.B.; Rebelo, S. *Nuclear*

Accumulation of LAP1:TRF2 Complex during DNA Damage Response Uncovers a Novel Role for LAP1; 2020; Vol. 9; ISBN 3519244063.

30. Gomes, A.; Fernandes, E.; Lima, J. Fluorescence probes used for detection of reactive oxygen species. *J Biochem Biophys Methods* **2005**, *65*, 45–80, doi:10.1016/j.jbbm.2005.10.003.

31. Aranda, A.; Sequedo, L.; Tolosa, L.; Quintas, G. Dichloro-dihydro-flurescein diacetate (DCFH-DA) assay: A quantitative method for oxidative stress assessment of nanoparticle-treated cells. *Toxicol. Vitr.* **2013**, *27*, 954–963, doi:10.1016/j.tiv.2013.01.016.

32. Pinho, A.R.; Martins, F.; Costa, M.E. V.; Senos, A.M.R.; Silva, O.A.B. d. C.E.; Pereira, M. de L.; Rebelo, S. In Vitro Cytotoxicity Effects of Zinc Oxide Nanoparticles on Spermatogonia Cells. *Cells* **2020**, *9*, doi:10.3390/cells9051081.

33. Zhao, H.; Huang, X.; Halicka, H.D. Detection of Histone H2AX Phosphorylation on Ser-139 as an Indicator of DNA Damage. *Curr. Protoc. Cytom.* **2019**, *89*, 1–10, doi:10.1002/cpcy.55.

34. García-Hevia, L.; Valiente, R.; Martín-Rodríguez, R.; Renero-Lecuna, C.; González, J.; Rodríguez-Fernández, L.; Aguado, F.; Villegas, J.C.; Fanarraga, M.L. Nano-ZnO leads to tubulin macrotube assembly and actin bundling, triggering cytoskeletal catastrophe and cell necrosis. *Nanoscale* **2016**, *8*, 10963–10973, doi:10.1039/c6nr00391e.

35. Valdivia, A.; Duran, C.; Martin, A.S. The Role of Nox-Mediated Oxidation in the Regulation of Cytoskeletal Dynamics The Role of Nox-Mediated Oxidation in the Regulation of Cytoskeletal Dynamics. *Curr. Pharm. Des.* **2015**, *21*, doi:10.2174/1381612821666151029112624.

36. Hussein, M.; Ali, H.; Saadeldin, I.; Ahmed, M. Querectin Alleviates Zinc Oxide Nanoreprotoxicity in Male Albino Rats. *J. Biochem. Mol. Toxicol.* **2016**, *30*, 489–496, doi:10.1002/jbt.

37. Özgür, M.E.; Ulu, A.; Noma, S.A.A.; Özcan, İ.; Balcıoğlu, S.; Ateş, B.; Köytepe, S. Melatonin protects sperm cells of Capoeta trutta from toxicity of titanium dioxide nanoparticles. *Environ. Sci. Pollut. Res.* **2020**, *27*, 17843–17853, doi:10.1007/s11356-020-08273-7.

38. Kong, L.; Hu, W.; Lu, C.; Cheng, K.; Tang, M. Chemosphere Mechanisms underlying nickel nanoparticle induced reproductive toxicity and chemo-protective effects of vitamin C in male rats. *Chemosphere* **2019**, *218*, 259–265, doi:10.1016/j.chemosphere.2018.11.128.

39. Hsu, H. Te; Tseng, Y.T.; Wong, W.J.; Liu, C.M.; Lo, Y.C. Resveratrol prevents nanoparticles-induced inflammation and oxidative stress via downregulation of PKC-α and NADPH oxidase in lung epithelial A549 cells. *BMC Complement. Altern. Med.* **2018**, *18*, 1–13, doi:10.1186/s12906-018-2278-6.

40. Liu, Y.K.; Yang, H.W.; Wang, M.H.; Wang, W.; Liu, F.; Yang, H.L. N-acetylcysteine Attenuates Cobalt Nanoparticle-Induced Cytotoxic Effects through Inhibition of Cell Death, Reactive Oxygen Species-related Signaling and Cytokines Expression. *Orthop. Surg.* **2016**, *8*, 496–502, doi:10.1111/os.12298.

41. Wang, J.; Sun, P.; Bao, Y.; Dou, B.; Song, D.; Li, Y. Vitamin E renders protection to PC12 cells against oxidative damage and apoptosis induced by single-walled carbon nanotubes. *Toxicol. Vitr.* **2012**, *26*, 32–41, doi:10.1016/j.tiv.2011.10.004.

42. Barkhoradi, A.; Hekmatimoghaddam, S.; Jebali, A.; Khalili, M.; Talebi, A.; Noorani, M. Effect

of zinc oxide nanoparticles on viability of human spermatozoa. *Iran. J. Reprod. Med.* **2013**, *11*, 767–771.

43. Han, Z.; Yan, Q.; Ge, W.; Liu, Z.-G.; Gurunathan, S.; Felici, M.; Shen, W.; Zang, X.-F. Cytotoxic effects of ZnO nanoparticles on mouse testicular cells. *Int. J. Nanomedicine* **2016**, *11*, 5187–5203.

44. Yu, Z.; Li, Q.; Wang, J.; Yu, Y.; Wang, Y. Reactive Oxygen Species-Related Nanoparticle Toxicity in the Biomedical Field. *Nanoscale Res. Lett.* **2020**, *15*, doi:doi.org/10.1186/s11671-020-03344-7.

45. Calarco, A.; Bosetti, M.; Margarucci, S.; Fusaro, L.; Nicolì, E.; Petillo, O.; Cannas, M.; Galderisi, U.; Peluso, G. The genotoxicity of PEI-based nanoparticles is reduced by acetylation of polyethylenimine amines in human primary cells. *Toxicol. Lett.* **2013**, *218*, 10–17, doi:10.1016/j.toxlet.2012.12.019.

46. Wigner, P.; Zielinski, K.; Michlewska, S.; Danielska, P.; Marczak, A.; Ricci, E.J.; Santos-Oliveira, R.; Szwed, M. Disturbance of cellular homeostasis as a molecular risk evaluation of human endothelial cells exposed to nanoparticles. *Nat. Sci. Reports* **2021**, *11*, 1–16, doi:10.1038/s41598-021-83291-0.

47. Dunleavy, J.E.M.; Bryan, M.K.O.; Stanton, P.G.; Donnell, L.O. The cytoskeleton in spermatogenesis. *Soc. Reprod. Fertil.* **2019**, *157*, 53–72, doi:https://doi.org/10.1530/REP-18-0457.

48. Wang, L.; Yan, M.; Wu, S.; Wu, X.; Bu, T.; Wong, C.K.C.; Ge, R.; Sun, F.; Cheng, C.Y. Actin binding proteins , actin cytoskeleton and spermatogenesis – Lesson from toxicant models. *Reprod. Toxicol.* **2020**, *96*, 76–89, doi:10.1016/j.reprotox.2020.05.017.

49. Lie, Y.; Mruk, D.D.; Lee, W.M.; Cheng, C.Y. Cytoskeletal dynamics and spermatogenesis. *Philos. Trans. R. Soc.* **2010**, *365*, 1581–1592, doi:10.1098/rstb.2009.0261.

50. Nekooki, Y.; Haruo, M. Role of tubulin acetylation in cellular functions and diseases. *Med. Mol. Morphol.* **2020**, *53*, 191–197, doi:10.1007/s00795-020-00260-8.

51. Ispanixtlahuatl-meráz, O.; Schins, R.P.F.; Chirino, Y.I. Environmental Science Nano Cell type specific cytoskeleton disruption induced by engineered nanoparticles. *Environ. Sci. Nano* **2017**, doi:10.1039/C7EN00704C.

52. Septiadi, D.; Crippa, F.; Moore, T.L.; Rothen-rutishauser, B. Nanoparticle – Cell Interaction : A Cell Mechanics Perspective. *Adv. Mater.* **2018**, doi:10.1002/adma.201704463.

53. Janke, C.; Montagnac, G. Causes and Consequences of Microtubule Acetylation. *Curr. Biol.* **2017**, *27*, doi:10.1016/j.cub.2017.10.044.

54. Kr, K.; Melounkov, L.; Slov, M.; Mannov, N.; Sedl, M.; Bart, J. Disruption of Cell Adhesion and Cytoskeletal Networks by Thiol-Functionalized Silica-Coated Iron Oxide Nanoparticles. *Int. J. Mol. Sci.* **2020**, *21*, doi:doi:10.3390/ijms21249350.

55. Pernodet, N.; Fang, X.; Sun, Y.; Bakhtina, A.; Ramakrishnan, A.; Sokolov, J.; Ulman, A.; Rafailovich, M. Adverse Effects of Citrate / Gold Nanoparticles on Human Dermal Fibroblasts. *Small* **2006**, *11733*, 766–773, doi:10.1002/smll.200500492.

Chapter 5

General conclusions and Future Perspectives

The first chapter of this dissertation was based on a review article that includes *in vitro* and *in vivo* studies, where it was demonstrated that MONPs can interfere with the male reproductive system at many levels. Most of these studies revealed that oxidative stress is the main molecular mechanism that contributes to the reproductive toxicity of these nanomaterials. Since oxidative stress interferes with biomolecules and reproductive hormones, inevitably, it affects the number, quality, morphology, and activity of germ cells. At the organ level, MONPs cause several histological alterations in tissues of the reproductive system. This finding was also supported by the presence of MONPs in the testis, which also confirmed MONPs' ability to cross the BTB in pre-clinical studies. However, from this review, it became clear that no enough studies are available to evaluate the reversibility of damage by MONPs. To understand the real effect of NPs on male reproductive health, it is crucial to understand whether the induced damage is permanent. Therefore, the next step of this research was to assess the recovery ability of GC-1 cells. This was acomplished by exposing cells to a previously established cytotoxic concentration of one type of MONPs – ZnO NPs (20 µg/mL) – for 6 and 12 hours. This exposure was followed by a four-day recovery period in which cells were allowed to proliferate in an NP-free environment. Cell viability assays upon NPs removal revealed that, at the end of the recovery period, although cell viability was very close to the control condition, cells were unable to fully recover. This suggests that the removal of ZnO NPs improves cell performance, however it is not sufficient to allow cell recover completely. Given these findings, in the following study, another strategy was proposed to neutralize the cytotoxicity of ZnO NPs.

Since there is a growing interest in the use of antioxidants to mitigate the negative effects of nanoparticles on human health [1–4], here, different concentrations of VS3 – a chalcone with antioxidant activity [5,6] – were assessed to evaluate its ability to protect GC-1 cells from ZnO NPs-induced damage. In this case, cells were pretreated with VS3 (0-12.5 µM) before being co-exposed to ZnO NPs (20 µg/mL) and VS3 (0-12.5 µM) for 6 and 12 hours. Results demonstrated that VS3 can partially recover the viability of GC-1 cells and may have protected microtubules from ZnO NPs. Additionally, this compound attenuates the NPs-induced genotoxicity and ROS production for shorter exposure times.

As future work, additional assays, such as GC-1 cells internalization of NPs and ZnO NPs dissolution should be performed to better understand the mechanisms of toxicity of these nanomaterials, which may also elucidate how VS3 behaves in its presence. Additionally, in this study, only the concentration and duration of exposure were considered to evaluate the reproductive toxicity of ZnO NPs. However, the size and surface area of NPs are two equally important parameters often overlooked, but should be considered in future work, since they greatly determine cytotoxicity [7,8]. Here, only the cytoskeleton was studied. However, nucleoskeleton alterations in GC-1 cells have been previously reported for 20 µg/mL of ZnO NPs [9]. Spermatogenesis can be compromised by changes in the nucleoskeleton because it can lead to genomic instability and meiosis impairment. Therefore, future studies should focus on this structure, since it is crucial for preserving male fertility.

As reproductive cells have been proven to be highly sensitive to ZnO NPs insults, it is crucial to continue the search for therapies that can protect these cells and preserve male fertility.

References:

1. Hussein, M.M.A.; Gad, E.; Ahmed, M.M.; Arisha, A.H.; Mahdy, H.F.; Swelum, A.A.; Tukur, H.A.; Saadeldin, I.M. Amelioration of titanium dioxide nanoparticle reprotoxicity by the antioxidants morin and rutin. *Environ. Sci. Pollut. Res.* **2019**, *26*, 29074–29084, doi:https://doi.org/10.1007/s11356-019-06091-0.

2. Jafari, A.; Karimipour, M.; Khaksar, M.R.; Ghasemnejad-Berenji, M. Protective effects of orally administered thymol against titanium dioxide nanoparticle–induced testicular damage. *Environ. Sci. Pollut. Res.* **2020**, *27*, 2353–2360, doi:10.1007/s11356-019-06937-7.

3. Hussein, M.; Ali, H.; Saadeldin, I.; Ahmed, M. Querectin Alleviates Zinc Oxide Nanoreprotoxicity in Male Albino Rats. *J. Biochem. Mol. Toxicol.* **2016**, *30*, 489–496, doi:10.1002/jbt.

4. Özgür, M.E. The protective effects of Vitamin C and Trolox on kinematic and oxidative stress indices in rainbow trout sperm cells against flower-like ZnO nanoparticles. *Aquac. Res.* **2019**, *50*, 2838–2845, doi:10.1111/are.14236.

5. Martins, T.; Silva, V.L.M.; Silva, A.M.S.; Lima, J.L.F.C.; Fernandes, E.; Ribeiro, D. Chalcones as Scavengers of HOCl and Inhibitors of Oxidative Burst: Structure-Activity Relationship Studies. *Med. Chem. (Los. Angeles).* **2020**, *17*, 1–9.

6. Sousa, A.; Lucas, M.; Ribeiro, D.; Correia, C.M.; Silva, V.L.M.; Silva, A.M.S.; Fernandes, E.; Freitas, M. Chalcones as Modulators of Neutrophil Oxidative Burst under Physiological and High Glucose Conditions. **2020**, doi:10.1021/acs.jnatprod.0c00728.

7. Shin, S.W.; Song, I.H.; Um, S.H. Role of Physicochemical Properties in Nanoparticle Toxicity. *Nanomaterials* **2015**, 1351–1365, doi:10.3390/nano5031351.

8. Sukhanova, A.; Bozrova, S.; Sokolov, P.; Berestovoy, M.; Karaulov, A.; Nabiev, I. Dependence of Nanoparticle Toxicity on Their Physical and Chemical Properties. *Nanoscale Res. Lett.* **2018**, *13*, doi:https://doi.org/10.1186/s11671-018-2457-x.

9. Pinho, A.R.; Martins, F.; Costa, M.E. V.; Senos, A.M.R.; Silva, O.A.B. d. C.E.; Pereira, M. de L.; Rebelo, S. In Vitro Cytotoxicity Effects of Zinc Oxide Nanoparticles on Spermatogonia Cells. *Cells* **2020**, *9*, doi:10.3390/cells9051081.

Annex

Cell culture solutions:

- **Complete DMEM medium**

DMEM Hugh Glucose with 10% FBS and 1% of PenStrep. Filter sterilize and store at 4ºC.

- **1x PBS**

Dissolve each pack of BupH Modified Dulbecco's Phosphate Buffered Saline Pack (Pierce) in 500 mL of deionized water. Filter sterilize and store at 4ºC.

Immunoblottingi solutions:

- **10% SDS**

Dissolve 1g of SDS in 10 mL of deionized water. Store at room temperature.

- **10% APS**

Dissolve 0.5g of APS in 5 mL of deionized water. Short term storage at 4ºC. Long term storage at -20ºC.

- **1M Tris solution**

Dissolve 30.3g of Tris base in 250 mL of deionized water. Adjust the pH to 6.8. Store at 4ºC.

- **Lower gel buffer (LGB) 4x**

Dissolve 181.65g of Tris and 4g of SDS in 1L of deionized water. Adjust the pH to 8.9

- **Upper gel buffer (UGB) 4x**

Dissolve 75.69g of Tris in 1L of deionized water. Adjust the pH to 6.8

- **10x Running buffer**

Dissolve 30.3g of Tris, 144.2 of Glycine, and 10g of SDS in 800mL of deionized water. Add 200mL of methanol. Adjust the pH to 8.3

- **10x Transfer buffer**

Dissolve 30.3g of Tris, and 144.1g of Glycine in 1L of deionized water. Adjust the pH to 8.3

- **10x TBS**

Dissolve 12.11g of Tris, and 87.66g of NaCl in 1L of deionized water. Adjust the pH to 8. Store at 4ºC.

- **10x TBS-T**

Dissolve 12.11g of Tris, and 87.66g of NaCl in 1L of deionized water and add 10 mL of Tween-20. Adjust the pH to 8. Store at 4ºC.

- **Stripping Mild Solution**

Dissolve 7.5g of Glycine, and 0.5g of SDS in 500 mL of deionized water and add 5 mL of Tween-20. Ajust the pH to 2.2, store in the dark, at 4ºC.

- **4x Loading buffer**

For a final volume of 8mL add 2.5mL of Tris 1M, 4mL of Glicerol, 0.8g of SDS, and 0.001g of bromophenol blue. Store in aliquots of 800µL at -20ºC. Before use, add 200µL of β-mercaptoethanol to each aliquot.

- **Resolving lower gel solution**

1 system – 1.5 mm	**5%**	**20%**
ddH_2O (mL)	18.59	7.34
Acrylamide/bis-Acrylamide (29:1) (mL)	3.75	15
LGB (mL)	7.5	7.5
APS (µL)	150	150
TEMED (µL)	15	15

- **Stacking upper gel solution**

1 system – 1.5 mm	**3.5%**
ddH_2O (mL)	13.85
Acrylamide/bis-Acrylamide (29:1) (mL)	1.75
UGB (mL)	4
SDS (µL)	200
APS (µL)	200
TEMED (µL)	20